*Russian Chemical Reviews* **82** (7) 648 – 685 (2013) © 2013 Russian Academy of Sciences and Turpion Ltd

DOI 10.1070/RC2013v082n07ABEH004413

# Target-oriented analysis of gaseous, liquid and solid chemical systems by mass spectrometry, nuclear magnetic resonance spectroscopy and electron microscopy

V V Kachala, L L Khemchyan, A S Kashin, N V Orlov, A A Grachev, S S Zalesskiy, V P Ananikov

## Contents


| | | |
|---|---|---|
| I. | Introduction | 648 |
| II. | Target-oriented analytical approach | 649 |
| III. | Gas-phase chemical systems | 651 |
| IV. | Liquid-phase chemical systems | 660 |
| V. | Solid-state chemical systems | 675 |
| VI. | Conclusions and outlook | 679 |


**Abstract. In the present review we describe the emerging tendency for creating target-oriented analytical approaches designed to solve important chemical tasks by using a combination of analytical tools. The concept is illustrated by selected examples of advances of NMR spectroscopy, mass spectrometry and electron microscopy in the analysis and study of gas-phase, liquid-state and solid-state chemical systems. Comparative description of chemical applications of these analytical methods is presented and discussed. The bibliography includes 359 references.**

## I. Introduction

Progress in organic chemistry, catalysis, asymmetric synthesis, polymer chemistry, material science and many related areas in a large extent was governed by the development of efficient analytical tools. NMR spectroscopy and mass spectrometry nowadays are the leading methods due to wide area of applications and unquestionable importance of problems. Development of nanoscience, taking place extremely rapidly in the recent years, has appointed electron microscopy as the necessary and complementary characterization tool. A powerful combination of NMR, mass spectrometry and electron microscopy becomes a must in modern chemical applications.

**V V Kachala, L L Khemchyan, A S Kashin, N V Orlov, A A Grachev, S S Zalesskiy, V P Ananikov** N D Zelinsky Institute of Organic Chemistry, Russian Academy of Sciences, Leninsky prosp. 47, 119991 Moscow, Russian Federation. Tel. (7-495) 135 90 79
e-mail: vvk@ioc.ac.ru (V V Kachala),
e-mail: khemchyan@ioc.ac.ru (L L Khemchyan),
e-mail: a.kashin@ioc.ac.ru (A S Kashin),
e-mail: onv@ioc.ac.ru (N V Orlov),
e-mail: grachevaa@mail.ru (A A Grachev),
e-mail: s.zalesskiy@ioc.ac.ru (S S Zalesskiy),
e-mail: val@ioc.ac.ru (V P Ananikov).

Received 21 May 2013
*Uspekhi Khimii* **82** (7) 648 – 685 (2013)

In spite of well-known areas of application and numerous examples available in the literature, each method has certain strong and weak points that are necessary to take into account for carrying out thorough compound characterization or reaction monitoring. The focus of the present article is to highlight application areas of the considered analytical methods applicable in the field of organic chemistry with a special attention paid to development of target-oriented approach. A rough summary presented in Table 1 might be used as a quick guide to select a proper combination of structural methods and to navigate through the discussion in the present article.

**Table 1**. Target-oriented map of applications of the considered analytical methods in organic chemistry and development of new synthetic methods.[a]

| Chemical system | NMR Spectroscopy | Mass spectrometry | Electron microscopy |
|---|---|---|---|
| Gas-phase | ★★ | ★★★ | |
| Liquid-phase | ★★★ | ★★ | ★ |
| Solid-state | ★★★ | ★★ | ★★★ |

[a] (★) Limited applications, (★★) some applications, (★★★) many applications.

There are many excellent review articles available in the literature dealing with NMR spectroscopy, mass spectrometry and electron microscopy (representative citations are made in each section below). Typically the reviews deal with certain analytical methods and highlight particular applications. We have arranged the discussion from the point of view of target-oriented analysis — the topics were divided into sections depending on the nature of chemical system (gas-phase, solution and solid-state), followed by comparative description of analytical methods in each part (see Table 1). No attempts were made to provide a comprehensive description of methods in the present review, since it is

hardly possible due to enormously wide subject coverage. Instead, we have selected few representative studies to illustrate the concept of target-oriented approach and its utility in modern chemistry.

## II. Target-oriented analytical approach

The present review starts with a basic introductory description of each analytical method (sections II.1. – II.3.), where the main features needed to highlight the concept are briefly mentioned. Comparative description of gas-phase (section III), liquid-phase (section IV) and solid-phase (section V) chemical systems gives an overview of possible applications of NMR spectroscopy, mass spectrometry and electron microscopy in each area.

### 1. Applications of mass spectrometry in organic chemistry

The history of the mass spectrometry begins from J J Thomson experiments to determine $m/z$ ratio of electron at 1897.[1] It is possible to say that from the first application till nowadays there was fascinating continuous progress in the development of mass spectrometry. Numerous hardware, software, methodological and data processing enhancements and updates were performed and plenty of articles, reviews and books have been published during the last decades.[2 – 13]

Due to outstanding sensitivity and easy to use design, mass spectrometry has become powerful practical tool not only for fundamental science but also for hundreds of other fields and practical applications. It is widely used in medicine, biology, biotechnology, pharmacy, food and environmental analysis, forensic applications, surface analysis, homeland security, geology, archaeology, space research, *etc*.[14, 15]

Undoubtedly, mass spectrometry is essential and one of the most important tools for chemical science. The method provides a wealth of valuable information: molecular weight, isotopic ratio, composition, structure, character of fragmentation, reactivity, *etc*., which quite often cannot be obtained using other analytical measurements. The key features of mass-spectrometric analysis (especially, sensitivity and rapid data collection) have already reached impressive level routinely utilized at chemical and biological laboratories worldwide, and the process of further developments is still going on.

Herein we have focused on the role of mass spectrometry in target-oriented analysis in organic chemistry. In this connection, we should separately mention feasibility of coupling gas and liquid chromatograph to mass spectrometer (GC-MS and LC-MS), which provides a vast array of data for complex mixtures including quantitative MS measurements.[9, 10]

Chemical reaction is the essence of molecular transformation, as well as rather difficult challenge to analytical methods (in contrast to static analysis of stable compounds). Main areas of application of mass spectrometry in the field of reactivity in organic chemistry can be divided into the following groups:

a) Characterization of starting materials: verification of purity and quality of reagents.

b) Reaction monitoring: mechanistic investigations, determination of composition, structure and stability of intermediate compounds, assessment of active and inactive forms of catalysts, conversion of reactants, identification of by-products.

c) Analysis of products: structure determination, verification of purity of products after isolation, examination for residual amounts of catalysts, *etc*.

Reaction monitoring can be carried out in two different ways:

a) Off-line monitoring: probing a reaction by aliquots. It is suitable for kinetic study of slow reactions and long-lived intermediates.

b) On-line monitoring: coupling a chemical reactor directly to ion source of a mass-spectrometer or performing ion-molecular reactions inside the mass-spectrometer. The method is suitable for fast reaction kinetics and short-lived unstable intermediates.

Checking starting materials is the first necessary step before starting the experiments, because it is of principal importance to know the exact composition of chemical system put into a reaction vessel. It is commonly accepted among the organic chemists to check starting materials by 1D NMR spectra, however, in many cases, sensitivity of NMR is not enough to detect trace impurities.

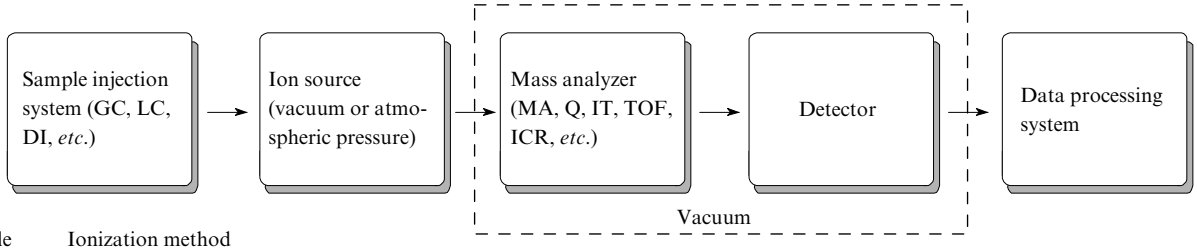
A representative example from our recent experience would involve atom-economic catalytic C – P bond formation.[16, 17] While working with H-phosphonates in our group, we usually check them by $^{1}H$ and $^{31}P\{^{1}H\}$ NMR. Before starting mechanistic investigations with commercially available diisopropyl H-phosphonate, $(Pr^{i}O)_2P(O)H$, we have checked it with ESI-MS as well. In addition to $(Pr^{i}O)_2P(O)H$, two more compounds: $(Pr^{i}O)(HO)P(O)H$ and $(HO)_2P(O)H$ were revealed in the mass spectrum although there was complete purity according to the $^{31}P\{^{1}H\}$ NMR spectrum.[18]

In this field of chemistry, it is well known that the presence of impurities even at trace levels can inhibit a target reaction. Impurities may cause degradation of catalyst and other difficulties, especially, concerning identification of active intermediates with concentrations comparable with (or less than) to the concentrations of impurities. As it can obviously be concluded, mass spectrometry may give an answer to frequently raised question: why the same reaction proceeds with different efficiency for starting materials from different commercial sources and even for different batches from the same supplier. Careful verification of purity of the starting materials should be carried out using both NMR and MS.

Particularly important is to evaluate the purity of isolated products by using mass spectrometry together with NMR. MS is essential as a rapid method for screening of small amounts of species giving no signals in $^{1}H$ and $^{13}C$ NMR spectra (metal compounds, salts, inorganic additives, *etc*.). Such impurities may be difficult to detect by routine NMR analysis.

Finally, reaction monitoring is the main tool for mechanistic studies and we will concentrate our attention on this topic within the present review. This research topic clearly shows that MS gives deep insight into mechanistic details during the course of the reaction.

MS analysis can be applied to samples in any aggregate state: gas, liquid (solution) or solid by selecting appropriate ionization method (Fig. 1). In this article we discuss a few representative examples of MS analysis suitable for reaction monitoring in the frameworks of gaseous, liquid and solid chemical systems.




| Sample | Ionization method |
|---|---|
| Gaseous | EI, CI, *etc.* |
| Liquid | ESI, APCI, *etc.* |
| Solid | MALDI, FAB, *etc.* |

**Figure 1.** Simplified representation of molecule/ion transfer in MS analysis.
GC is gas chromatograph, LC is liquid chromatograph, DI is direct infusion, MA is magnetic analyzer, Q is quadrupole, IT is ion trap, TOF is time-of-flight analyzer, ICR is ion cyclotron resonance mass analyzer; EI, CI, ESI, APCI, MALDI, FAB, see in text.

Understanding reaction mechanisms is always the most intriguing issue, and information about intermediates is a highly valuable target in this regard. Literature examples demonstrate that MS analysis of liquid systems (solutions) was mainly performed for probing intermediates of different reactions. Indeed, widely used EI (electron impact) to analyze gaseous systems is a 'hard' method that causes extensive but uncontrollable fragmentation; another method for gaseous system analysis, CI (chemical ionization), is 'softer' but works due to ion-molecular reactions between neutral analyte molecules and ions of reagent gas (methane, hydrogen, isobutane, ammonia, dimethyl ether, benzene *etc.*). In the case of methods for solid samples in MS analysis [*e.g.* MALDI (matrix-assisted laser desorption ionization), FAB (fast atom bombardment)], auxiliary substances (matrices) are required, *e.g.*, α-cyano-4-hydroxycinnamic acid, 2,5-dihydroxybenzoic acid, 5-chlorosalicylic acid, glycerol, *m*-nitrobenzyl alcohol, *etc.* The choice of the matrix demands special attention and sample preparation needs dedicated efforts.

In mechanistic investigations, quick data acquisition of the analytical procedure applied is of key importance. In addition, extensive fragmentation of unstable intermediates should be avoided, and their reactions with auxiliary substances (reagent gas ions or matrices) can complicate interpretation of spectral information.

In contrast to gaseous and solid systems, MS analysis of liquid systems allows transferring of intact molecules (and intermediates, if present) directly to mass analysis step without uncontrolled fragmentation and avoiding auxiliary substances. The main ionization techniques widely used for analysis of liquid chemical systems involve ESI (electrospray ionization), APCI (atmospheric pressure chemical ionization) and APPI (atmospheric pressure photoionization).

Herein, gaseous and solid chemical systems are discussed together in Section III.1 and special attention is paid to liquid chemical systems described in Section IV.1.

## 2. Applications of NMR spectroscopy in organic chemistry

Nuclear magnetic resonance spectroscopy (NMR) is a proven analytical method in organic chemistry. Fast development of NMR hardware, improvement of computational methods, and use of new materials and technologies expanded the scope of NMR analysis significantly over the last decades. However, in the terms of routine organic chemistry applications, most methodological developments have involved the application of NMR to the study of isotropic liquids and solutions. Simultaneous development of the method took place for gaseous and solid states of matter, though less commonly applied to laboratory practice in organic synthesis. The main reason that little attention was paid to these applications is the broadening of NMR resonances in the solid or gas phase, which complicates interpretation and hides characteristic line shape of individual peaks.

Extreme broadening of signals in the solid state is caused primarily by chemical shift anisotropy (CSA), direct dipole–dipole and quadrupole interactions (for spins with $I > 1/2$).[19–22] Special techniques, like fast rotation of the sample at so called magic angle, are required for narrowing the signals in the solid state spectra. In the case of gas and liquid samples, these effects are averaged by Brownian molecular motion.

In gaseous samples line widths of peaks can reach hundreds of Hz, because relaxation *via* intramolecular dipole–dipole mechanisms can be very effective.[23,24] At the same time, gas phase NMR has poor sensitivity due to low concentrations of compounds in the gas phase, although rapid relaxation may help to acquire spectra fast enough in some cases.

The main areas of application of NMR in the organic chemistry include:

— Verification of molecular structure of known compounds together with determination of purity.

— Structure elucidation of unknown compounds and revealing of stereochemical properties.

— Study of molecular dynamics, determination of conformation changes, inversion and rotation barriers, thermodynamic parameters.

— Reaction monitoring, on-line control of yield and selectivity, measuring kinetics and *in situ* investigations of catalytic systems.

— Detailed analysis of mixtures, especially for natural products.

A valuable benefit of NMR spectroscopy is the absence of sample destruction during the experiment (*i.e.* non-destructive analysis). The principle of NMR involves inter-

action of radio frequency with nuclei of studied sample in strong and highly homogeneous magnetic field. The most sensitive and most convenient nucleus for organic chemistry applications is proton, so the vast majority of NMR experiments is performed by observing $^{1}H$ signals. All other atomic nuclei present in organic molecules can be divided into three groups: very common to NMR analysis, rarely used and NMR-inactive. The first group includes nuclei with high natural abundance, good relative sensitivity and narrow spectral lines, which makes their observation very practical using conventional procedures ($^{2}H$ in labelled compounds, $^{7}Li$, $^{11}B$, $^{14}N$ for $NO_2$ and $NR_4^+$ groups, $^{19}F$, $^{27}Al$, $^{29}Si$, $^{31}P$, $^{77}Se$, $^{119}Sn$, $^{195}Pt$). Although less sensitive, $^{13}C$ NMR is also a common choice owing to great structure elucidation potential in organic chemistry. Rarely used nuclei have lower sensitivity, lower natural abundance, or quadrupolar nature: $^{2}H$ and $^{15}N$, $^{17}O$, $^{33}S$, $^{35/37}Cl$, $^{77/79}Br$, *etc*. Acquisition of NMR spectra on these nuclei usually requires a larger amount of sample and longer experimental time. Nevertheless, modern detection methods allow observation of such 'difficult' nuclei and avoiding several limitations. For example, $^{15}N$ at natural abundance can be observed using indirect methods with up to 300 times higher sensitivity.[25] Unfortunately, several elements do not have magnetically active isotopes, thus measuring spectral data is impossible. For instance, NMR-inactive nuclei include Pd, which is very important for catalysis, and some lanthanides and actinides.

The major observable parameters in NMR spectra are chemical shifts of the signals, their integral intensities, multiplicity patterns and relaxation rates. Chemical shift represents a variation of nucleus resonant frequency depending on the chemical environment. Chemical shift is directly associated with position of certain atom in the molecule and intramolecular connection to functional group(s). It is important to mention that chemical shifts are hardware-independent reproducible parameters, which can be estimated by quantum chemistry calculations[26] or additive schemes[27] with a good precision. Modern commercially available databases and spectra prediction software packages are helpful in verification and identification of many types of organic molecules.

The quantitative measure in NMR spectroscopy is provided by integral intensity of certain signals, which is proportional to the number of resonating atoms (nuclei). It is really hard to overestimate the role of quantification and quality control by NMR. Simple spectral analysis and easy sample preparation makes identification and sample purity analysis possible in automated manner. Modern NMR instruments are capable of measuring micrograms of sample making the observation of minor compounds feasible.

Spin–spin couplings are determined by the number of bonds between interacting atoms, plain and dihedral angles and properties of neighbouring atoms (like electronegativity, hybridization, *etc*.). The signals of spin-coupled nuclei are represented by splitted lines such as doublets, triplets and more complex multiplets, where the overall multiplet structure depends on the number of interacting atoms, their spin numbers, symmetry of molecule and coupling constant values. Analysis of spin–spin coupling data is of principal importance to determine structures, stereochemistry, three-dimensional molecular arrangement and dynamical behaviour. Relaxation times $T_1$ and $T_2$ depend on the origin of object, temperature, viscosity and, sometimes, on spectrometer's magnetic field strengths. The knowledge of $T_1$ and $T_2$ values is necessary for proper setting up of the NMR experiment.[28]

The structure of complex molecules and composition of chemical systems often cannot be established using only simple 1D NMR spectra because of strong overlap of signals. Two-dimensional NMR methods allow fast and reliable structure elucidation as well as simplification of spectral assignment.[28] 2D NMR provides the information about connectivity between different atoms through scalar couplings or spatial (nuclear Overhauser effect, NOE) interactions in a clear and descriptive way.

### 3. Applications of electron microscopy in organic chemistry

In the recent decades, rapid development of nanotechnology, nanocatalysis and material science changed the concept of routinely used structure investigation methods. Nowadays, high resolution electron microscopy became a widely-utilized tool among 'classical' chemistry applications. Unlike NMR spectroscopy and MS, electron microscopy often does not require special skills to interpret the results at a first glance. Microscopy images provide structural information with direct visualization of the studied objects. Modern instruments with high lateral resolution [1 nm for the scanning electron microscopes (SEM) and 1 angstrom for the transmission electron microscopes (TEM)] can be used to investigate various objects with a wide range of sizes. However, it should be noted that image quality and instrument performance do strongly depend on the sample. Sample preparation for electron microscopy is a much more challenging task compared to NMR and MS. The operating principle of electron microscopy is the analysis of the signals produced from the interaction of the electron beam with the sample.[29, 30] In order to eliminate possible distortions of the electron trajectories, all measurements must be carried out in a high vacuum, thus several limitations and restrictions on sample types should be considered.

## III. Gas-phase chemical systems

Gas-phase reactions can be divided into two major groups: those which include only gaseous reactants and those proceeding on the surface of a solid metal catalyst.[31] In general, the latter are large-scale industrial processes such as pyrolysis,[32] hydration,[33] oxidation,[34–36] and epoxidation[37] of hydrocarbons and Fischer–Tropsch synthesis.[38] In addition, investigation of metal-catalyzed C–H and N–H bond activation is of great importance due to utilization in methane conversion,[39] hydroamination of olefins, oxidative amination of arenes and C–N cross-coupling with ammonia.[40] During the last decades, tremendous growth of studies concerning gas-phase preparation of nanomaterials has taken place. Flash vacuum pyrolysis and shock wave pyrolysis are used to obtain nanostructured chalcogen-containing materials and films from organic selenides and tellurides,[41] as well as carbon nanoparticles[42] and nanotubes.[43] Another area of investigation of gas-phase reactions is mass-spectrometric studies of structure, dynamics and reactivity of stable and unstable molecules and ions including metal complexes[44–48] and ionized fullerenes[49] and cycloaddition reactions between neutral or ionized molecules[50–53] that are suitable to detect elementary reaction steps. Investigation of gas-phase photodissociation reactions of simple molecules gives valuable information

about main thermodynamic and electronic properties and reaction mechanisms,[54] besides it has found practical utilization in analyzing and modelling of the reactions of simple molecules in the atmosphere[55] and interstellar medium.[56]

## 1. Mass spectrometry of gaseous samples

Fourier transform ion cyclotron resonance mass spectrometry (FTICR-MS) and high-pressure mass spectrometry (HPMS) are powerful tools in the field of gas-phase ion chemistry, the topics were reviewed in details by Wu and McMahon.[57] Many experimental methods and instrumental developments based on FTICR-MS and HPMS, including the coupling of a high-pressure external ion source to a FTICR mass spectrometer, were listed. HPMS instruments equipped with electron gun operate as CI with different reagent gases, providing formation of both positive and negative ions.[57] A number of applications of HPMS for gas-phase MS analysis, such as gas-phase acidities, proton and metal cation affinities were also described. HPMS was shown to be well-suited for monitoring gas-phase $S_N2$ reactions.[57]

Various charge states of the buckminsterfullerene $C_{60}$ became available by conventional EI of the compound vapour, thus allowing mass-spectrometric study of the ion $C_{60}^{n+}$ reactivity to be carried out.[49] Generation of singly and multiply charged fullerene cations under EI conditions and MS investigations of their reactivity including reactions of $C_{60}^{+}$, $C_{60}^{2+}$ and $C_{60}^{3+}$ with H atoms, ammonia, aliphatic amines, nitrogen heterocycles, nitriles, water, alcohols, ethers, aldehydes, ketones, *etc*. were reviewed by Bohme.[49] Another interesting example of EI-MS study of $C_{60}$ and $C_{70}$ fullerene reactivity was demonstrated later.[58] The reactions of $C_{60}$ with organo- and organoelement mercury derivatives [$CF_3HgBr$, PhHgBr, *p*-$CH_3C_6H_4HgBr$, *p*-$CH_3OC_6H_4HgCl$, $CF_3HgPh$, $Ph_2Hg$, (*o*-carboran-9-yl)$_2$Hg, (*m*-carboran-9-yl)$_2$Hg, (*p*-carboran-9-yl)$_2$Hg and (*m*-carboran-9-yl)HgCl] in the ionization chamber (IC) of the EI ion source of a mass spectrometer at 250–300 °C results in the transfer of the corresponding organic or organoelement radicals from the mercury species to the fullerene. Some of the processes are accompanied by hydrogen addition (Fig. 2).[58]

$C_{70}$ reacts with $Ph_2Hg$ and (*o*-carboran-9-yl)$_2$Hg at 300 °C in a similar fashion. A homolytic reaction path is considered for the reactions. MS study indicated both the thermal and EI initiated homolytic dissociation of the mercurials to the intermediate organic or organoelement radicals followed by their interaction with the fullerenes at the metallic walls of the IC.[58] There is also another example of a comparative study of homolytic reactions of fullerenes with aldehydes (RCHO: R = Ph, *p*-$FC_6H_4$, $F_5C_6$, *p*-$MeOC_6H_4$, α-thienyl, *etc*.) in a mass spectrometer under EI and in solution under UV irradiation.[59]

The tautomerism of substituted 2-phenacylquinolines (**1a**–**h**) was studied by EI-MS.[60] The EI mass spectra of eight 2-phenacylquinolines (ketimine form) were recorded at 70 eV in order to determine the fragmentation routes and to check the presence of their enaminone tautomers, (*Z*)-2-benzoylmethylene-1,2-dihydroquinolines, in the gas phase.

Detailed analysis of observed fragmentation pathways was performed (Fig. 3).[60] The relative abundances or total ion currents of some ions correlated with the Hammett substituent constants and Hammett–Brown constants. The product ions $[M-CO]^{+\bullet}$ and $[M-HCO]^{+}$ were also observed (see Fig. 3). A mechanism of formation of these ions was suggested based on collected set of EI-MS data.[60] A key feature of the mechanism was the involvement of skeletal rearrangements. The results furnish important information relating to tautomerism in the gas phase.[60]

The GC-EI-MS technique together with NMR were successfully utilized for identifying 4,5-indandiol as indan metabolite *via* its aromatic hydroxylation with *Rhodococcus* sp. strain DK17.[61]

Ion-molecular reactions between various organic compounds and the electron-deficient reagent ion $CCl_3^+$, generated by using tetrachloromethane as the reagent gas, were studied by GC-ITMS (ITMS is ion trap mass spectrometry) equipped with hybrid (positive and negative CI) ionization source.[62] The ion-molecular reactions of aromatic hydrocarbons, aliphatic ketones and alcohol derivatives with the reagent ion $CCl_3^+$ were investigated and the mechanisms were proposed according to the information provided by MS/MS experiments and theoretical calculations. The method was then successfully applied to study volatile organic compounds in *Dendranthema indicum* var. *aromaticum* and 20 compounds including monoterpenes and their oxygen-containing derivatives, aromatic hydrocarbons and sesquiterpenes were identified using such ion-molecular reactions. Therefore, the study offers a useful tool for the analysis and identification of various volatile compounds.[62]

A very interesting example of gaseous mixture investigation by APCI-MS was recently published.[63] The authors observed ion-molecular non-dissociative charge transfer reaction according to Eqn (1) upon introducing a $CF_2Br_2$/

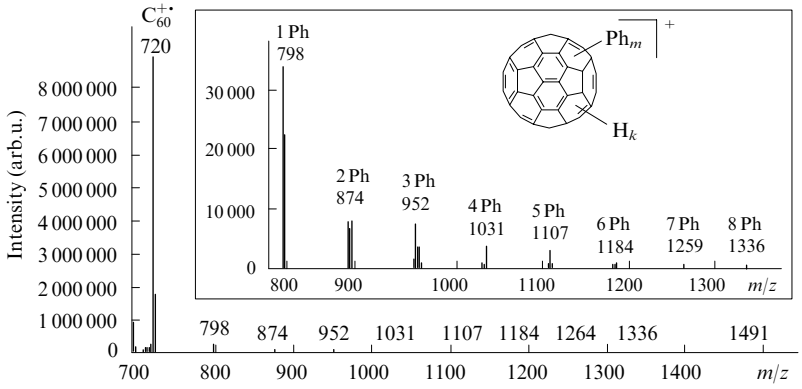



**Figure 2.** High mass region of the mass spectrum recorded during the reaction of $C_{60}$ with $Ph_2Hg$ in the IC at 70 eV and 270 °C (for simplicity of the spectrum, the background peaks are omitted).[58]

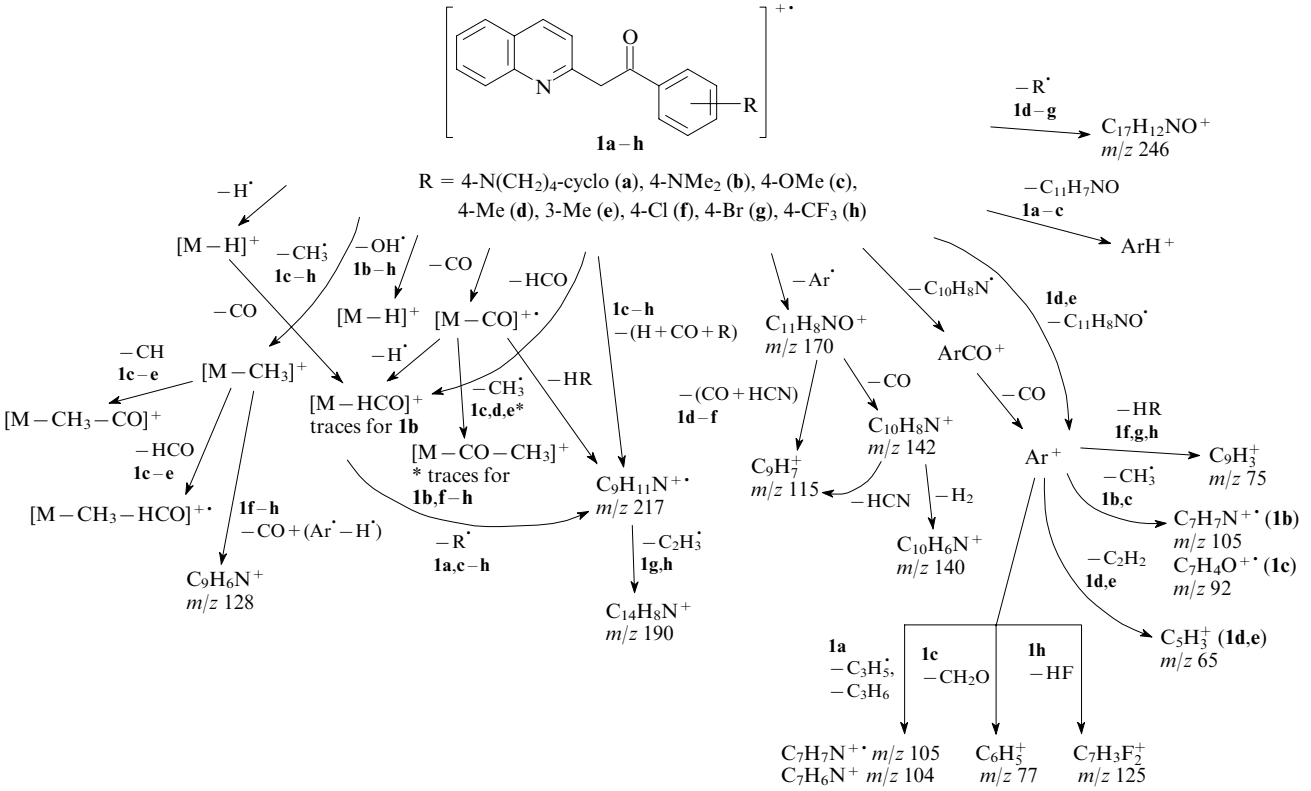



**Figure 3.** Typical fragmentation pathways in 70 eV mass spectra of 2-phenacylquinolines **1a**–**h**.[60]

air mixture into the APCI ion source. The obtained negative ion mass spectra are presented in Fig. 4.[63]

$$CF_2Br_2 + O_2^- \longrightarrow CF_2Br_2^- + O_2 \quad (1)$$

The signal of $CF_2Br_2^-$ ion ($m/z = 210$) together with other signals, including ion-molecular complexes, such as $O_3^-(CF_2Br_2)$ and $Br^-(CF_2Br_2)$ were well observed (Fig. 4). This fact clearly shows how APCI, which is known to be well-suited for HPLC and operates with liquid flows ($CH_3CN$, MeOH, *etc.*), can also work with gases (as in the case of classical CI). In the above example $O_2$ from air serves as a reagent gas.

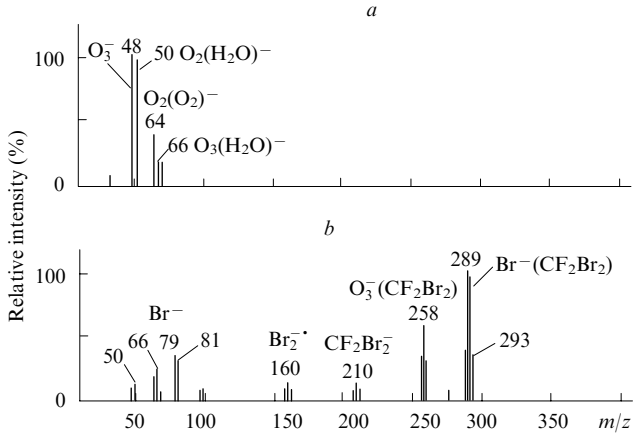



**Figure 4.** Negative ion APCI mass spectra obtained at 30 °C with air (background) (*a*) and $CF_2Br_2$ in air (*b*).[63]

Indeed, the protocol above[63] is one of the representative examples. All three ion sources, ESI, APCI and APPI, which were initially intended for liquid samples (DI-MS, LC-MS), were successfully coupled with GC.[64–68] The possibility of such coupling already led to creation of the MS instruments with rapidly switchable LC/GC flows connected to the same ion source.

The gas phase kinetic measurements for reactions of three deuterated toluenes ($C_6H_5-CD_3$, $C_6D_5-CH_3$, $C_6D_5-CD_3$) with hydroxyl radicals were performed within 298–353K temperature range using MS technique with mass spectrometer operating in the SIM (selected ion monitoring) mode.[69] The experiments were conducted in cylindrical quartz reaction chamber located in the oven of the GC (to provide temperature control) and interfaced to a quadrupole MS instrument with EI ion source. This on-line MS monitoring system was effective to control disappearance of reactants and demonstrated high time resolution, resulting in the large amount of collected data used for the determination of the Arrhenius parameters. The following Arrhenius expressions were elucidated for these reactions ($cm^3$ molecule$^{-1}$ $s^{-1}$):

$$\text{toluene-d}_3 \quad k = (6.42^{+1.17}_{-0.99}) \times 10^{-13} \exp[(661 \pm 54)/T]$$

$$\text{toluene-d}_5 \quad k = (2.11^{+1.03}_{-0.69}) \times 10^{-12} \exp[(287 \pm 128)/T]$$

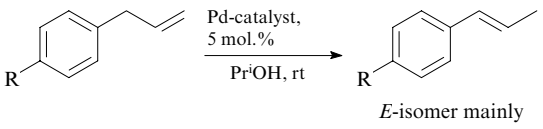
$$\text{toluene-d}_8 \quad k = (1.40^{+0.44}_{-0.33}) \times 10^{-12} \exp[(404 \pm 88)/T]$$

Yet example of gas-phase kinetic investigations utilizing MS methodology was recently published.[70] The authors successfully applied GC-MS operating with EI and CI

(both positive and negative) to monitor the reactions of 2-butoxyethanol and benzyl alcohol with the nitrate radical. Gas-phase products were identified and rate coefficients of the reactions were measured. Based on the obtained MS data the mechanisms of formation of the observed products were proposed.[70]

The GC-EI-MS monitoring of reaction progress and product formation was utilized for mechanistic studies of Pd(II)-catalyzed selective isomerization of allylbenzenes (Scheme 1).[71] The characteristic key fragments of the deuterated starting material and the products were identified (see Scheme 1 and Fig. 5).[71] The study allowed clear differentiation as to whether or not deuterium has incorporated at C(2). Even though starting materials and products exhibit the same molecular ion in the higher mass region and benzyl fragmentation in the lower mass region, the initial fragmentation of 1,1-$D_2$-prop-1-en-3-ylbenzene generates a fragment with $m/z = 104.1$ by loss of the $d_2$-methylene group whereas $m/z = 103.1$ is expected for the product, regardless of isomer configuration ($E/Z$).

Scheme 1




R = OH, OMe, $CF_3$

This fragment originates from α-methyl cleavage of the terminal methyl group within the product. Contrary to this, $m/z = 104.1$ was detected for the initial fragment of the *E*- and the *Z*-product, which clearly demonstrated deuterium incorporation at the C(2) position of propenylbenzene (see Fig. 5). Based on the obtained MS data together with kinetic measurements, the mechanism of Pd-catalyzed isomerization of allylbenzenes *via* a hydride addition–elimination starting with palladium hydride species generated *in situ* was proposed.[71]

A unique GC-Cold EI-MS technique was presented as being promising for monitoring of various organic reactions, mechanism elucidation and identification of the reaction products.[72] This technique allows an effective rapid analysis (Fig. 6) of crudes and enhances molecular ion peak compared to standard GC-EI-MS.[72]

Detailed mass spectrometric study of combustion of isomeric butenes,[73] isomeric butanols,[74] and morpholine[75] was performed using GC-EI-molecular-beam-MS (GC-EI-MBMS) and EI-MBMS. The experimental data showed different destruction pathways for the three butene isomers (but-1-ene, *trans*-but-2-ene and isobutene). By applying low nominal electron energies of 10.6, 12.0 and 13.4 eV, the authors were able to detect intermediate species and 18.0 eV were applied for detection/determination of major species. The destruction pathways of the butenes and the products formed were described in detail.[73] In the case of isomeric butanols, high mass-resolution EI-MBMS also provided the exact elementary composition of the combustion intermediates.[74]

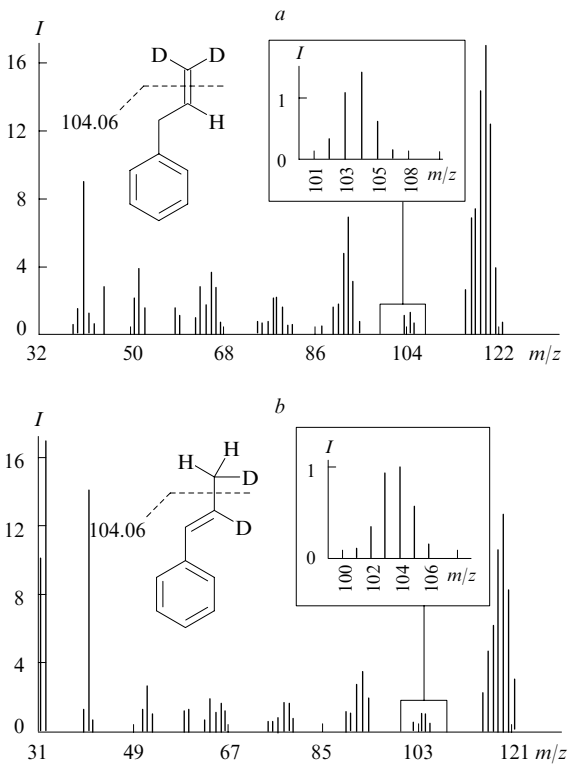



**Figure 5.** Mass spectra showing the characteristic fragments of 1,1-$D_2$-prop-1-en-3-ylbenzene (*a*) and 2,3-$D_2$-(*E*)-prop-1-en-1-ylbenzene (*b*).[71]
*I* is relative intensity ($10^4$ arb.u.)

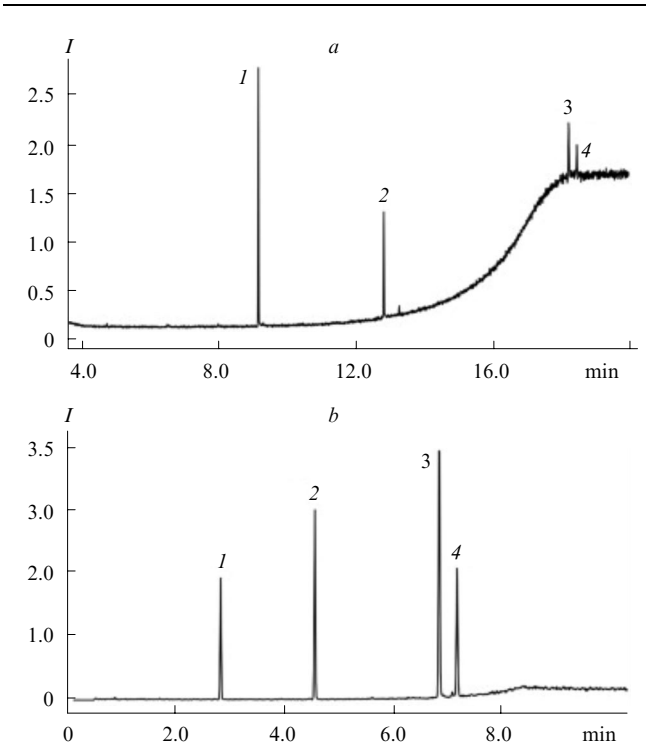
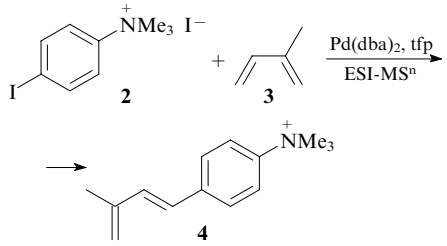



**Figure 6.** Analysis of a mixture of n-$C_{16}H_{34}$ (*1*), methyl stearate (*2*), cholesterol (*3*) and n-$C_{32}H_{66}$ (*4*) at about 0.25 ng on-column amount with standard GC-EI-MS (*a*) and GC-Cold EI-MS (*b*).[72]
*I* is relative intensity ($10^6$ arb.u.)

A few more vivid examples were recently published: EI and APCI to study the kinetics of gas phase C – H activation of the halomethanes $CH_2F_2$ and $CH_2Cl_2$,[76] GC-EI-MS in the SIM mode for analysis of cypermethrin residues and main degradation products,[77] and *de novo* analysis of EI mass spectra: the automated fragmentation analysis of high resolution EI mass spectra based on a fragmentation tree algorithm.[78]

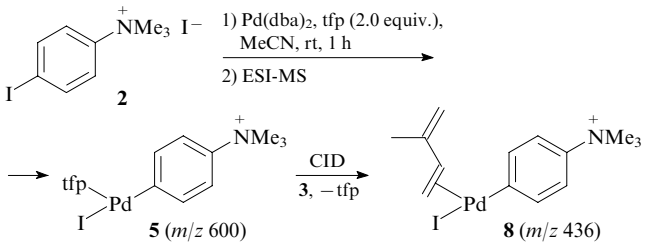
On-line MS monitoring with two independent gas (vaporized olefin) and liquid (acetonitrile solution of Pd catalyst and aryl iodide) flows was utilized for examination of the Heck reaction mechanism in the gas phase by ion-molecular reactions.[79] The hybrid MS instrument equipped with an ESI ion source, linear ion trap (LTQ), octapole collision cell (HCD cell †), and an Orbitrap mass analyzer was used to perform and monitor the gas phase Heck reaction of (*p*-iodophenyl)-trimethylammonium iodide (**2**) with isoprene (**3**) leading to formation of product (**4**) (Scheme 2).

Scheme 2




To provide isoprene **3** for gas-phase ion-molecular reactions, the vaporized olefin was introduced *via* the nitrogen bath gas of the HCD cell using a small (250 ml) stainless steel autoclave which was furnished with the reagent **3** and put between the nitrogen source and the gas inlet.[79] First, the oxidative addition of aryl iodide **2** to bis(dibenzylideneacetone) palladium [$Pd(dba)_2$] in the presence of tri(2-furyl)phosphine (tfp) was examined in acetonitrile solution by introducing the solution through ESI source (Scheme 3).

Scheme 3




The respective mass spectrum exhibited the signal for product of oxidative addition, cation **5** ($m/z$ 600) with prominent abundance. This ion was selected for LTQ-$MS^2$ experiments and the characteristic fragment ions formed upon CID (collision induced dissociation) (**6** and **7**) apparently supported the structure assignment for the Pd complex ion **5** (Fig. 7 *a*).[79] After introducing gaseous isoprene into the instrument *via* the collision gas inlet of the HCD cell, the mass spectrum substantially changed after a delay time of some minutes. Isoprene adduct ions **8** and **9** of complex ions **6** and **7** (see Scheme 3) were formed in the gas phase by reactive collisions and can be found in the mass spectrum with $m/z$ 436 and $m/z$ 474, respectively (characteristic mass shift $\Delta m$ = 68 Da) (Fig. 7 *b*).

Upon activation of complex ion **8** ($m/z$ 436) in a similar LTQ-$MS^3$ experiment, fragment cation **4** ($m/z$ 202), which corresponds to the product of Heck reaction between **2** and **3**, was detected (see Schemes 2 and 4).

The described example representatively shows how mass spectrometer equipped with a typical 'liquid' ion source, such as ESI, can operate with gas through independent flow allowing gas-phase ion-molecular reactions to be carried

† High-energy Collisional Dissociation.

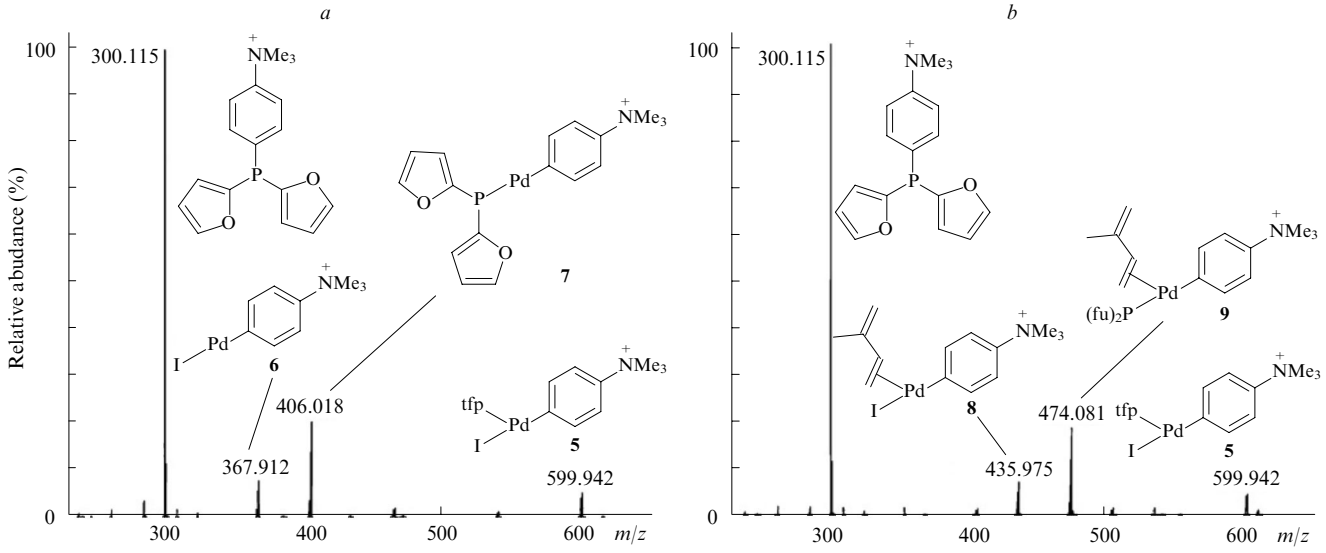
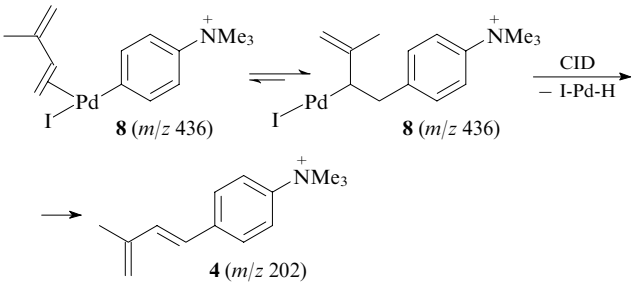



**Figure 7.** Representative mass spectra obtained during on-line MS monitoring of the Heck reaction with two independent flows, a gas (vaporized olefin **3**) and a liquid (acetonitrile solution of Pd catalyst and aryl iodide **2**) flow: product ion spectra of Pd complex ion **5** ($m/z$ 600) in the absence (*a*) and in the presence (*b*) of gaseous isoprene **3**.[79]
fu is 2-furyl.

Scheme 4

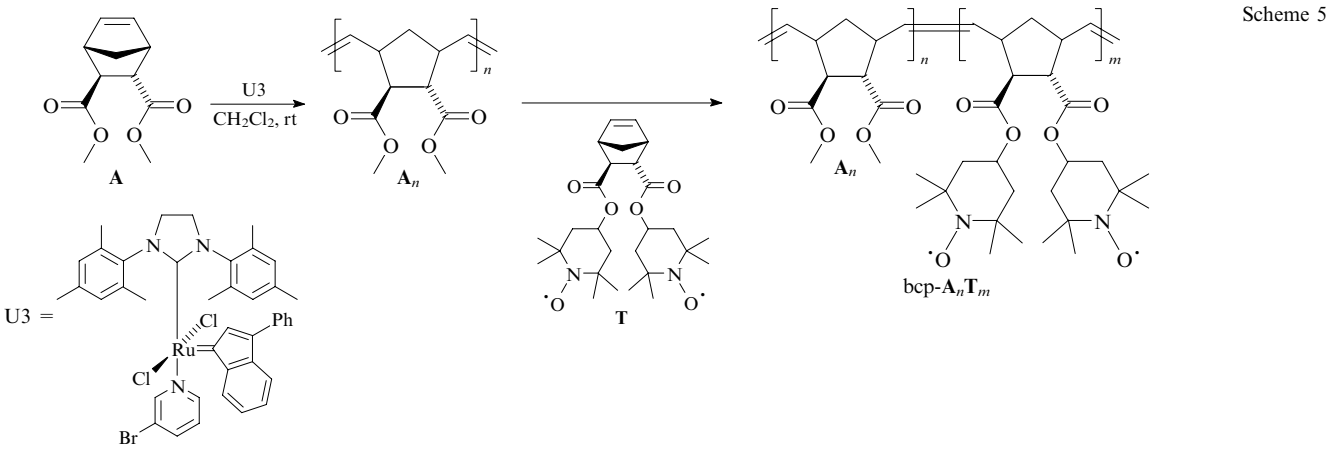



out. Another good demonstration of ambient version of ESI for on-line characterization of particles and gases was presented.[80] It should be emphasized that ambient ionization is an advanced method for rapid, high throughput MS analysis with little or no sample pretreatment — essential requirement when dealing with mechanistic investigations. Different ambient ionization techniques suitable for analysis of gaseous, liquid and solid samples are listed and well described in a detailed tutorial article[81] and recent thorough reviews,[82, 83] mainly devoted to reaction monitoring by ambient MS techniques.

Undoubtedly, side by side with other MS techniques, modern rapidly developing tools for MS analysis of solid samples, such as MALDI, greatly contribute to the progress of chemical science. Indeed, analysis of peptides, proteins, lipids, nucleic acids, together with non-biological polymers and other high-molecular-weight objects became easily available due to MALDI-MS since its discovery by Tanaka in the 1980s.[84–91]

The block copolymerization of two structurally different norbornene monomers **A** and **T** catalyzed by Umicore type initiator U3 was investigated using MALDI-MS and NMR (Scheme 5).[92] Initially, the authors demonstrated that homopolymer $\mathbf{A}_{25}$ can be effectively desorbed in MALDI, yielding the respective $\mathbf{A}_n\mathrm{Na}^+$-ions as a pure series (Fig. 8 *a*). Thus the homopolymer $\mathbf{A}_n$ could serve as a molecular probe for the subsequent desorption of the individual $\mathbf{A}_n\mathbf{T}_m$ species. Afterwards MALDI-MS was applied to block copolymer bcp-$\mathbf{A}_{25}\mathbf{T}_{25}$ in order to check for the presence of residual homopolymer $\mathbf{A}_{25}$ in the polymer mixture. No residual $\mathbf{A}_{25}$ was detected in the mixture showing a complete crossover reaction after the addition of 25 equivalents of the second monomer **T** (Fig. 8 *b*).[92]

Scheme 5



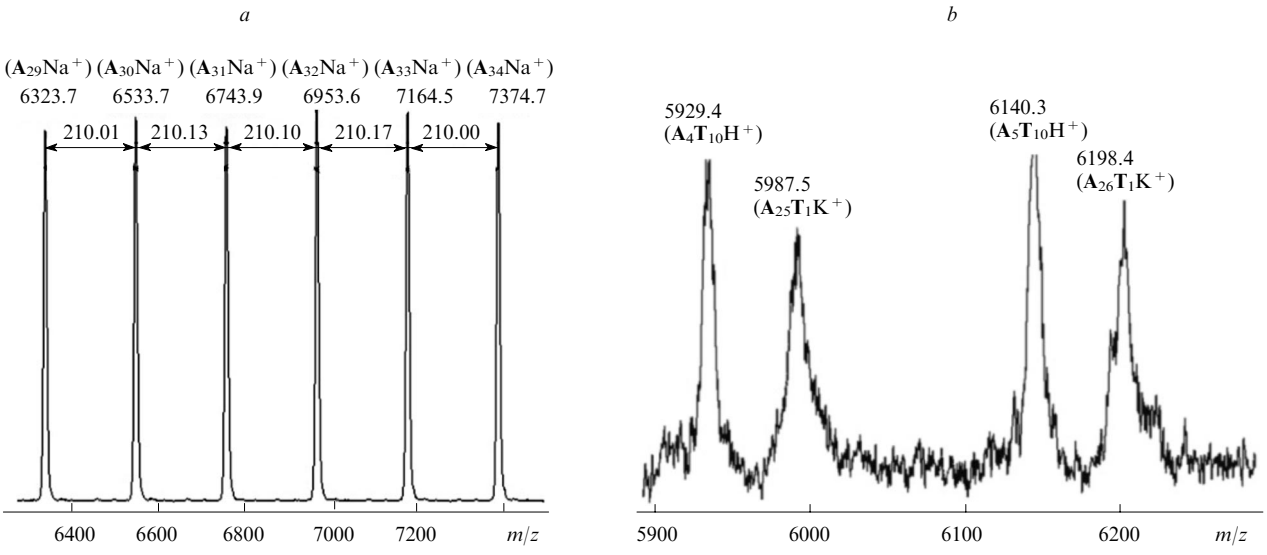




**Figure 8.** Expansion of MALDI-TOF mass spectra of homopolymer $\mathbf{A_{25}}$ (*a*) and bcp-$\mathbf{A_{25}T_{25}}$ (*b*) synthesized with U3 catalyst.[92]

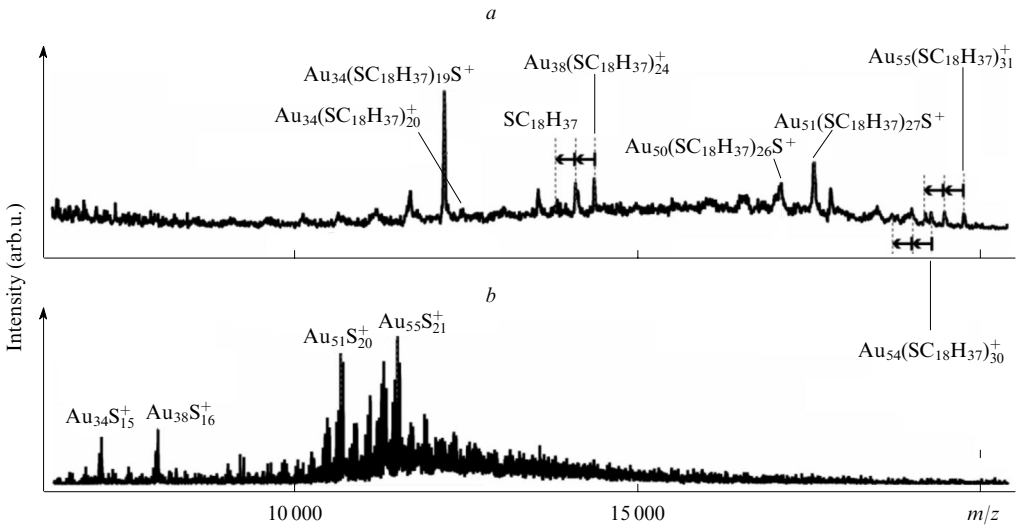
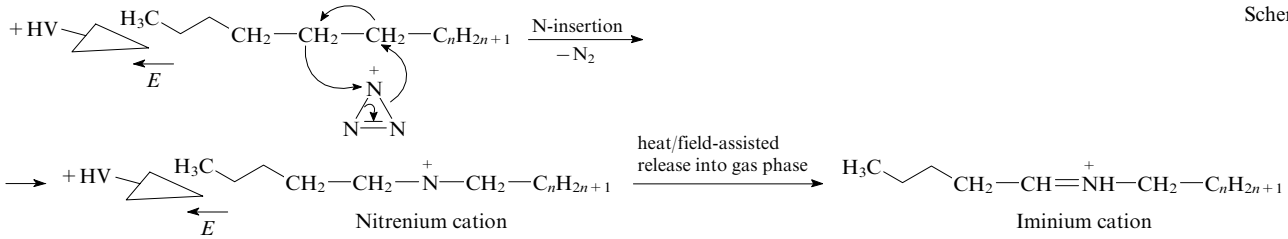



**Figure 9.** Assignment of positive-ion MALDI mass spectra of 11 kDa $Au_n(SC_{18}H_{37})_m$ clusters recorded at low (*a*) and high (*b*) laser power.[96]

Scheme 6




Similar example of the crossover reaction of various monomers in presence of the Grubbs type catalysts G1 – G3 was studied in detail by MALDI-MS as well as other mechanistic investigations *via* MALDI-MS of oligomers were also recently published.[93 – 95]

Another example of MALDI-MS efficiency towards non-biological high-molecular-weight compounds is related to metal clusters. Nowadays metal clusters play outstanding role in catalysis and their catalytic activity mostly depends on size and morphology. Therefore, information about cluster molecular weight plays a crucial role for the development and optimization of catalytic reactions and MALDI-MS provides easy access to this information.

The 11 kDa core mass $Au_n(SC_{18}H_{37})_m$ clusters were synthesized in the reaction of Au clusters stabilized by poly(*N*-vinyl-2-pyrrolidone) with n-$C_{18}H_{37}SH$.[96] Based on MALDI-MS spectra recorded with different laser power, it was possible to identify the synthesized clusters as a mixture of $Au_{54}(SC_{18}H_{37})_{30}$, $Au_{55}(SC_{18}H_{37})_{31}$ and $Au_{38}(SC_{18}H_{37})_{24}$ (Fig. 9).[96] There are also other studies brightly illustrating the performance of combined application of MALDI and ESI for comprehensive characterization of Au clusters.[97, 98]

An unconventional and promising MS method for exploring carbon – carbon bond activation in solid saturated hydrocarbons was recently presented by Cooks and co-workers.[99] Insertion of atomic nitrogen ion into C – C bonds of large n-alkanes was successfully carried out. The model n-$C_{60}H_{122}$ alkane was deposited as a thin film onto the tip of a triangular filter paper and the experiment was performed in an $N_2$ atmosphere in an isolated chamber used for APCI electrically heated to 150 – 400 °C, with a potential of 5 – 6 kV applied to paper substrate (HV in Scheme 6) on the tip of which the sample had been deposited.[99] The cations leaving the paper were either deposited on a surface and analyzed independently or transferred into the vacuum system of a mass spectrometer for on-line analysis. The proposed tentative mechanism of nitrogen insertion into alkanes and a representative mass spectrum thus obtained are presented (Scheme 6, Fig. 10).[99] The mass spectrum dominated by the ion $[M+N]^+$ where M is the alkane

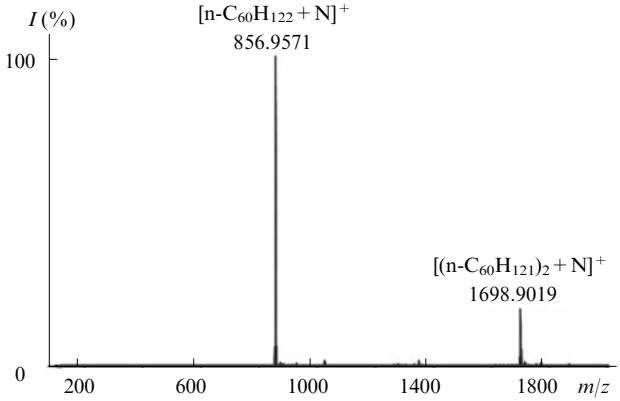



**Figure 10.** Mass spectrum obtained in the model experiment of nitrogen insertion into the C – C bond of n-$C_{60}H_{122}$ alkane.[99]

(verified by exact mass measurements). A minor product corresponded to the dimeric species $[2M+N-2H]^+$. Nitrogen incorporation was observed for the $C_{31}$, $C_{35}$, $C_{40}$, $C_{41}$, $C_{46}$ and $C_{50}$ n-alkanes as well.[99]

The authors cited provide detailed description of on-line MS monitoring, nanoESI and $MS^n$ experiments.[99] It should be pointed out that the discussed example is not only a metal-free alkane transformation but also the onset of a new approach for MS analysis of petroleum products.[99]

Briefly summing up, there is a number of MS techniques (ionization methods) for analysis of gaseous and solid chemical systems. These techniques are complementary and the choice depends on the properties of compound (or mixture) to be analyzed: molecular weight, polarity, reactivity in ion-molecular reactions, *etc*. Some of the techniques work with the solid phase only (*e.g*. MALDI), some are applicable to gaseous and solid samples (*e.g*. EI), some of them are 'hard' (*e.g*., EI), some other are 'soft(er)' (*e.g*., MALDI, CI, APCI), certain methods operate in a vacuum (*e.g*., EI, CI, MALDI), other methods are used under atmospheric pressure (AP version of MALDI, APCI). The methods which are able to operate with gases (*e.g*., EI, CI, APCI) can be easily coupled with GC allowing analysis of complex mixtures. However, despite the large number of achievements in the field of gas- and solid-phase MS, organic reactions mainly take place in liquid phase. The MS analysis of liquid chemical systems is discussed at the section IV.1 of the review.

## 2. NMR spectroscopy of gaseous samples

As it was mentioned above, gas phase NMR has poor sensitivity due to low concentrations of compounds in the gas phase; however, rapid relaxation helps to acquire spectra fast enough. On the other hand, rapid nuclei relaxation leads to broad signals (sometimes hundreds of Hz) in gas spectra, which hides characteristic line shapes of individual peaks.[23,24]

Molecules in the gas phase can be considered as isolated, thus, the effects of intermolecular interactions may be neglected. This gives a way for determination of solvent effects on NMR parameters of a molecule (chemical shifts[100] and coupling constants[101,102]) or activation parameters of reactions.[103–106] It also helps to investigate isolated molecules[107,108] and associates and compare them with the condensed state.[108]

Gas-phase NMR was used for determination of the dependence of experimental $^1J(C-H)$, $^1J(Si-H)$ and $^1J(Ge-H)$ values on the density of the medium (Fig. 11).[101] It was shown that the $^1J$ values decrease with the density decreasing. The extrapolation of this dependence to 'zero density' was used to eliminate effects from intermolecular interactions. The values obtained in this way served for estimation of correctness of theoretical calculation of the coupling constants. The calculations were carried out at the non-relativistic level coupled cluster perturbation theory (CCSD) including the basis set convergence test. The relativistic corrections were estimated according to Dirac–Hartree–Fock (DHF) approach. The final theoretical values were obtained by applying the available estimates of the vibrational and temperature corrections. The difference between the calculated and experimental $^1J(XH)$, X = C, Si, Ge, constants was small and did not exceed 3%.

Temperature-dependent gas-phase $^1H$ NMR was used for the characterization of the internal rotation about the

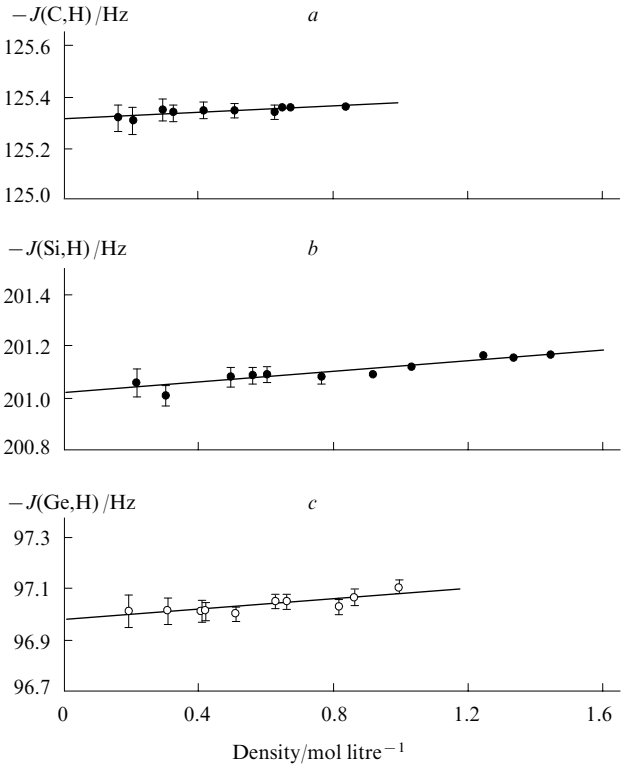



**Figure 11.** Linear dependences of experimental one-bond spin–spin coupling on the density observed for neat methane-$^{13}C$ (*a*), silane (*b*) and germane (*c*) at 300 K.[101]

peptide bond in a series of *N,N*-asymmetric dialkylformamides ($HCONR^1R^2$: $R^1 = Me$, $R^2 = Pr^n$, $Bu^n$, $Br^i$) (Fig. 12).[103] It was shown that the preferred conformer of

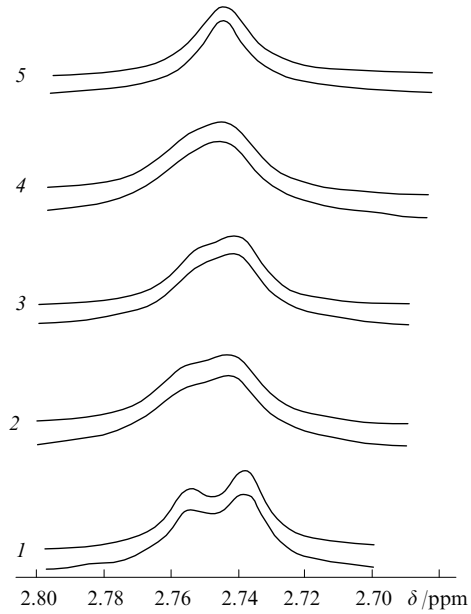



**Figure 12.** Temperature dependence of the *N*-methyl $^1H$ resonances in gaseous *N*-methyl-*N*-propylformamide at 300 MHz. The upper and lower traces correspond to calculated (DNMR5) and experimental spectra.[103]
Temperature/K: 1 (*1*), 344 (*2*), 349 (*3*), 353 (*4*), 391 (*5*).

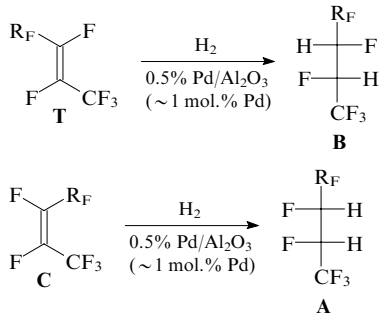
these formamides in the gas phase has the *N*-methyl group *syn* to the carbonyl oxygen as in the liquid phase. The free energy difference [$\Delta G^{\circ}_{298}(syn-anti)$], and activation free energies ($\Delta G^{\neq}_{298}$), in kcal mol$^{-1}$, for the conformers were calculated from the experimental NMR data.

| $R^2$ | $\Delta G^{\circ}_{298}(syn-anti)$ /kcal mol$^{-1}$ | $\Delta G^{\neq}_{298}$ /kcal mol$^{-1}$ |
|---|---|---|
| $Pr^n$ | −83 | 19.4 |
| $Bu^n$ | −80 | 19.3 |
| $Pr^i$ | −91 | 19.1 |

Moreover, NMR opens up large possibilities for investigation of reaction mechanisms in gaseous phase, especially gas adsorption and gas phase catalysis.[109, 110]

The vapour phase hydrogenation of *cis*/*trans* mixtures of perfluoro-2-butenes and perfluoro-2-pentenes over palladium supported on alumina was studied by gas phase $^{19}$F NMR (Scheme 7).[109]

Scheme 7




$R_F$ = $CF_3$, $CF_2CF_3$

Spectral data show the time dependence of the concentrations of the reactants and products in the hydrogenation of the *cis*/*trans* mixture of perfluoro-2-pentenes (Fig. 13). It should be noted that for the studied reaction such information is difficult to obtain using other analytical methods. The approximation of the measured curves by exponential functions suggests pseudo-first order kinetics. The reaction was reported to be highly stereospecific, as formation rate for every diastereomeric product is equal to consumption rate of the corresponding reactant. The *cis* olefin **C** gave the *erythro* hydrofluorocarbon HFC **A** and the *trans* olefin **T** gave the *threo* HFC **B** (see Scheme 7). Thus, the addition of dihydrogen to the double bond occurs *via* the *cis*-mechanism. Also, it is worth noting that the hydrogenation of the *trans* olefin is faster than that of the *cis* olefin ($k_{trans}/k_{cis}$ = 2.4).

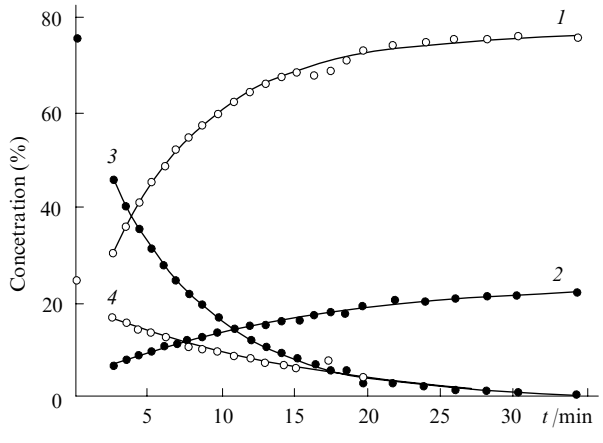



**Figure 13.** Kinetic plot for the $Pd/Al_2O_3$-catalyzed hydrogenation of a 24.8% : 75.2% *cis*/*trans* mixture of perfluoro-2-pentenes at 65 °C obtained by gas phase $^{19}$F NMR monitoring.[109]
(*1*) HFC **B**, (*2*) HFC **A**, (*3*) *trans* olefin **T**, (*4*) *cis* olefon **C**.

Gas-phase NMR was successfully applied for determination of the equilibrium constant ($K_p$) of isotopic exchange reaction between DCl and HBr according to Eqn (2).[111]

$$DCl + HBr \rightleftharpoons DBr + HCl \quad (2)$$

Meanwhile other methods did not lead to reliable results. Here the relative concentrations of the reactants ($p_{HCl}/p_{HBr}$ and $p_{DBr}/p_{DCl}$) [Eqn (3)] were determined by means of integral intensities of corresponding signals in $^1$H and $^2$H spectra (Fig. 14).

$$K_p = \frac{p_{DBr}p_{HCl}}{p_{DCl}p_{HBr}} \quad (3)$$

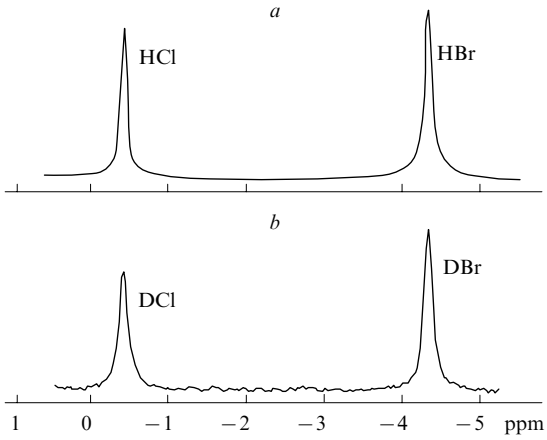



**Figure 14.** NMR spectra of a gas mixture of DCl (0.5 atm) and HBr (0.5 atm). $^1$H spectrum (400 MHz) (*a*) and $^2$H spectrum (61.4 MHz) (*b*).[111]

Not only reaction monitoring by recording 1D spectra was possible in the gas phase, but also 2D experiments, although the sensitivity for gaseous samples is usually relatively low. Indeed, several reports [112, 113] point out the fascinating opportunities of 2D NMR for structure elucidation in the gas phase.

It was demonstrated that standard homonuclear [correlation spectroscopy (COSY), total correlation spectroscop (TOSCY)] and heteronuclear [heteronuclear single quantum coherence (HSQC), heteronuclear multiple-bond correlation (HMBC)] were feasible in the gas phase (Fig. 15).[112] However, due to rapid diffusion, it was not always possible to apply pulsed field gradients (PFG) for coherence selection as it led to significant signal losses. In the case of COSY experiment, the observed signal loss reached 25%, which still left some space for the use of PFG but for heteronuclear correlations the signal was almost completely lost during evolution delay. Turning to $^{19}$F it was shown that very fast

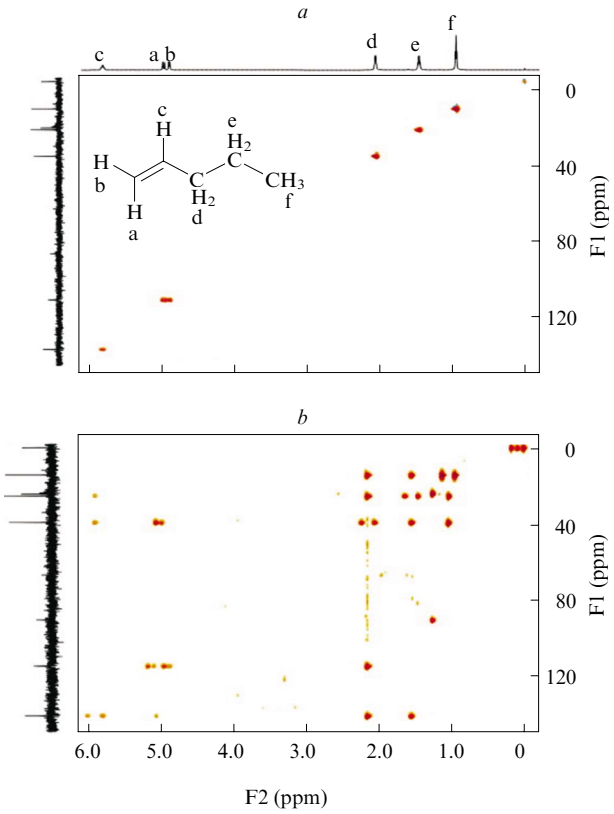



**Figure 15.** $^{1}H-^{13}C$ 2D correlation experiments at 700 MHz on a gaseous 1-pentene and TMS mixture at saturated vapour pressures (303 K, ~105 Pa).[112]
(*a*) HSQC, (*b*) HMBC; the 1D spectra are shown along axes, each spectrum acquired in *ca.* 1 h.

spin rotation relaxation of this nucleus in the gas phase made ultrafast acquisitions possible. As a proof of concept, $^{19}F-^{19}F$ COSY was acquired only in 6 s using standard pulse program.[112] The same holds true for the $^{13}C$ relaxation times. For example, a $^{13}C$ INADEQUATE (incredible natural-abundance double-quantum transfer experiment) for propene at natural abundance was completely acquired in only 14 hours. Unfortunately, the authors did not succeed in application of NOESY (nuclear Overhauser effect correlation spectroscopy) method to gaseous sample due to short relaxation times. The study of diffusion NMR in the gas phase was also presented.[113] Fast diffusion in gaseous samples imposed some limits on the length and strength of gradient pulses applied. In general, shorter PFG with less gradient power were required to obtain reasonable diffusion spectra. An example of $^{19}F$ DOSY (diffusion ordered spectroscopy) acquired with GCSTE (gradient compensated stimulated spin-echo) pulse program is shown (Fig. 16).[113]

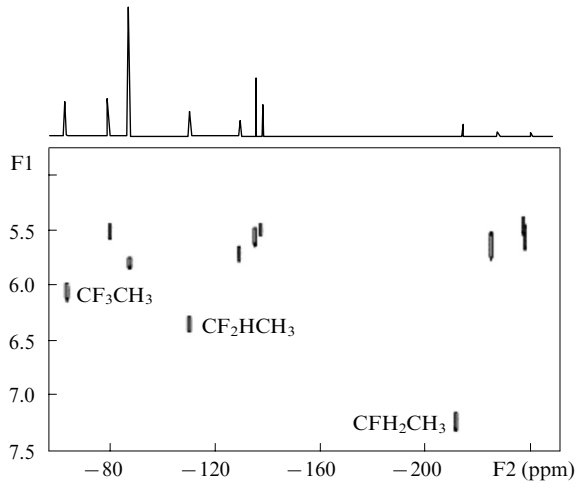



**Figure 16.** $^{19}F$ GCSTE spectrum of a mixture of fluorinated ethanes in the gas phase.[113]
Ordinate axis in units of $10^{-7}$ m$^2$ s$^{-1}$.

## IV. Liquid-phase chemical systems

Development of modern organic synthesis during last decades has led to significant increase in the number of practical methods for selective formation of chemical bonds (carbon–carbon, carbon–heteroatom, heteroatom–heteroatom). As a result, compounds with fairly complex structures, including analogues of natural molecules, can be efficiently synthesized. A real revolution in the practice of organic synthesis was made by transition-metal catalysis[114–121] as well as outstanding development of organocatalysis.[122–132] The introduction of homogeneous catalysis methods into organic synthesis resulted in implementation of various transformations such as cross-coupling or metathesis reactions, and in substantial increase in the yields and selectivities including enantioselectivities for well-known transformations.[133–135] The majority of chemical processes dealing with fine chemicals both in industry and in academia are performed in the liquid state. Nowadays, these include not only traditional organic solvents but also alternative 'greener' media. First of all, this concerns ionic liquids,[136–151] water,[152–168] supercritical fluids like supercritical $CO_2$ (Refs 169–183) as well as solvent-free conditions.[184] These novel systems were designed inspired by Green Chemistry principles,[185,186] namely, decreasing amount of wastes and performing reactions under milder conditions, simpler product isolation and purification, regeneration and reuse of catalysts and obtaining better selectivity and yields.

Development of new types of reactions including catalytic ones needs thorough mechanistic investigations, which are impossible without utilization of modern analytical methods. High-resolution NMR spectroscopy and mass spectrometry widely used nowadays have become powerful tools to study chemical transformations in solution.

### 1. Mass spectrometry of liquid samples

As it was mentioned in section III.1, ESI, APCI and APPI can be coupled with GC.[64–68] In this section it should be pointed out that EI, initially made for MS of gaseous samples (GC-MS), can also be coupled with LC.[187–190] LC-EI-MS provides new promising opportunities for analyzing thermally labile organic compounds, but in most cases, it still remains a 'hard' MS method, leading to extensive fragmentation during ionization and, unfortunately, it is not well-suited for compounds with high molecular weights.

Certainly, among other ionization methods working with liquid-phase samples, ESI holds a leading position

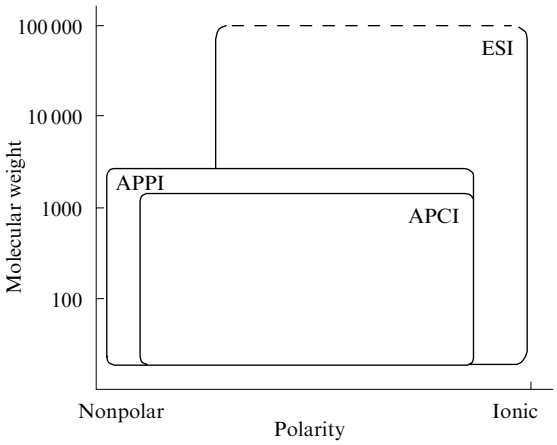


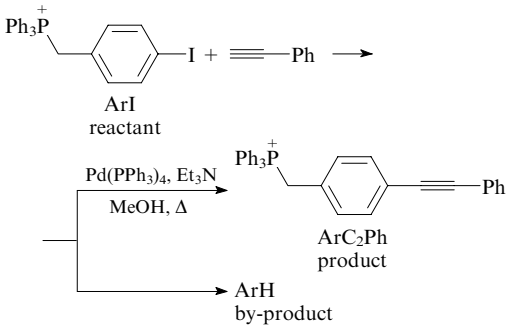

**Figure 17.** General scheme of applicability of API techniques for small molecules as a function of polarity and molecular weights.[191]

(Fig. 17).[191] This 'soft' method deals with solutions, the 'real-life' media of most organic reactions, allowing their quick off-line and on-line monitoring with minimal or no sample pretreatment. The method provides opportunity to study gas phase ion chemistry and ion-molecular reactions inside an MS instrument. Ionization occurs under gentle conditions at atmospheric pressure and leads to formation of gas-phase singly and/or multiply charged ions often due to protonation of neutral species (reactants, intermediates, products) (Fig. 18). In the cases of initially charged dissolved species (*e.g.*, carbocations, carbanions, organo-ligated metal cations, *etc.*), ESI may simply serve as a 'bridge' for transferring intact analytes from liquid reaction media to vacuum stages of a mass spectrometer [mass analyzer(s) and detector] without additional ionization (see Fig. 18).

Being reliable and sensitive,[191–195] ESI-MS has been widely used since its discovery by J Fenn in the 1980s[8,196] and it was repeatedly surveyed including the application for reaction monitoring.[197–211]

On-line ESI-MS monitoring was utilized to get insight into the mechanism of copper-free Sonogashira reaction (Scheme 8).[212] The authors used ESI-MS for '*keeping an eye on all the players*', *i.e.*, for simultaneous monitoring of reactants, products (by-products) and intermediates.[212] A bulky phosphonium group ($Ph_3P^+$) was applied as a charged tag to detect species of interest (see Scheme 8). Charged tags are required for the detection of species otherwise invisible to ESI-MS.[208,213,214] Pressurized sample infusion was used to deliver the reaction mixture to ESI ion source avoiding the contact with atmospheric air ($N_2$ was used as the pressurizing gas).[215,216]

Scheme 8




The kinetics of the Sonogashira cross-coupling was studied by on-line ESI-MS monitoring (Fig. 19) and mechanism of the reaction was proposed based on the obtained mass spectral data (Scheme 9).

A single spectrum obtained by on-line ESI-MS, is presented in Fig. 20. The lines of the plot (Fig. 19) were obtained by extracting intensity data from each spectrum.

The intermediate $[Pd(PPh_3)_2(Ar)(C_2Ph)]$ was always observed in this form, whereas no other species containing both coupling partners were observed. However, the $[Pd(PPh_3)_n(Ar)(I)]$ intermediate was observed for $n = 1$ and 2. Since both of these complexes could conceivably be converted to the product (see Scheme 9), they were summed together in the kinetic plot (see Fig. 19).

A key observation is the change of mechanism early in the studied reaction, whereby the initial fast rate is replaced with a much slower, zero-order process. The rate of for-

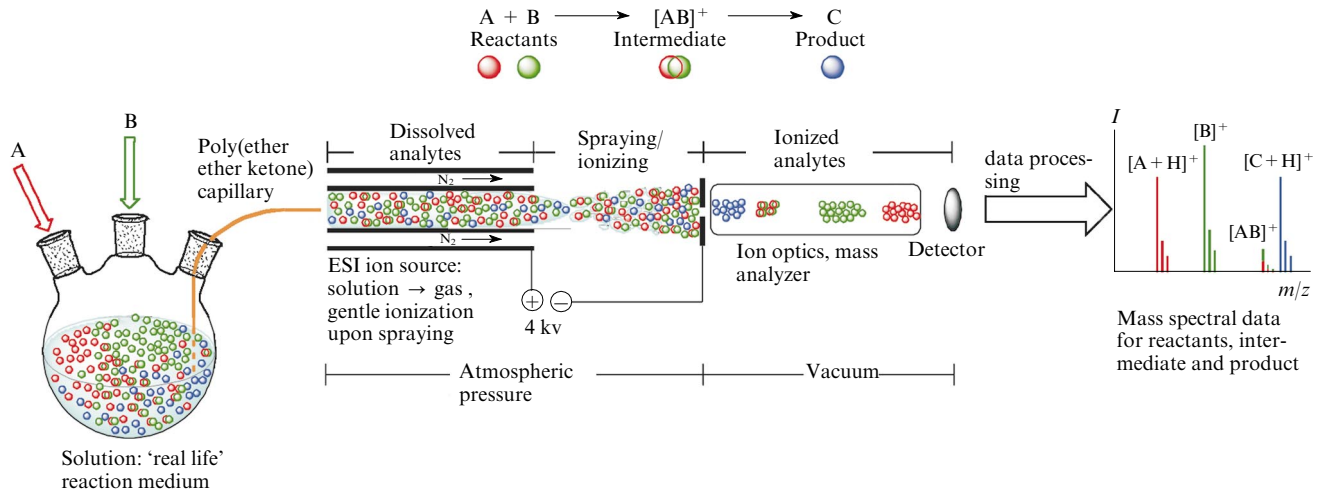



**Figure 18.** Sketch of ESI-TOF-MS analysis for a liquid phase reaction: liquid → spraying/ionization → gas.

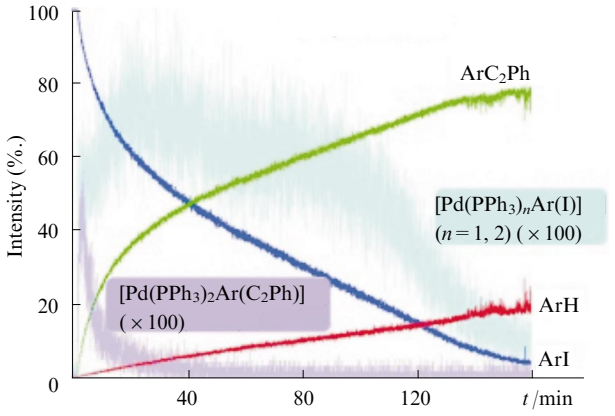
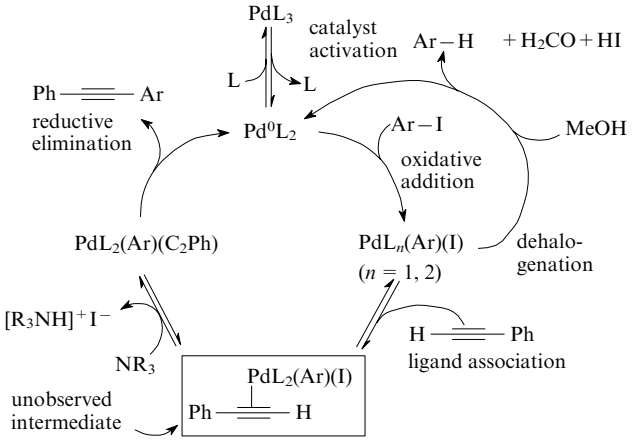



**Figure 19.** Kinetic plot of the copper-free Sonogashira reaction: ESI-MS intensity data over time for all key species containing Ar = *p*-$C_6H_4CH_2PPh_3^+$.
The intensity has been multiplied by 100 for the palladium-containing intermediates.[212]

Scheme 9




L = $PPh_3$

mation of the by-product (ArH) through dehalogenation was essentially constant throughout (zero order). The changeover in the mechanism corresponds to the onset of the disappearance of $[Pd(PPh_3)_2(Ar)(C_2Ph)]$ (Ar = *p*-$C_6H_4CH_2PPh_3^+$). In contrast, $[Pd(PPh_3)_n(Ar)(I)]$ ($n$ = 1 or 2, sum of both species) reaches a maximum concentration at the time of the mechanistic changeover, stays roughly constant, then diminishes to zero at the end of the reaction (see Fig. 19).[212] By performing ESI-MS monitoring for different test reactions, it was possible to make conclusions about rate-determining steps of the studied cross-coupling process.[212]

Therefore, the combination of charged tags and pressurized sample infusion enables efficient on-line ESI-MS monitoring. Valuable data were obtained on the relative concentrations of several components of a catalytic reaction, such as the discussed Pd-catalyzed coupling of an aryl iodide with phenylacetylene (see Scheme 8).[212]

It should also be pointed out that pressurized sample infusion to ESI ion source directly from the reaction vessel is a practically convenient technique, suitable for handling unstable species due to the absence of contact with atmospheric air.[215] Another option well-suited for this purpose, namely, coupling a glovebox with a ESI-MS instrument, was also reported by the same group.[217]

The Pauson–Khand reaction (Scheme 10) was carried out in a chlorobenzene solution and studied by means of on-line ESI-MS (Fig. 21).[218]

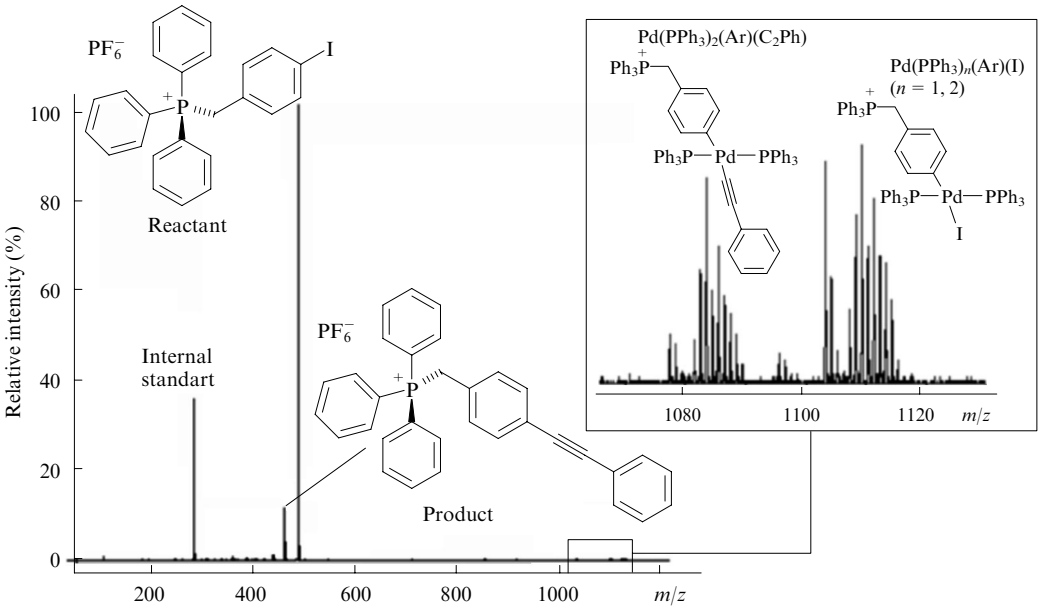
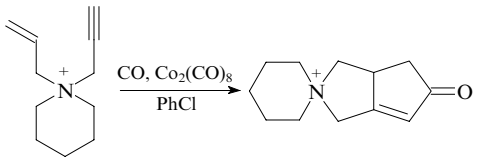



**Figure 20.** Single ESI-MS spectrum registered upon monitoring of the Sonogasira reaction.[212]
The intensities of signals of Pd-containing intermediates (in the inset) have been multiplied by 100 to become appreciably intense with respect to the reactants and products.

Scheme 10



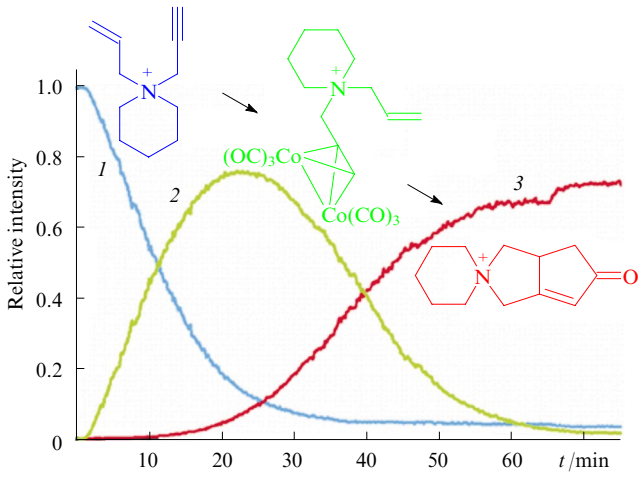
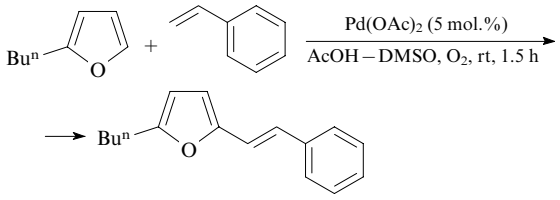




**Figure 21.** Kinetic plot of the intramolecular Pauson–Khand reaction studied by on-line ESI-MS monitoring.[218]
Abundance *vs.* time data for the reactant (*1*), intermediate (*2*) and product (*3*). Data have been normalized to the total ion current.

The results revealed only the hexacarbonyl complex as a detectable intermediate (see Fig. 21), and the reaction was shown to have a large enthalpy and entropy of activation, consistent with ligand dissociation being the rate limiting step.[218] The reaction kinetics was studied by using the dependence of abundance of each ion of interest (reactant, intermediate and product) on the reaction time (see Fig. 21).[218] In this case, CO was used as a reactant and as the pressurizing gas to deliver the reaction mixture to ESI ion source.

Aerobic dehydrogenative Heck reaction of heterocycles with styrenes (the model reaction of n-butylfuran with styrene is presented in Scheme 11) was studied by ESI-MS.[219] By performing ESI-MS monitoring with subsequent ESI-MS/MS and HRMS experiments, the catalytic intermediates and species formed in the presence of metallic co-oxidant (AgOAc) were detected and characterized.

Scheme 11




One of the key intermediates, Pd-activated n-butylfuran, was detected as sodium adduct (**A**) with $m/z = 389.1$ (Fig. 22*b*). The most abundant signal with $m/z = 411.1$, corresponding to another metal-containing intermediate (**B**), resulted from styrene insertion into the Pd–C bond of n-butylfuryl–Pd complex with $m/z = 389.1$ (Fig. 22*a*). The structure of complex **B** ($m/z = 411.1$) was additionally confirmed by ESI-MS/MS experiment and showed the loss of Pd and DMSO.[219] Unsolvated (**C**) and hydrated (**D**) species related to Pd-complex **B** were also observed with $m/z = 333.1$ and $m/z = 351.1$, respectively, together with other Pd-containing compounds (Fig. 22*b*).

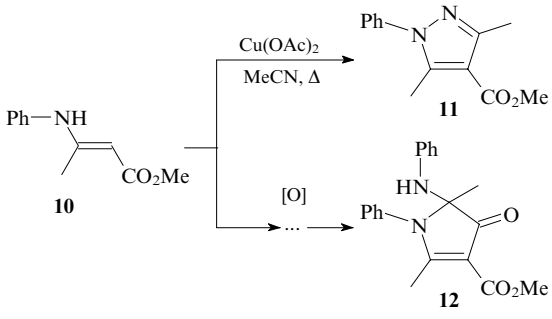
Based on the obtained MS data, the catalytic cycle of the aerobic dehydrogenative Heck reaction was proposed and the negative influence of metallic co-oxidant (AgOAc) caused by formation of insoluble or inactive Pd–Ag mixed species was revealed.[219]

Previously the same group reported representative ESI-MS mechanistic studies of the Pd-catalyzed dehydrogenative Heck reaction of furans with acrylates using benzoquinone as the reoxidant[220] and Wacker oxidation of alkenes,[221] where, based on ESI-MS, dinuclear Pd complexes were shown to be more involved as active catalytic intermediates than mononuclear species.[221]

It was demonstrated that the enantioselectivity of a chiral catalyst can be easily determined from its racemic form by ESI-MS screening of a non-equal mixture of two mass-labelled quasi-enantiomeric substrates (A and B, Fig. 23).[204, 222] The experimental protocol was proven to be simple and fast, as no workup or product isolation is necessary. The chart representing the ESI-MS screening methodology is presented in Fig. 23, which shows two limiting cases: the absence of selectivity and perfect selectivity).

The conversion of enamine (**10**) to pyrazole (**11**) *via* the C–C/N–N bond-formation cascade in the presence of $Cu(OAc)_2$ was investigated by means of ESI-MS (Scheme 12).[223] The off-line ESI-MS monitoring together with CID experiments were utilized to detect and characterize a number of different forms of Cu catalyst ($[(CH_3CN)_2Cu]^+$, $[(CH_3CN)_2Cu(OAc)]^+$, $[Cu(\mathbf{10})(\mathbf{11})]^+$, $[(CH_3CN)Cu(\mathbf{10}-H)]^+$, $[Cu(\mathbf{10})(CH_3CN)]^+$, $[Cu(\mathbf{10})_2]^+$, $[Cu(\mathbf{11})(CH_3CN)]^+$, $[Cu(\mathbf{11})_2]^+$, *etc.*) and revealed the unexpected product **12** (see Scheme 12).[223] The kinetics of formation of pyrazole **11** and derivative **12** was studied based on the dependence of the total relative intensity of all ions of relevant compounds on the time of heating.

Scheme 12




The off-line ESI-MS monitoring was performed by taking aliquots of the reaction mixture and diluting them 100-fold with acetonitrile before analysis. As it is seen from detected Cu-containing species (see Scheme 12), acetonitrile acts not only as a solvent but also as a reactant (in the case of pyrazole **11**) and as a ligand (*e.g.*, in the case of $[Cu(\mathbf{11})(CH_3CN)]^+$ complex). To distinguish between covalently embedded $CH_3CN$ and non-covalent complexes, two

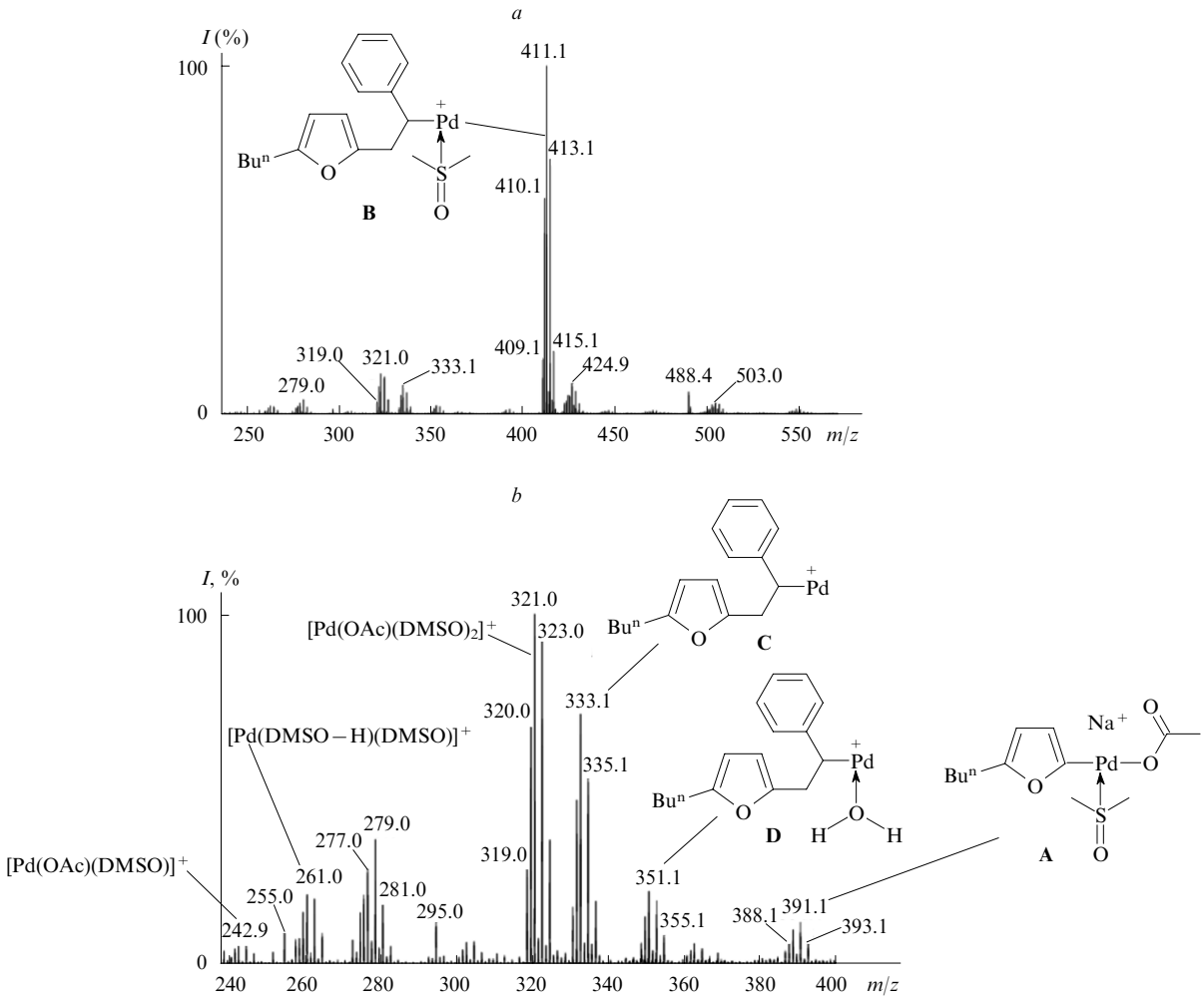



**Figure 22.** Representative mass spectrum obtained by ESI-MS monitoring of aerobic dehydrogenative Heck coupling reaction between n-butylfuran and styrene (*a*) and fragment of this spectrum (*b*).[219]

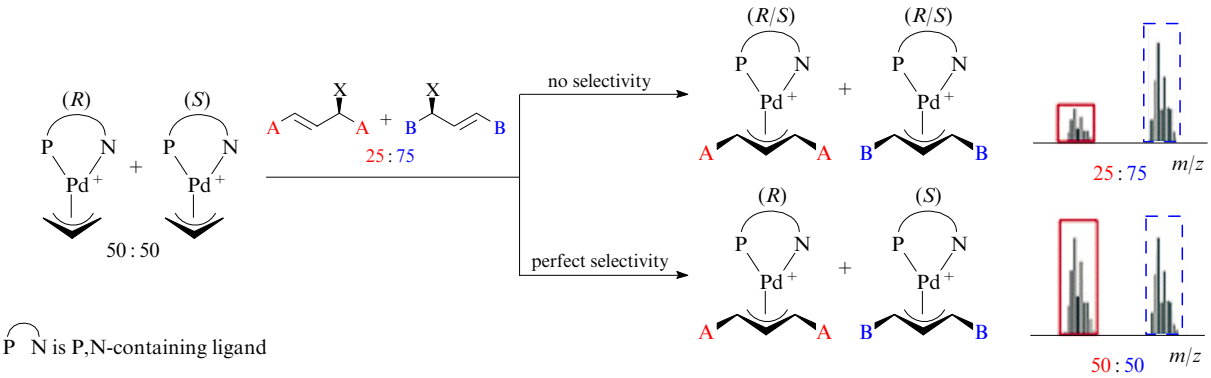



**Figure 23.** Determination of enantioselectivity of a chiral catalyst by ESI-MS screening.[222]
The continuous and dashed frames mark the peaks referring to A- and B-containing products, respectively.

independent series of ESI-MS analysis with $CD_3CN$ as a dilution solvent and as a reaction solvent were performed. Deuterium labelling of acetonitrile confirmed the assignments of signals in obtained mass spectra. For instance, when the reaction was carried out in $CH_3CN$, while $CD_3CN$ was used as a dilution solvent for ESI-MS, a mass shift of +3 Da was observed for $[Cu(\mathbf{11})(CH_3CN)]^+$ due to formation of $[Cu(\mathbf{10})(CD_3CN)]^+$ *via* rapid ligand exchange. The +3 Da shift suggests that $[Cu(\mathbf{11})(CH_3CN)]^+$ contains one non-covalently bound acetonitrile ligand and one covalently embedded acetonitrile unit (within molecule **11**).[223] A set of reactions and ESI-MS experiments with labelled

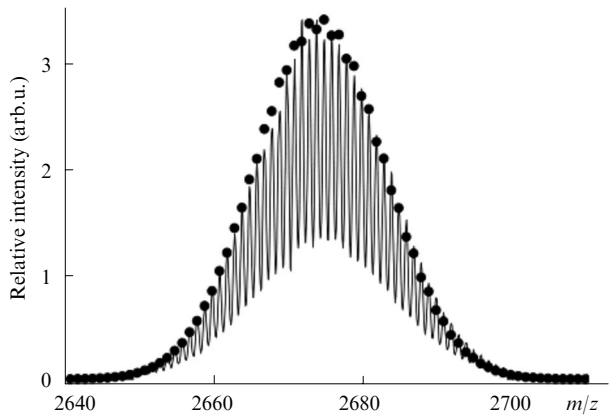



**Figure 24.** Mass spectrum obtained by electrospraying $Zn_{14}Se_{13}Cl_2(tmeda)_6$ in dichloromethane.[224] Dots indicate the expected isotope pattern.

starting material **10** and deuterium labelled copper diacetate were also successfully carried out to get deeper insight into the structure of compound **12**.

Recently, ESI-MS investigations of $M_{14}E_{13}Cl_2(tmeda)_6$ nanoclusters, where M is a transition metal (Zn or/and Mn), E represents a chalcogen (S or Se) and tmeda is *N*,*N*,*N*′,*N*′-tetramethyl-ethylenediamine, were conducted.[224] This work confirms the validity of ESI-MS as a versatile tool for the analysis of high-molecular-weight (more than 2600 Da) organometallic nanoclusters and, as noticed by the authors, a proper adjustment of MS instrument parameters allows good-quality spectra to be obtained.[224] Note that dichloromethane solutions of the clusters were infused into the ESI source and, although dichloromethane is not a typical electrospray solvent (most often, acetonitrile and methanol are used), good quality of mass spectra was reached (Fig. 24).[224]

An interesting example of ESI-MS studies of chiral cobalt coordination cluster with polynuclear $Co_{16}$ core was recently published.[225] The polynuclear core was shown to be stable in methanol. Both elimination and substitution reactions of the $Co_{16}$ complex were successfully monitored by ESI-MS.

The reactions between urea and $Sr^{2+}$ in the gas phase were investigated by ESI-MS.[226] Equimolar aqueous mixtures of strontium chloride and urea ($10^{-4}$ mol litre$^{-1}$) were introduced into ESI source and the formation of $[Sr(urea)]^{2+}$ complex was observed. The $[Sr(urea)]^{2+}$ complex detected as the most abundant signal with $m/z$ = 73.96 was then subjected to the CID experiment, resulting in the formation of both singly and doubly charged fragment ions (Fig. 25).[226] Signals assignments and detailed analysis of fragmentation character provided a valuable information about the stability of the dication $[Sr(urea)]^{2+}$ (Ref. 226).

This example clearly indicates how ESI-MS/MS ($MS^n$, CID) answers the question about the stability of species. The two key issues are: (i) which bond is broken under CID and (ii) how much energy is required for the breakage. The first issue is solved by fragment spectrum analysis and the second one is elucidated from CID experiment parameters.[227]

The C–N coupling in the gas-phase ion-molecular reactions of ammonia and $[M(CH)]^+$ (M = Ni, Pd, Pt) was studied by ESI-MS.[228] It was shown that the ESI of methanolic solutions of monomeric nickel(II) acetate, $[Ni(CH_3COO)_2]$ and tetrameric platinum(II) acetate, $[Pt_4(CH_3COO)_8]$, leads to the formation of the corresponding methylidyne complexes $[M(CH)]^+$ (M = Ni, Pt), which react with ammonia *via* C–N coupling. Although the product pairs $M/[CH_4N]^+$ and $[M(CH_2N)]^+/H_2$ were observed for both metals, hydrogen atom expulsion to generate $[M(CHNH_2)]^+/H$ was only observed in the case of the nickel-containing system and the proton transfer leading to $M/[NH_4]^+$ was limited to platinum. However,

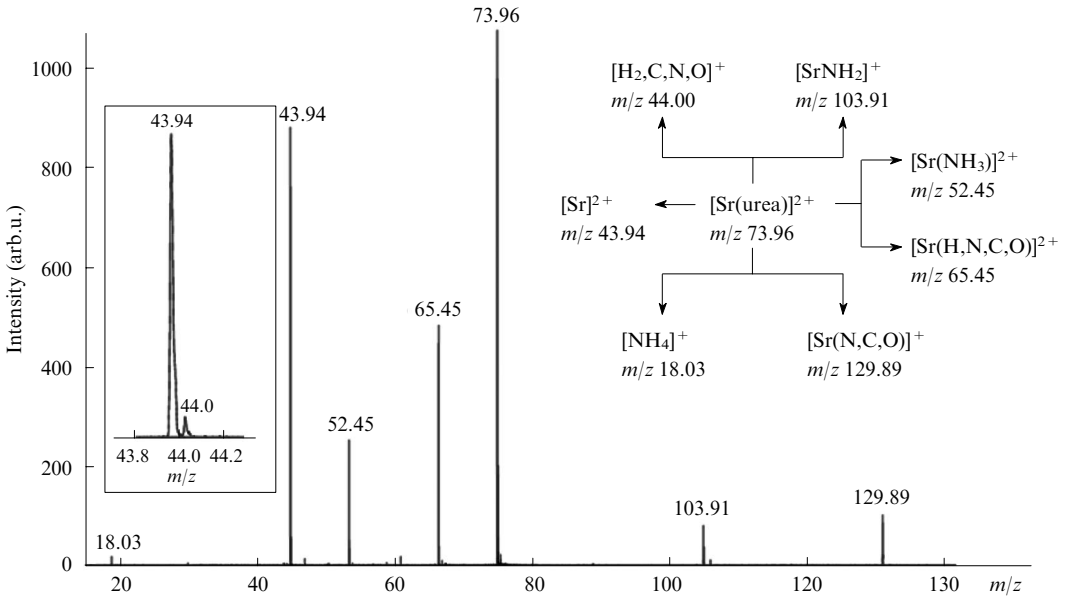



**Figure 25.** The CID spectrum of the $[Sr(urea)]^{2+}$ complex.[226]

attempts to conduct similar experiments with $[Pd(CH)]^+/NH_3$ failed.[228]

A tris(2,2′-bipyridine) ruthenium perchlorate solution in methanol (0.1 mmol litre$^{-1}$) was electrosprayed to produce $[Ru(bipy)_2]^{2+}$ ions. Upon ion-molecular reaction with CO inside the MS instrument, $[Ru(bipy)_2]^{2+}$ gave the new $[Ru(bipy)_2(CO)]^{2+}$ ion, which was detected.[229] The ion-molecular reactions of $[Ru(bipy)_2]^{2+}$ and $[Ru(bipy)_2(CO)]^{2+}$ with 2-methylpropane, propane and propene were then investigated. The reactions of $[Ru(bipy)_2]^{2+}$ resulted in all cases only in the addition of the hydrocarbon; representative mass spectra are presented in Fig. 26.[229] In the reactions of 2-methylpropane and propane with $[Ru(bipy)_2(CO)]^{2+}$, dehydrogenation and demethanation were observed. In contrast with the reactions of propane and 2-methylpropane, propene simply associated with or replaced CO in the reaction with the $[Ru(bipy)_2(CO)]^{2+}$ dication. This work is a bright example of ligand tuning (CO or CO-free) and testing: comparing the reactivity in the gas-phase ion-molecular reactions was performed directly inside the MS instrument by on-line ESI-MS for a solution of organometallic compound.

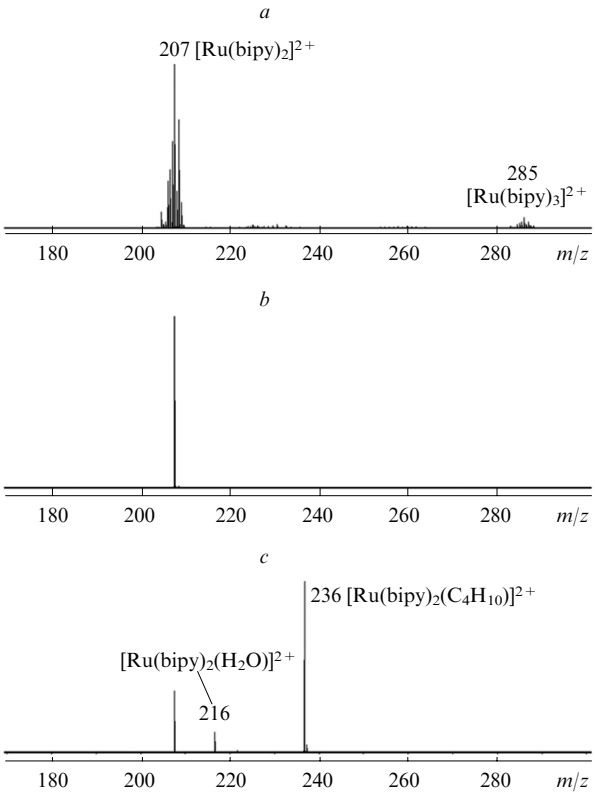
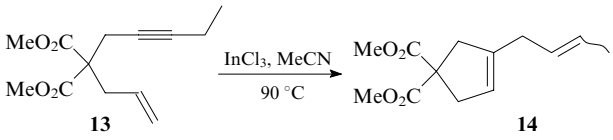



**Figure 26.** Mass spectra: (*a*) CID of $[Ru(bipy)_3]^{2+}$, (*b*) isolated $[^{102}Ru(bipy)_2]^{2+}$; (*c*) reaction between $[Ru(bipy)_2]^{2+}$ and 2-methylpropane.[229]

The effectiveness of ESI-MS in the monitoring of elementary reactions of organotin complexes was also demonstrated during mechanistic studies of tin-catalyzed hydrolysis of 3-acryloxypropyltrimethoxysilane with mono- and multifunctional mercaptans.[230] The unique isotopic distribution of tin successfully proved experimental results in identifying the presence and number of tin atoms in given complexes. ESI-MS and NMR data provided a deeper insight into mechanism of the studied chemical transformation. Noteworthy, together with tin complexes involved in the target process, a number of undesirable tin complexes caused by the presence of impurities in starting materials (mercaptans) were also observed in ESI-MS spectra.[230] This is an additional example of MS benefit when dealing with mechanistic investigations, especially with systems sensitive to impurities contained in starting materials.

$InCl_3$-mediated cycloisomerization of 1,6-enyne **13** was monitored by means of ESI-MS and, as a result, *in situ* generated $InCl_2^+$ was proposed as the real catalyst of this reaction (Scheme 13 and Fig. 27).[231] Indeed, $InCl_2^+$ was clearly observed in the obtained ESI-HRMS spectra as a complex with product **14** (see Fig. 27).

Scheme 13



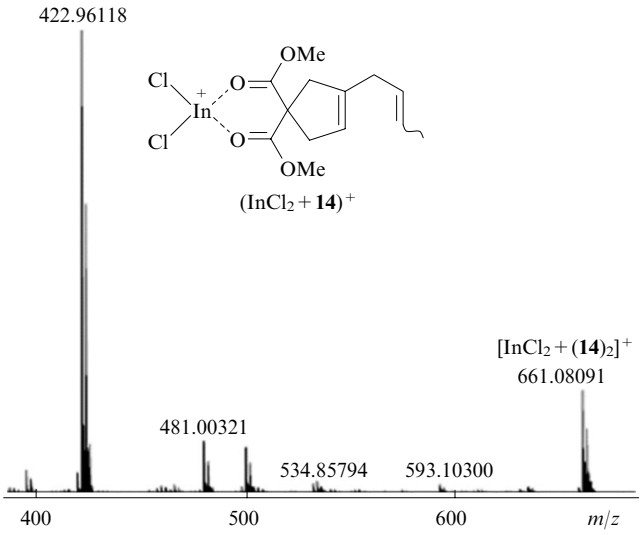




**Figure 27.** ESI-MS spectrum (positive mode) of the reaction mixture of $InCl_3$-mediated cycloisomerization of **13** to **14** and proposed structure for the ion with 422.96 *m*/*z* (corresponds to complex of $InCl_2$ with product **14**).[231]

Note that electrospray principles underlie not only such powerful analytical tool as ESI-MS and its modifications but also successfully serve for preparative purposes as was described in the literature: 'Charged microdroplets act as microreaction vessels, extending the use of electrospray mass spectrometry from chemical analysis to synthesis'.[232]

Despite wide applicability, ESI, however, has certain limitations. ESI-MS is 'blind' towards nonpolar compounds, which cannot be ionized by electrospraying (see Fig. 17).[192, 193] In some cases, the problem can be solved by charged tags mentioned above.[208, 212, 213] However, when it is impossible to tag the molecule of interest by a charged group, the problem can also be solved by APCI or APPI, which are known to be applicable to nonpolar compounds (see Fig. 17). Comparative study of ESI, APCI and APPI in

detection and monitoring of poly-aromatic hydrocarbons (PAHs) and oxy-PAHs was recently reported.[233] A complex mixture of PAHs and oxy-PAHs obtained after the air oxidation of fluoranthene on mineral substrates was used to establish the ionization abilities of these methods (ESI, APCI and APPI). It was shown that APPI-MS is the best suited method for analysis of the PAHs, allowing detection of the full range of studied compounds from low to high molecular weight. APCI was less effective and ESI did not provide satisfactory results. Similar example, demonstrating effectiveness of APPI-MS for PAHs (acenaphthalene, phenanthrene, benz[b]anthracene, pyrene and fluoranthene), was also reported.[234]

Another common advantage of APCI and APPI compared to ESI deals with their ability to operate with high flow rates (typically 0.2 to 2 ml $min^{-1}$), thus allowing rapid LC-APCI(APPI)-MS experiments to be carried out.[235] On the other hand, it can be a problem when sample quantity is strongly limited and high flow rates (*i.e.* rapid sample consumption) are unacceptable. In the last case, ESI, which easily operates with low (1–3 μl $min^{-1}$) flow rates at direct infusion, is the method of choice. Moreover, nanoESI operates with even lower values below 20 nl/min (Refs 236 and 237). This is essential for MS investigation of micro- and nanoscale chemical reactions (*e.g.*, nanogram scale catalyst loadings, *etc.*) and especially when dilution is undesirable.

## 2. NMR spectroscopy of liquid samples

The dissolution of a sample results in averaging of chemical shift anisotropy (CSA) and vanishing of direct dipole–dipole interactions due to rapid molecular tumbling, which gives rise to narrow signals in NMR spectra.[28] The benefits of liquid NMR include detailed information about fine molecular structure, simple sample preparation, high throughput ability and absence of sample destruction during the experiments.

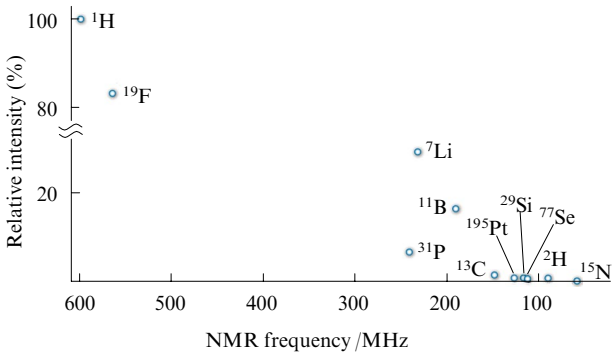



**Figure 28.** NMR frequency and relative sensitivity of various nuclei (scaled to 600 MHz of $^{1}$H NMR).

$^{1}$H NMR experiments are most required in organic chemistry due to superior sensitivity of $^{1}$H compared to other nuclei (Fig. 28). Proton spectra of dissolved organic compounds provide quantitative information including compound purity, structure and stereochemical information. Even though the compounds produced by modern organic synthesis may exhibit very complex multiplet patterns in the $^{1}$H NMR spectra, their assignment can be successfully simplifed *via* the use of iterative spectra prediction tools (Fig. 29).

The NMR measurements are fast enough for high-throughput applications.[239] Disadvantages of $^{1}$H spectra are connected with the dependence of chemical shifts on

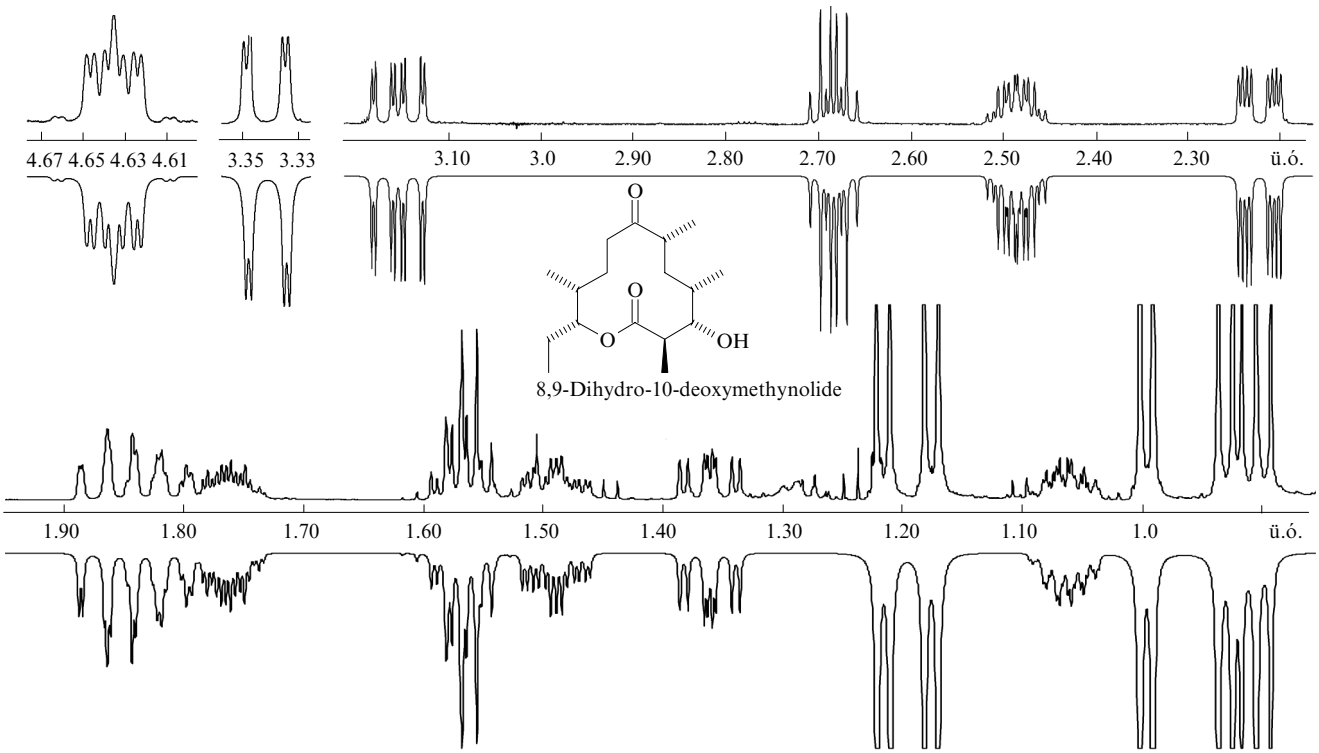



**Figure 29.** Experimental (top) and calculated (bottom) $^{1}$H NMR spectra for the compound shown.[238]

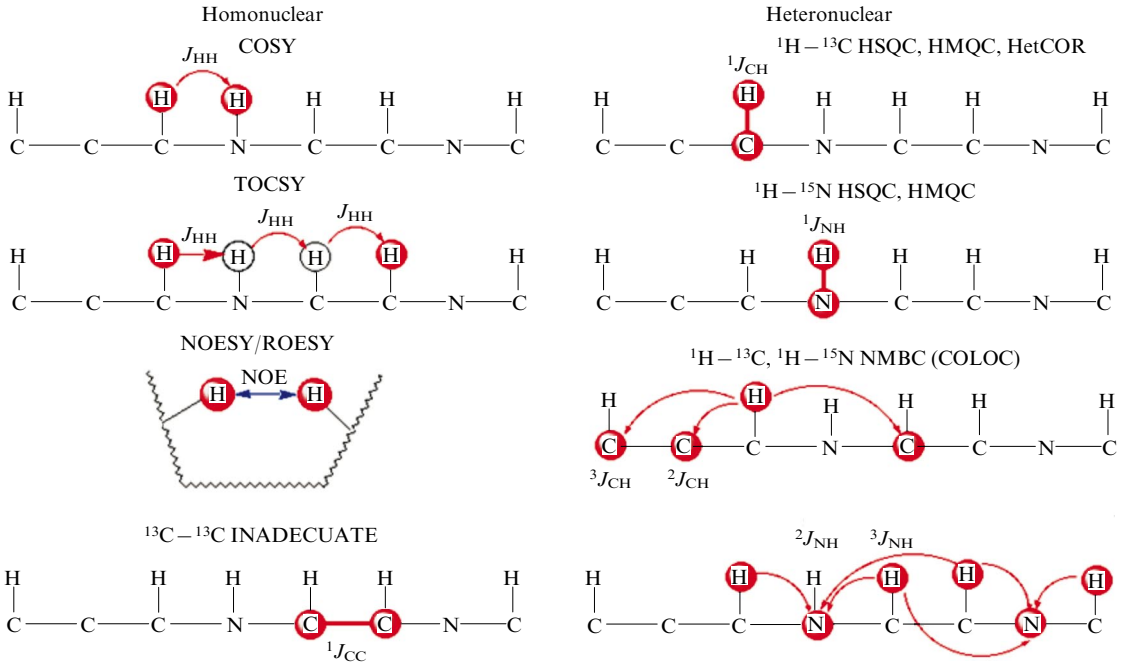



**Figure 30.** Major types of correlations for homonuclear and heteronuclear 2D NMR methods for determination of complex molecules.[246]

solvent polarity, temperature and pH. Presence of many protons makes spectrum hard to assign, whereas for proton-deficient molecules (substituted heterocycles, fused aromatic systems) proton spectrum brings too few information about molecular structure. Carbon-13 spectra have they own advantages like good reproducibility of chemical shifts, minor signal overlap for small- and medium-sized molecules, wide range of chemical shifts, many characteristic regions for functional groups and possibility of spectral editing (*i.e.*, determination of $CH_3$, $CH_2$, CH and Cq carbon atoms).[239] On the other hand, the sensitivity of $^{13}C$ is dramatically lower compared to $^{1}H$. This brings the limits for sample preparation regarding detection amount (milligrams of sample and more) and experimental time (from minutes to hours scale). Longer relaxation times and NOE transfer cause some difficulties in quantitative analysis.

A variety of 1D methods were developed for structure elucidation [240] but increasing complexity of objects of interest, especially biomolecules and natural compounds defined the limitations of 1D NMR spectroscopy. For example, steroids have always been in focus of organic chemistry, but often only X-ray diffraction provided all necessary information as $^{1}H$ NMR spectra were too complicated, $^{13}C$ required too large samples due to the low sensitivity of spectrometers. Usually information taken from $^{13}C$ spectra was not sufficient for determination of fine structure properties, whereas the application of 2D methods was strongly limited in the past.

The interest in investigation of biomolecules and, particularly, biological polymers (proteins, nucleic acids and polysaccharides) set the requirements for NMR hardware and software, including building of new magnets for higher frequencies and higher resolution, development of new electronics, new probe design for extra sensitivity, as well as new software concepts for data acquisition and processing. The development of 2D NMR methods has been started since the 1980s. These experiments allow structure identification by atom connectivity information and Nuclear Ovehauser Effect (spatial interactions). They provide information about the connectivity between different atoms through scalar couplings or spatial (NOE) interactions (Fig. 30).[28, 241 – 246]

The game-changing digital NMR spectrometers were developed in the mid-1990s, together with high-end workstations [247] capable to perform 2D data processing and output at reasonable time, equipped with graphical user interface, convenient and clear for users. This new generation of instruments was equipped with digital RF synthesizers, providing RF pulses with stable and reproducible phase and amplitude, digital receiver demonstrating decreased artifacts and distortions, Z-gradient probeheads, which gave rise to gradient-selected experiments with short experimental time and better selectivity. Since that time, 2D methods have developed rapidly, with increased sensitivity, selectivity, including combination of different correlation techniques (HSQC-TOCSY, HSQC-NOESY, SelCOSY-TOCSY, *etc.*).[28, 248]

Typical NMR analysis strategy for liquid systems is presented below (Fig. 31).[28]

2D HSQC and COSY spectra are very helpful for investigation of reactions, as they are fast enough, provide rapid H – H and C – H connectivity in molecules which can be thought of as 'fingerprints' of every component. The only disadvantage of HSQC is limited quantification abilities due to dependence of signal intensity on $^{1}H$ relaxation times and $^{1}H-^{13}C$ coupling constants.[249]

The structure elucidation for typical molecules like steroids became efficient with this strategy (Fig. 32).[250] Even the basic HSQC experiment was able to recognize stereochemically different protons previously left unassigned in so called 'methylene hump'[251] as well as unrevealed $^{13}C$ chemical shift dependences on configuration.

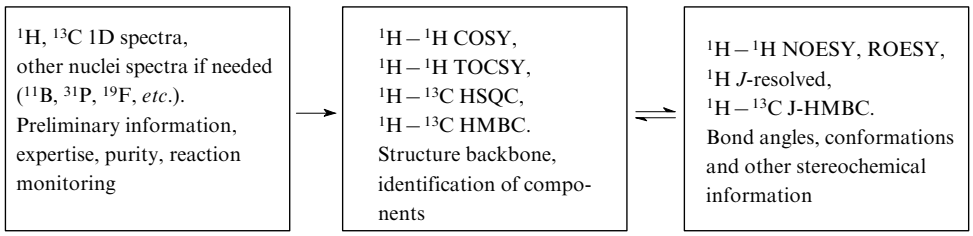



**Figure 31.** Typical NMR analysis strategy for liquid systems.[28]

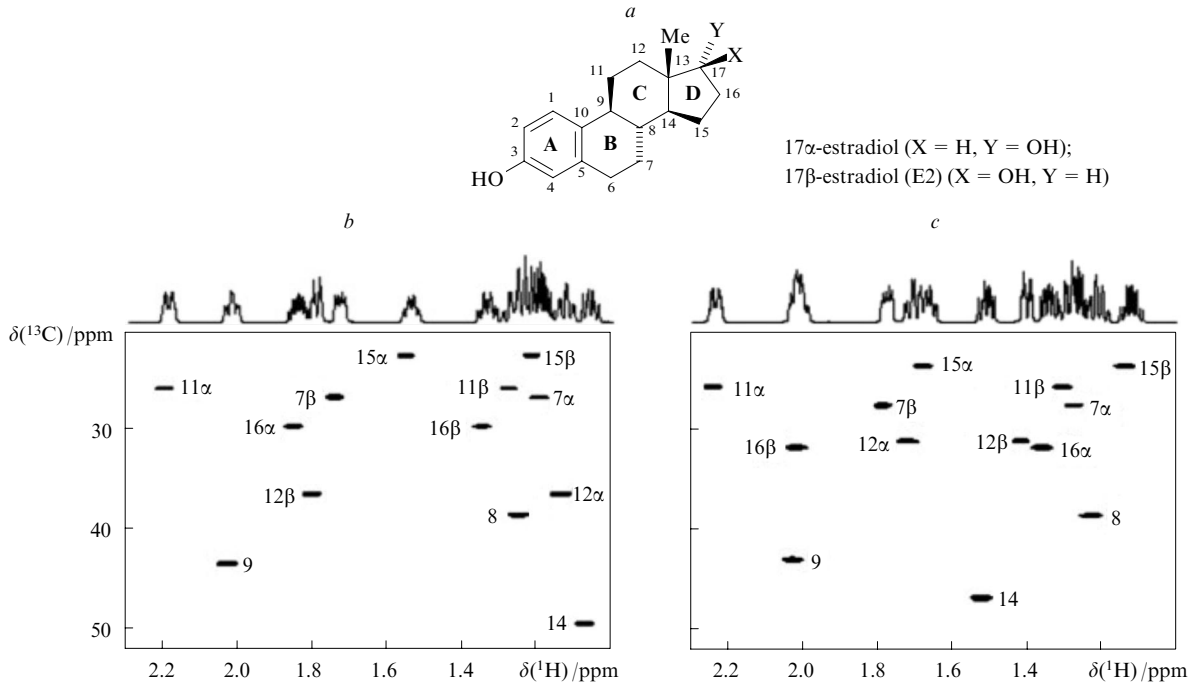



**Figure 32.** 17α- and 17β-estradiols (*a*) and their HSQC spectra (*b*, 17β-estradiol, *c*, 17α-estradiol) showing the difference in configurations.[250]

The efficiency of this approach was proved by increased number of publications dedicated to 2D NMR structure elucidation. The modern state of the art allows performing 2D experiments with high efficiency for set of steroid molecules establishing unambiguously their fine structure.[252] Heteronuclear correlation experiments are also performed on $^1$H with $^{31}$P, $^{19}$F, $^{11}$B or $^{29}$Si and other important nuclei,[253 – 256] or $^{19}$F – $^{13}$C, $^{31}$P – $^{13}$C or $^{31}$P – $^{31}$P correlations.[254, 256, 257]

For higher efficiency, in the case of simple molecules or when the number of correlated atoms is limited, alternative 1D versions of well-known methods, selective COSY, TOCSY, NOESY and ROESY (rotating frame nuclear Overhauser effect correlation spectroscopy) are used.[28, 258 – 262]

2D INADEQUATE experiment, despite its exceptional informativity as it can reveal the carbon skeleton of a molecule, is still rare due to exceptionally low sensitivity and rather long experimental times (days or even weeks) and requirement of tens or even hundreds milligrams of the sample. Several approaches like proton-enhanced INADEQUATE called ADEQUATE (astonishingly sensitive double quantum transfer experiment)[263] help to improve the sensitivity of this method. In addition, this method can have more applications on the instruments with cryoprobes.[264]

The nuclear Overhauser effect is the change in the NMR signal intensity of a nucleus upon saturation of the signal of another nucleus interacting with the former through the dipole – dipole mechanism.[28, 247] The nuclear Overhauser effect is a 'wish' of a system of interacting nuclei to come to the thermal equilibrium state after the perturbation of the occupancies of the spin states of the irradiated nucleus. This process is accompanied by the excess energy redistribution to other nuclei of the system, which results in a change in the signal intensities of the non-irradiated nuclei. As the dipole – dipole interactions depend on the distances between atoms, the NOE can be used for studies of the mutual spatial arrangement of the nuclei separated by many bonds.

The formula that describes the dependence of transient NOE for nucleus *d* (upon irradiation of nucleus *k*) on the distance between these nuclei $r_{kd}$ can be approximated as Eqn 4:

$$f_k^d = c r_{kd}^{-6} \tau_m \qquad (4)$$

where *c* is the constant including the fundamental constants and the correlation time of the molecule, $\tau_m$ is mixing time,

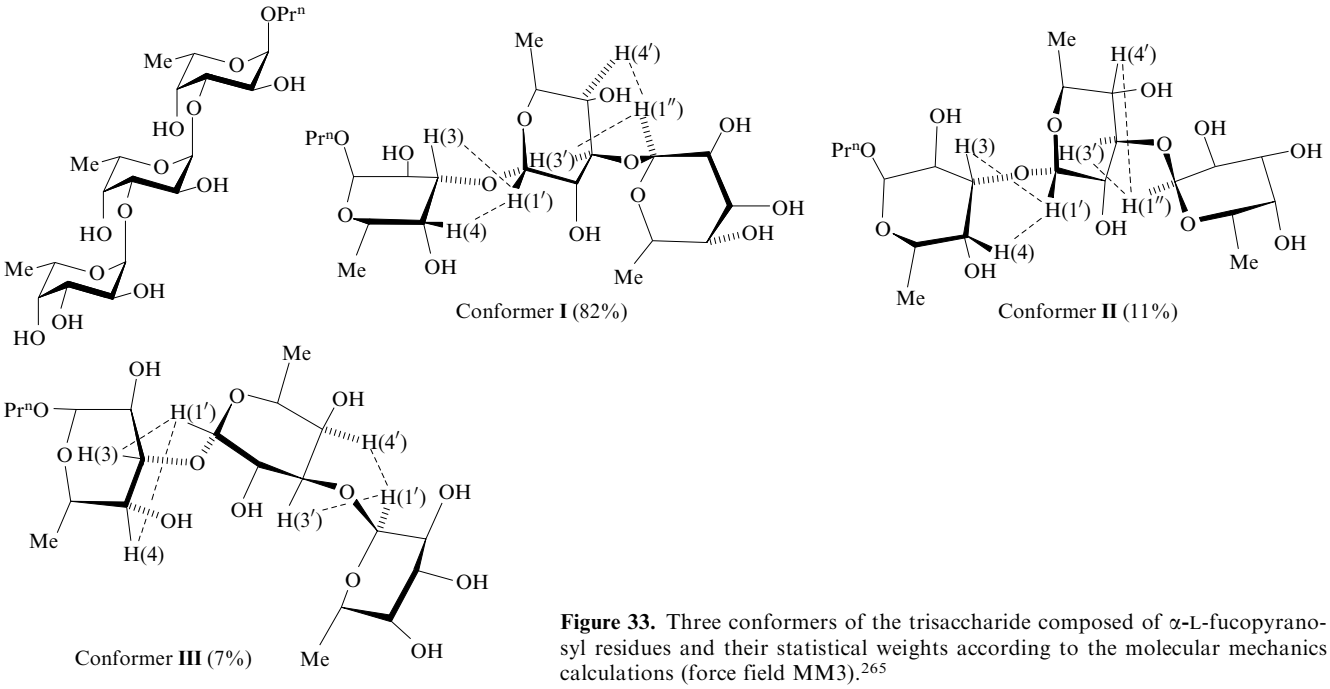



**Figure 33.** Three conformers of the trisaccharide composed of α-L-fucopyranosyl residues and their statistical weights according to the molecular mechanics calculations (force field MM3).[265]

*i.e.*, the time for redistribution of the excitation introduced into the site occupancies of energy levels of the nucleus $k$ to other nuclei of the system (the appearance of the NOE). This equation can be used for determination of the interproton distances $r_{kd}$ from the known NOE values. The reproducibility of measurements of the NOE values depends on several experimental conditions: the nature and concentration of the sample, the presence of paramagnetic impurities, the degree of saturation of irradiated signal and specific properties of the instrument and experiment setup.

However, the ratio of two NOEs within one molecule, which is referred to as the relative NOE, is less sensitive to all these factors and its value is roughly inversely proportional to the sixth power of the ratio of the corresponding interproton distances (Eqn 5).

$$\frac{f_k^d}{f_n^m} = \left(\frac{r_{kd}}{r_{nm}}\right)^{-6} \tag{5}$$

In the recent study,[265] the use of transient NOE, namely 2D NOESY experiment, is applied to determine the conformational properties of trisaccharide (Fig. 33). Intensive correlation signals between protons H(1) of glycosylating fucopyranose residues and protons H(3) and H(4) of the glicosylated residues (Fig. 34) are observed in the 2D NOESY spectrum. At the same time, the theoretical conformational analysis based on the molecular mechanics calculations (force field MM3) found three possible conformers (**I**, **II** and **III**) for this molecule (Fig. 33). The NOE values calculated by the molecular mechanics (Eqn 5) were in good agreement with the experimental values (Table 2), indicating reliability the chosen model.

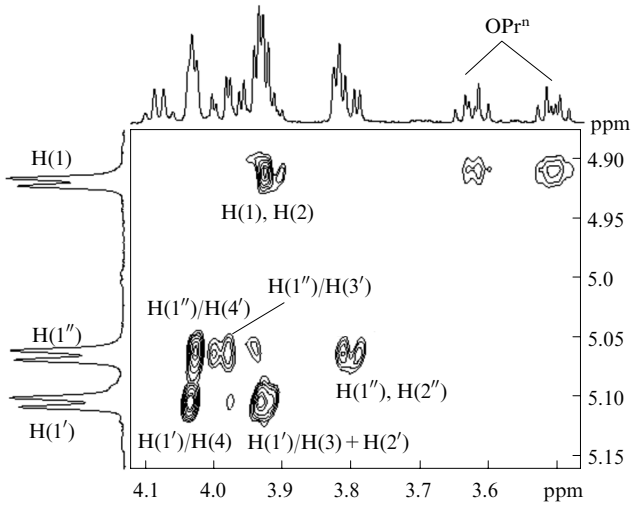



**Figure 34.** Part of the 2D NOESY spectrum for the trisaccharide (see Fig. 33) demonstrating inter-residue correlations.[265]

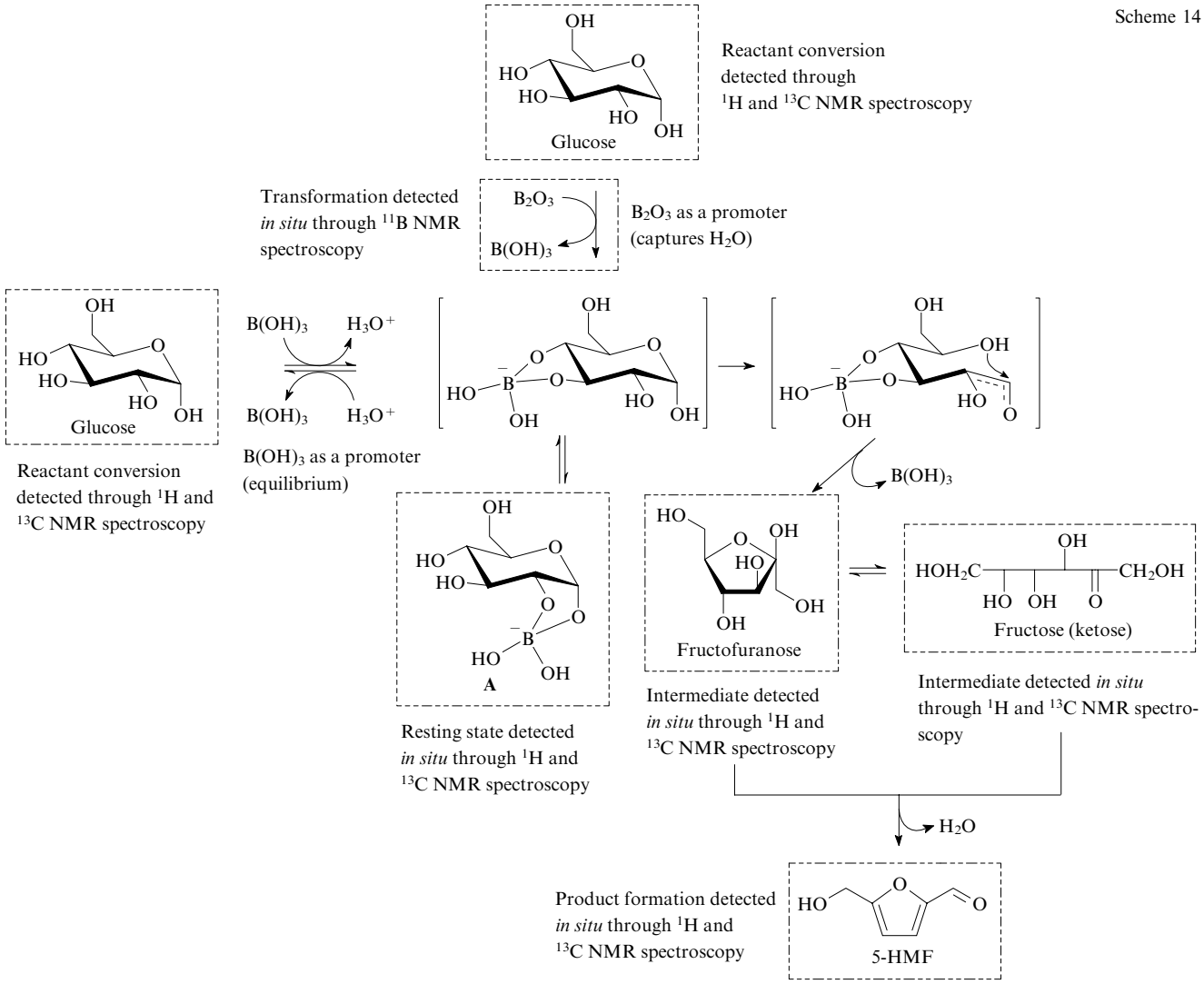
**Table 2**. Experimental relative integral values of cross-peaks in the 2D NOESY spectra of the trisaccharide and computed[a] relative transient NOE values (in parentheses).[265]

| Linkage | H(2′)/H(1′) | H(3)/H(1′) | H(4)/H(1′) |
|---|---|---|---|
| α-L-Fuc-(1→3)-α-L-Fuc-OPr$^n$ | | 214 (120 + 100) [b] | 143 (155) |
| α-L-Fuc-(1→3)-α-L-Fuc | 119 (110) | 100 (100) | 143 (160) |

[a] Theoretical NOEs calculated over all conformations lying within 10% from the global energy minimum. [b] Measured for the sum of H(3)/H(1′) and H(2′)/H(1′) cross-peaks.

The NMR methodology was extended to include non-standard reaction media without conventional organic solvents.[148] Direct NMR monitoring of sugar conversion in ionic liquids was performed involving structure elucidation of the intermediate and characterization of all reaction

Scheme 14



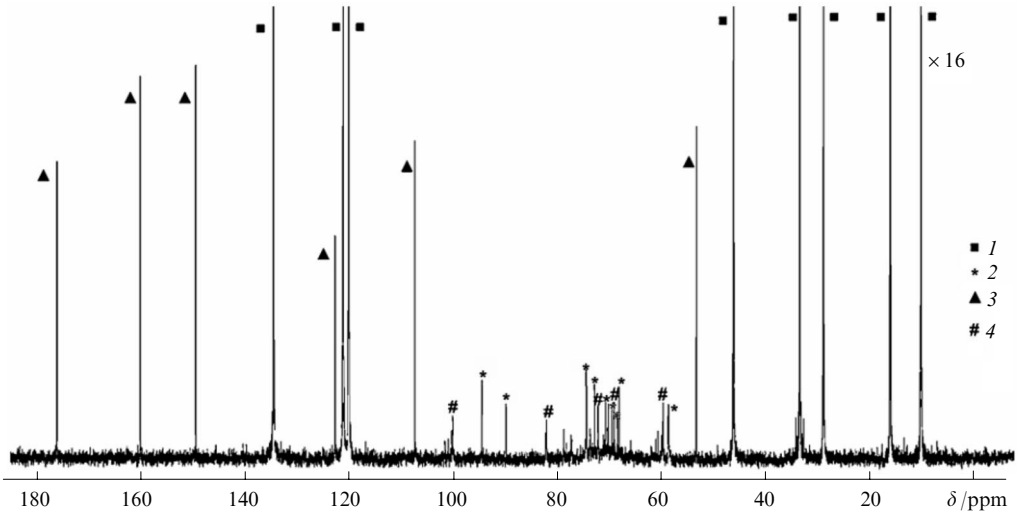




**Figure 35.** $^{13}$C {$^1$H} spectrum of native reaction mixture: solvent – [bmim]Cl (*1*), glucose, the reactant (*2*), 5-HMF, the product (*3*), and intermediate borate complex **A** (*4*) (see Scheme 14 for structure of **A** and the reaction details).[147]
bmim is 1-n-butyl-3-methylimidazolium.

components by 1D and 2D NMR spectra.[147] The reaction was conducted directly in the NMR tube; hence, the structure of the intermediate was determined and a plausible mechanism of the reaction was suggested (Scheme 14). The dashed frames enclose compounds that were detected in the NMR spectra). In this study, 1D selective TOCSY and NOESY spectra were very helpful for the determination of intermediate structure together with 2D correlation methods.

$^1$H reaction monitoring was really complicated because of strong signal overlap. Thus, $^{13}$C monitoring was applied taking into account $^{13}$C and $^1$H relaxation rates. As a result, all the signals were assigned with assistance of $^1$H$-^{13}$C and $^1$H$-^1$H correlation procedures (Fig. 35). The approach allowed efficient structure elucidation along with kinetic measurements using the developed quantification protocol.

During monitoring of the reaction, quantitative measurements can provide the necessary information about the degree of conversion, yield and kinetics. For absolute concentration measurements, especially in high-throughput NMR applications (quality control, metabolomics) an artificial internal standard, ERETIC (electronic reference to access *in vivo* concentrations) was developed. A special signal with calibrated integral intensity was synthesized by NMR hardware and allowed high-precision quantitative measurements without disturbing the system under study.[266] Together with automatic sample changing, this technique provides fast, reliable and high-throughput quantitative measurements.

Finally, worth mentioning is another recent trend in NMR, namely, ultrafast 2D spectroscopy. This approach was recently developed by Frydman and co-workers.[267, 268] Ultrafast 2D NMR allows acquisition of a 2D spectrum in a single scan, thereby reducing the time needed for the registration of an experiment by several orders of magnitude. The main type of 2D spectra, particularly COSY, HMQC, HSQC, TOCSY, *J*-resolved [269] (Fig. 36) have been obtained using such ultrafast method. This NMR technique was already applied to a wide range of problems, including the measurement of specific isotopic enrichments in biological mixtures,[270–272] or kinetic studies occurring on a short timescale,[271, 272] or *in vivo* spectroscopy in biological systems. A number of other applications are currently investigated; however, even when the acquisition of ultrafast spectra is carried out under optimized conditions, the results are often not satisfactory compared to conventional 2D spectra. Ultrafast 2D NMR usually demonstrates lower sensitivity, spectral width, resolution and distorted line shapes. Nevertheless, the method is being intensively developed nowadays.[273–275]

Diffusion NMR spectroscopy is another widely applied analytical NMR method. The main principle is the dependence of NMR signal amplitudes on molecular mobility in experiments with pulsed-field gradients. This effect is suitable for determination of self-diffusion coefficients ($D$), which are calculated by Einstein–Stokes equation (Eqn 6):

$$D = \frac{k_B T}{6\pi\eta r_h} \tag{6}$$

This equation states that for a spherical particle in isotropic medium under laminar flow conditions, the diffusion coefficient depends on hydrodynamic radius ($r_h$) of the molecule, temperature ($T$) and viscosity ($\eta$) of the solvent ($k_B$ is the Bolzmann constant).[28] The unique ability of the method is discrimination of component signals without physical separation into individual compounds. Processes of aggregation and complexation can also be detected and characterized. Moreover, in certain cases diffusion spectroscopy may provide useful information about molecule size even in complex mixtures of compounds.[276] For diffusion experiments, a probe with gradient coil and gradient amplifier are required in order to establish pulsed gradient fields (Fig. 37). So-called Specialized Diffusion NMR probes capable of delivering strong gradients were developed for slow motion of large molecules and viscous

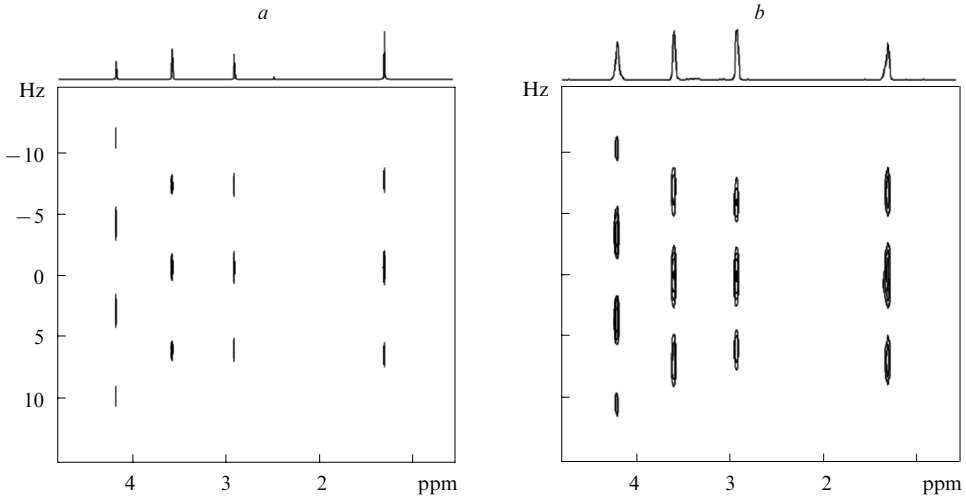



**Figure 36.** Comparison between 500 MHz *J*-resolved spectra acquired on a 100 mmol litre$^{-1}$ ethyl 3-bromopropionate sample in $CDCl_3$ at 298 K.[269]
(*a*) Conventional spectrum acquired in 3 h 8 min with 32 $t_1$ increments and 16 scans. (*b*) Ultrafast spectrum obtained in 500 ms. All spectra presented in the magnitude mode were processed with the same apodization function and post-processing parameters. Note that *J*-resolved spectra separate chemical shift and coupling constant information along two distinct axes.

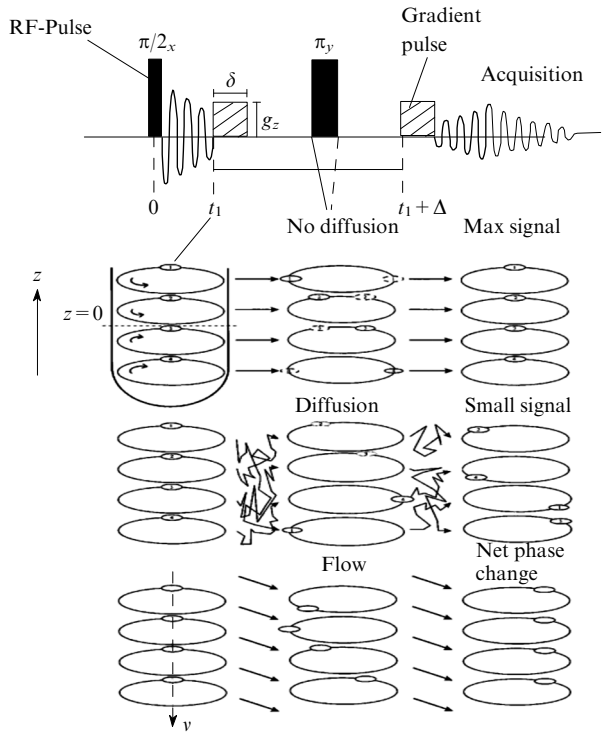



**Figure 37.** Diffusion experiment scheme and signal evolution along NMR tube during applied Z-gradient pulses.[277]

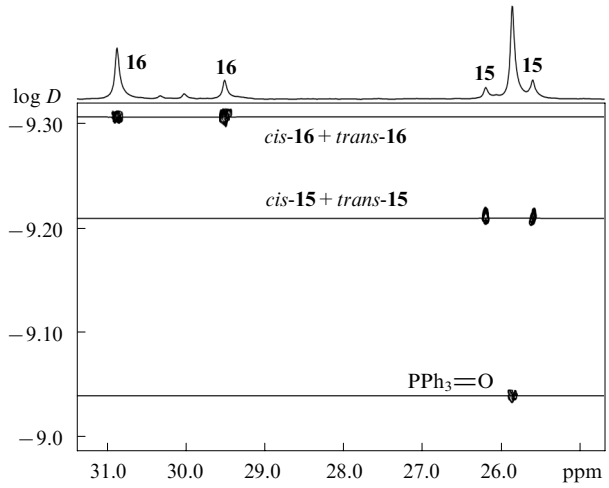
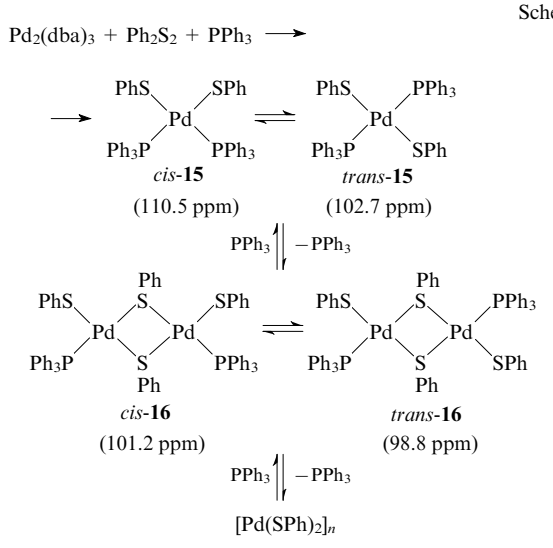



**Figure 38.** $^{31}$P DOSY spectrum and assignment of signals in $^{31}$P spectrum with mono- (**15**) and dinuclear (**16**) *cis*- and *trans*-Pd complexes.[278]
*D* is expressed in $m^2\ s^{-1}$

colloid systems. However, simple diffusion measurements of small molecules can be provided by standard high-resolution probe with *Z*-gradient coil with maximum amplitude to 50 – 60 G $cm^{-1}$ on $^1$H and other abundant nuclei ($^{31}$P, $^{31}$F).

Heteronuclear Diffusion Ordered spectroscopy (DOSY) was successfully employed for identification of mono- (**15**) and dinuclear (**16**) palladium complexes formed *in situ* in the benzene solution of tris(dibenzylideneacetone)dipalladium [$Pd_2(dba)_3$], diphenyl disulfide and triphenylphosphine (Scheme 15).[278] These complexes played the key roles in the catalytic addition reaction and development of new synthetic methods.[279 – 281] However, dynamic nature of the catalytic system precluded isolation of either **15** or **16**.

Scheme 15




Performing $^{31}$P DOSY analysis made it possible to sort out mononuclear and dinuclear complexes and make assignments in the $^{31}$P NMR spectrum (Fig. 38).[278]

The further extension of DOSY spectra was developed in the form of Pureshift DOSY, where $^1$H signals were collapsed into singlets. This technique removes one of the main obstacles for DOSY measurements — resonance line overlap. However, the benefit is gained at the cost of drastically reduced sensitivity, making the method applicable only to concentrated samples.[282, 283] 3D and 2D combinations of traditional 2D methods and diffusion techniques bring unique combined experiments like COSY – DOSY, TOCSY – DOSY and HSQC – DOSY.[284 – 286] An ultrafast 2D DOSY spectroscopy (Difftrain) was also reported.[287]

When the liquids system is too complicated (contains many overlapping signals) or the main aim of study is the detection of minor compounds against the background of intensive ones, the hyphenation of NMR with liquid chromatography or even with LC-MS can help to solve the problem.[288] The flow probes designed for both LC-(MS)-NMR and high-throughput screening allow one to measure spectra from 30 μl of solution. Except investigation of natural compounds and metabolites, these hyphenated methods are very useful for general liquid systems.[288, 289] Different types of analysis including on-flow and stop-flow processes were developed for different tasks and systems (Fig. 39).

Hyphenated LC-MS-NMR systems combine the strengths of both methods. NMR and ESI-MS are used for characterization of compounds while high performance separation is achieved with HPLC. Information about molecular weights obtained from MS analysis gives exceptionally valuable aid for structure determination.[288 – 291]

Not only experimental approaches are used to speed up the experimental workflow, improve sensitivity and quality of spectral data. Digital signal processing and algorithms implemented in modern computational hardware stimulated a giant leap in the NMR methodology development. As it was mentioned with 2D methods above, many hardware

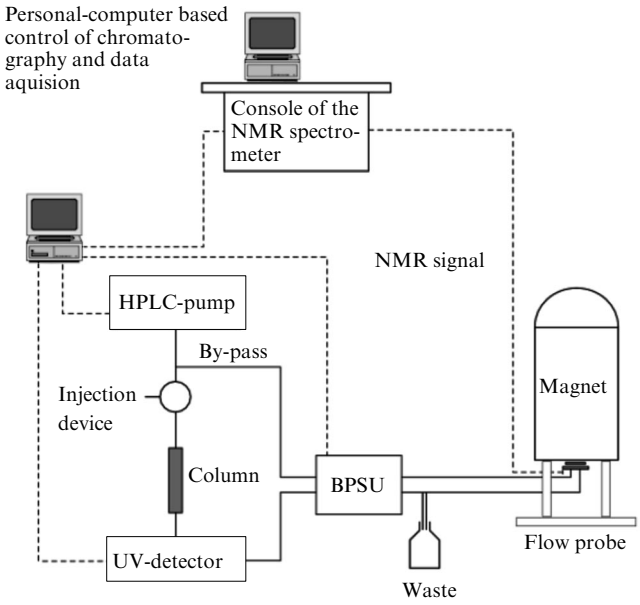



**Figure 39.** An example setup of LC-NMR workflow.[288]
Solid lines represent capillary connections, dotted lines show electrical circuitry. The system can operate either in on-line or off-line mode using storage loops in the Bruker peak sampling unit (BPSU).

improvements came from biomolecular NMR to the applications in organic chemistry.[248]

A representative example is non-uniform sampling algorithm, NUS, invented by Orekhov and co-workers.[292, 293] The principle of this method is sampling of certain percent of data points by special selection methods. For 3D methods, which are absolutely necessary for protein investigation, it brings four-fold faster acquisition, whereas for 2D, used routinely in organic chemistry, it can speed up experiment by a factor of up to 12 without any losses in both sensitivity and resolution (Fig. 40).

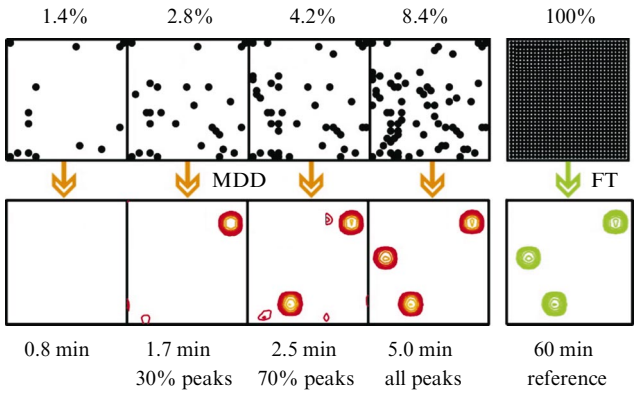



**Figure 40.** An example of NUS-scheduled experiment: properly designed sparse sampling provides a 12-fold decrease in the total experiment time.[292]
MDD is multidimensional decomposition, FT is fourier transformation.

Another method, covariance spectroscopy, deals exceptionally with post-processing. The idea lies in statistical treatment of 2D data. Covariance on COSY can transform it into artificial TOCSY, data from HSQC and COSY can be joined into HSQC-TOCSY and 2D INADEQUATE 'double-quantum correlation plot' can be transformed into COSY-like.[294, 295]

## 3. Electron microscopy of liquid samples

Routine microscopy techniques are unacceptable for the majority of gaseous, liquid or wet samples due to requirements of vacuum conditions. There is one type of the liquid media, which is compatible with the high-vacuum conditions. Because of their extremely low vapour pressures, ionic liquids can be used as a sample environment. Youshida *et al.*[296] used *N*,*N*,*N*-trimetyl-*N*-propylammonium-bis(trifluoromethanesulfonyl)imide as a solvent for the direct observation of the photochemical deposition of the gold particles onto the surface of $TiO_2$. The reaction was carried out directly in the microscope specimen chamber. Figures 41 *a*,*b* show low-magnification TEM images and diffraction patterns of $TiO_2$ particles in ionic liquid before and after irradiation, respectively. Formation of gold

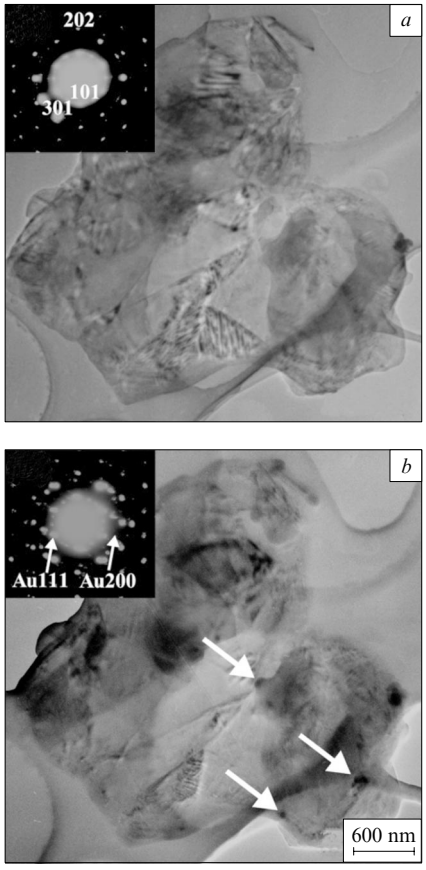



**Figure 41.** Low-magnification TEM images and diffraction patterns (in the insets) of $TiO_2$ particles in ionic liquid before (*a*) and after 3 h of UV irradiation (*b*).[296]
The arrows in the images point to $Au^0$ particles formed in the reaction.

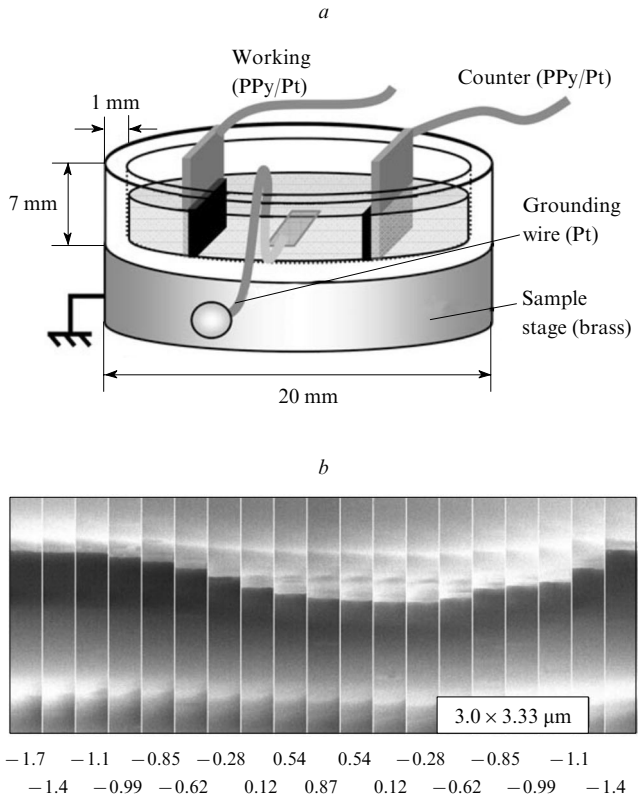



**Figure 42.** Schematic illustration of the electrochemical cell for *in situ* SEM observations (*a*) and SEM images of a polypyrrole film (PPy) at various electrode potentials (*b*).[297] (V, *vs.* $Ag/Ag^+$).

nanoparticles was detected *in situ* without the use of any specific sample treatment procedures.

Due to their electrical conductivity, ionic liquids can serve as electrolytes. Electrochemical cells containing ionic liquids can be assembled inside the electron microscope and used for the real-time observations of the redox processes on the electrode surface.[297] Schematic illustration of the electrochemical cell is shown in Fig. 42*a*. Two platinum plates electrochemically coated with polypyrrole film were immersed into the Petri dish containing 1-n-butyl-3-methylimidazolium bis(trifluoromethanesulfonyl)imide. Platinum grounding wire was used in order to enable electrical conduction between the cell and the sample stage. Cross-section of the electrode surface was observed by the high-magnification SEM. Electrochemical behaviour of the polymeric coating was studied by changing the applied dc voltage (Fig. 42*b*). SEM investigation of the polarized polypyrrole film clearly revealed that the coating thickness changes during oxidation and reduction.

Besides the observation of chemical transformations, electron microscopy in the liquid media provides the unique opportunity for direct visualization of the dynamic processes such as Brownian motion. For example, the movement of polystyrene diblock copolymers with poly(2-vinylpyridine) assemblies in the [emim][$EtOSO_3$] thin films was observed.[298] Conventional TEM technique was used for microscopy imaging.

## V. Solid-state chemical systems

Utilization of solid-state synthesis has grown considerably in the recent decades. The attractiveness of such reactions is determined not only by acceleration of reactions and enhanced selectivity, but also by the appearance of new ways of interaction compared to processes in solutions. The most widespread technique of carrying out such reactions is mechanochemical interaction of powder components in a ball mill or mortar with mechanical force being the promoter of the process.[299 – 301] This methodology has been successfully implemented in various organic reactions including aldol condensation,[302 – 304] Reformatsky,[305] Biginelli,[306] Morita – Baylis – Hillman,[307] Knoevenagel[308] and Wittig[309] reactions, as well as in the synthesis of heterocyclic compounds,[310 – 315] peptides[316, 317] and transition metal complexes.[318, 319] In addition, recent years have seen a growing tendency to perform transition-metal catalyzed[320 – 324] and asymmetric organocatalytic reactions[325 – 329] under milling conditions. It is interesting to mention that material of the ball mill chamber can sometimes serve as a catalyst.[310, 330]

Another approach to chemical transformations in the solid state is crystal engineering based on proper orientation of molecules due to non-covalent interactions (hydrogen bonding, $\pi - \pi$ stacking). As a result, oriented molecules are close enough to provide selective interaction upon suitable source of energy.[331 – 333] This strategy was successfully used in topochemical photoinitiated [2 + 2], [2 + 4] and [4 + 4] cycloaddition reactions and polymerization.[334 – 338]

Though the experimental procedures of mechanochemical and topochemical reactions are often quite simple, the main challenge is mechanistic understanding because limited number of methods are suitable for real-time study of transformation in solid mixtures of organic compounds. Quite often, solid products obtained are dissolved in a proper organic solvent for further analysis by high-resolution NMR or mass spectrometry. However dissolving can cause structural changes and disappearance of solid-stabilized intermediates and phase structure. To solve this problem, powder X-ray diffraction method has proven to be quite useful, especially for *in situ* investigation which allows real-time monitoring of reacting solid powders.[339, 340]

### 1. Mass spectrometry of solid samples

There are different ion sources that can operate with solid samples, for instance, EI, CI, MALDI, FAB *etc.* (see Fig. 1). Some of them work due to preliminary thermal vaporization of solid analyte directly in the ion source and then the obtained vapour is immediately ionized (*e.g.*, EI, CI). Evidently, this imposes a number of limitations, and the main limitation concerns inability to analyze thermally labile and non-volatile compounds. The solution of these problems lies in the ion sources which do not require a preliminary vaporization, where ionization occurs directly for solid analyte deposited in special matrix (*e.g.*, MALDI, FAB). The latter, especially MALDI, are extensively used to analyze high molecular weight (both biological and non-biological polymers) compounds, which is out of scope of this review.

Since during MS analysis in many cases (EI, CI *etc.*) the borders between solid and gas are quite formal due to preliminary vaporization of the solid analyte, MS analysis

of solid chemical systems was already discussed together with gaseous chemical systems in section III.1.

## 2. NMR spectroscopy of solid samples

The applications of solid-state NMR in the past were limited because of extreme line broadening. Two major factors leading to this phenomenon are chemical shift anisotropy (CSA) and dipole–dipole interactions (also quadrupole interactions for nuclei with $I > 1/2$), which are averaged due to molecular motion in solution NMR.[19, 22] Their influence is critical leading to line widths up to tens and hundreds kHz in solid samples, whereas the whole $^1$H spectrum of liquid or gaseous sample fits in a frequency range of 10 to 20 kHz (Fig. 43).

Fast spinning of the sample at so called magic angle (MAS, magic-angle spinning) can significantly reduce the contribution of these factors. It most cases, the higher the spinning speed, the less the line broadening. This is exemplified in Fig. 44, which shows $^{13}$C NMR spectra of glycine recorded at different spinning speeds.

The high speeds necessitate a special sample preparation procedure, which is much more complicated than in liquid-phase NMR. A solid sample is packed in special $ZrO_2$ (zirconia) rotor tolerant to extreme forces. Special pneumatic bearings keep rotor levitating, rotor cap with blades acts as air turbine, providing necessary spinning speed. Sample volume is limited by the rotor diameter, while the rotor diameter is determined by maximum possible spinning speed, as the rotor wall cannot move faster that the speed of sound in bearing gas medium (air or nitrogen). Therefore, the sensitivity has inverse relation to spinning speed, whereas spectral resolution increases with the speed increase in some cases.

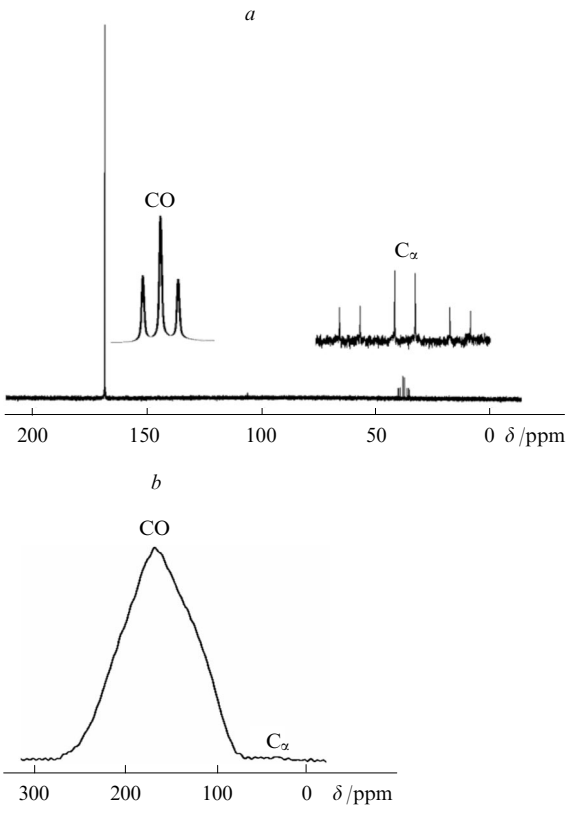



**Figure 43.** Comparison of line widths in $^{13}$C spectra of liquid sample (*a*) and solid sample (*b*) of $^{13}$C-labelled glycine (in the CO group, 10% $^{13}$C) (the integral intensity ratio $CO : C_\alpha = 10 : 1$).[19]

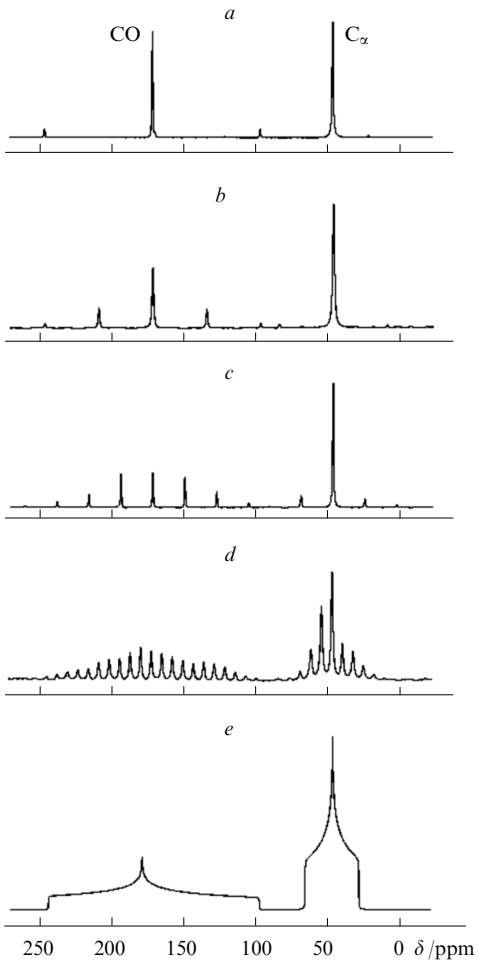



**Figure 44.** Effect of magic angle spinning at different speeds on glycine sample.[19]
Spinning speed /kHz: 10 (*a*), 5 (*b*), 2 (*c*), 1 (*d*); static sample (*e*); $CO : C_a \approx 1 : 1$

| | | | | |
|---|---|---|---|---|
| Sample volume /μl | 300 | 80 | 30 | 10 |
| Rotor diameter /mm | 7 | 4 | 3.2 | 1.9 |

Anyway, strong dipolar interactions between magnetically active nuclei cannot be eliminated only by MAS, thus strong homo- or heteronuclear decoupling is required during the acquisition. Unlike spin–spin decoupling with characteristic constants within hundreds Hz, $^1$H–$^{13}$C dipolar coupling constants are up to 120 kHz. In these conditions, decoupling RF fields with appropriate strengths are necessary for elimination of dipolar couplings. Tens and hundreds of Watts for solid state dipolar decoupling compared to hundreds milliwatts for spin decoupling require special NMR power amplifiers and probe.

Another complicating factor consists in very slow relaxation rates in solid states which is especially true for $^{13}$C spectroscopy. To overcome this problem, a special technique called cross-polarization (CP) is applied. The idea is

similar to liquid state INEPT (insensitive nuclei enhanced by polarization transfer) experiment. The polarization transfer from $^{1}H$ to the nuclei of interest (*e.g.*, $^{13}C$) switches operation to the $T_1(^{1}H)$ from $T_1(^{13}C)$ mode, simultaneously gaining sensitivity. The most required NMR methods for solid organic samples are 1D $^{13}C$ and $^{15}N$ CP-MAS experiments. They provide reliable spectra for partially soluble or almost insoluble samples.

$^{13}C$ CP-MAS spectroscopy is also useful for investigation of nanomaterials, like carbon nanotubes,[341] nanodiamonds,[342] and other materials (Fig. 45). Distinctive features can be easily traced using 1D spectra.

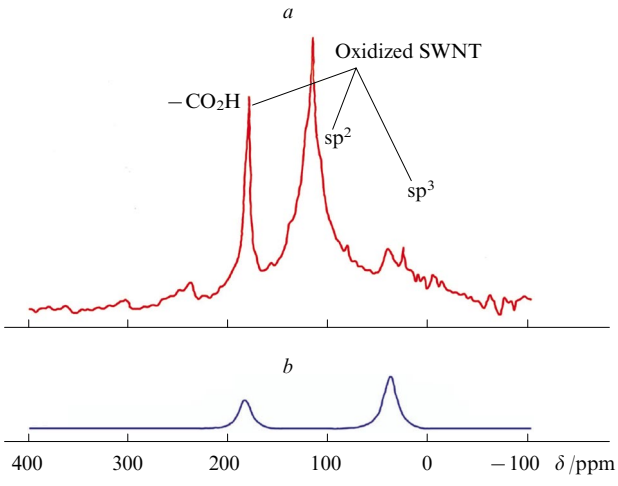



**Figure 45.** $^{13}C$ CP-MAS spectrum of functionalized SWNT (single wall nanotubes) (*a*) and simulated spectrum of polyacrylic acid (*b*).[341]

$^{1}H$ solid-state NMR spectroscopy is limited due to strong dipole homonuclear couplings by some systems, as well as $^{1}H-^{13}C$ 2D correlation spectroscopy. Instead, 2D $^{13}C-^{1}H$ correlation spectra are the good possibility to indirectly observe $^{1}H$ signals.

Nevertheless, there are many applications of solid-phase NMR like structure elucidation, conformation analysis, heterogeneous catalytic systems, investigation of sorption processes, supramolecular interactions. Structure elucidation has different aims compared to liquid-state NMR such as elucidation of the amorphous and crystalline samples, including polymers, analysis of multi-component systems, nanostructure analysis.

Even complicated molecules like steroids, terpenoids and their derivatives can be investigated with $^{13}C$ CP-MAS NMR spectroscopy which provides good spectral resolution. As an example, Fig. 46 shows the spectra of steroids **17a – b**.[343] The sample preparation is essential in this stage, as different crystalline forms can provide numerous signals in the spectra.[343]

Biosolids is another field of solid-state NMR application, including methods for protein structure determination in the crystallized state. Stereochemical deductions can be made on the basis of precise dipole – dipole constant measurements in the solid state. Proper experimental setup combined with theoretical calculations allows full 3D structure for complex objects, such as protein fibrils, to be determined.

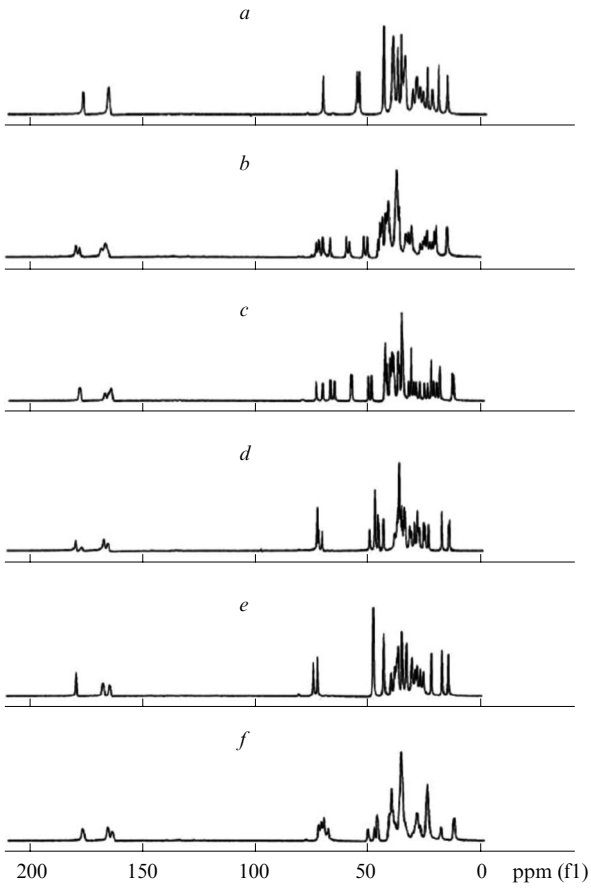
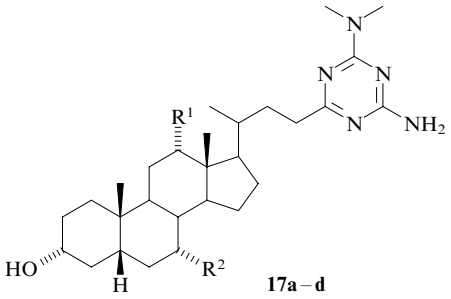



**Figure 46.** $^{13}C$ CP-MAS spectra of steroids (**17a – d**) crystallized from different solvents: **17a** from *p*-xylene (*a*), **17b** from *p*-xylene (*b*), **17b** from DMF/MeCN (*c*), **17d** from EtOAc/MeCN (*d*), **17c** from MeCN (*e*), **17d** from MeOH (*f*).[343]

Structures **17a – d**




**17a – d**

$R^1$ = H: $R^2$ = H (**a**), OH (**b**); $R^1$ = OH: $R^2$ = H (**c**), OH (**d**)

Considering the sensitivity enhancement, dynamic nuclear polarization (DNP) procedure should be mentioned. The resonance frequency of electrons is 660 times higher than that of protons, thus, the enhancement by magnetization transfer can theoretically reach this limit.[343-346] However, DNP experiments require special conditions like cryogenic temperatures (100 K and below) where excited state is stable enough to enhance NMR signal. Actual sensitivity growth is from 20 to 100 times, which makes possible the observation of less abundant

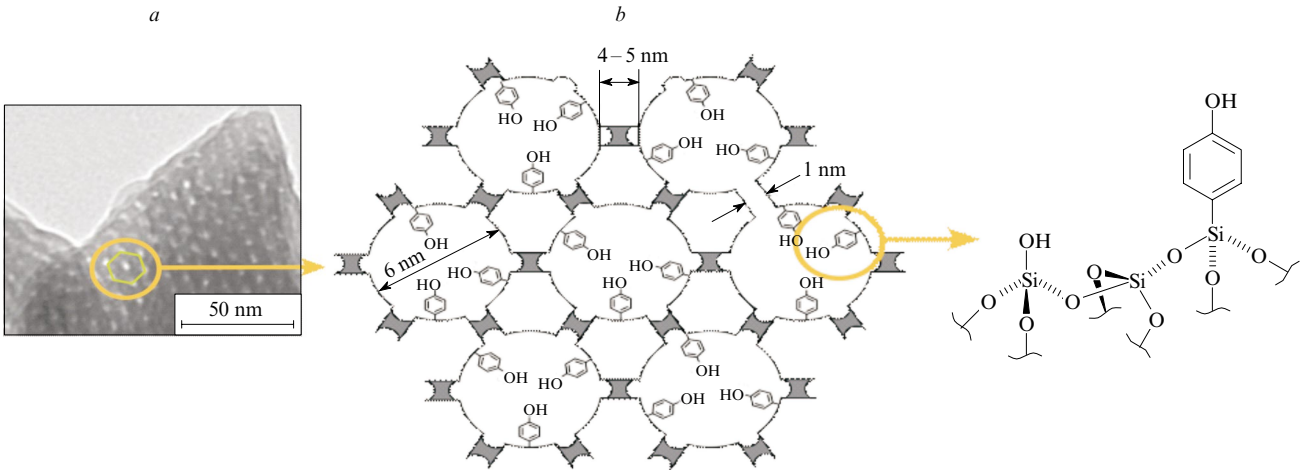



**Figure 47.** The SEM image (*a*) and structure of nanoporous material (*b*).[347]

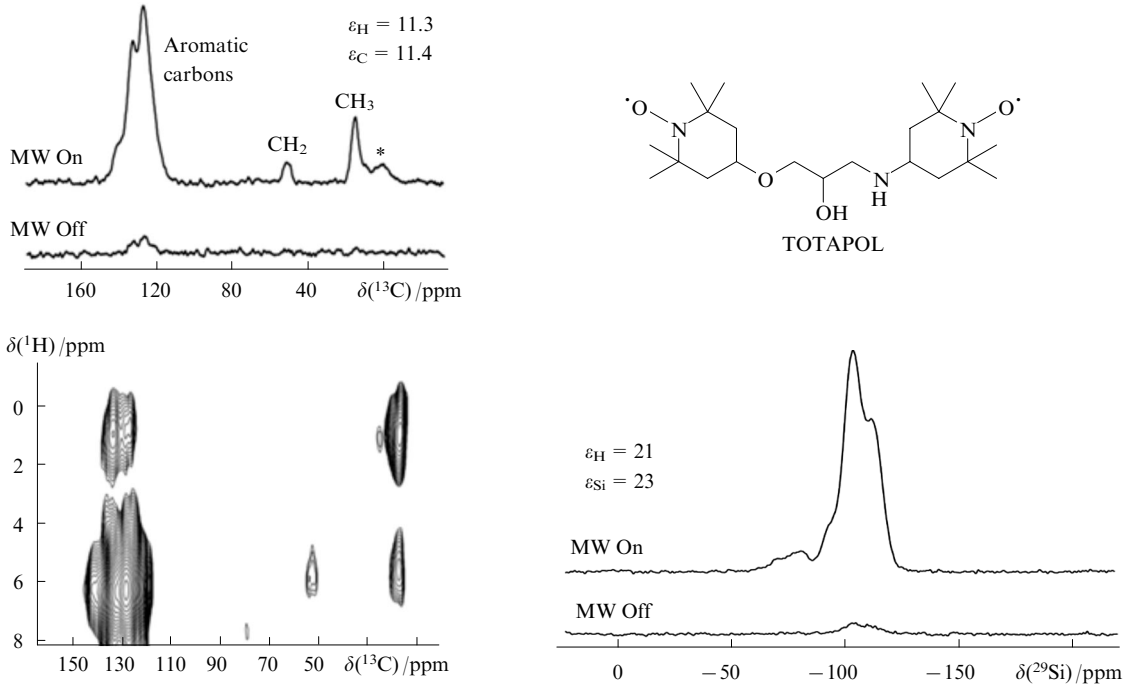



**Figure 48.** $^{13}C$ and $^{29}Si$ DNP-CP-MAS experiments of mesoporous material.[347]
TOTAPOL (25 mmol litre$^{-1}$), MAS = 12.5 kHz, 100 K, 3 h ($\varepsilon$ is amplification); MW is irradiation at 263 GHz to induce DNP. The asterisks mark the side signal caused by sample rotation.

nuclei, $^{13}C-^{13}C$ INADQUATE on solids and opens a new page of NMR spectroscopy, where it competes with X-ray diffractometry (NMR crystallography). Considerable disadvantage of DNP NMR systems is very high price of hardware; but in the nearest future we may expect implementation of cheaper DNP instruments available for chemists.

A good example of $^{13}C$ and $^{29}Si$ DNP-CPMAS investigation of real catalytic system based on mesoporous hybrid materials containing perfectly distributed and tunable ligands along each pore channel was published (Figs 47 and 48).[347]

## 3. Electron microscopy of solid samples

For more than half a century, solid-state electron microscopy has been known as an outstanding powerful tool for the observations of micro- and nano-size levels. Heterogeneous catalysts and characterization of novel nanostructured materials by electron microscopy are of particular interest for organic chemists.[348,349] A great number of studies dedicated to determination of heterogeneous catalyst morphology have appeared since the electron microscopy techniques were introduced into chemical research. Several recent reviews describe advances in SEM, TEM and STEM in the field of catalyst structure characterization.[350-354] General improvements include: high-angle annular dark

field (HAADF) STEM, aberration-corrected electron microscopy and environmental transmission electron microscopy.

Nanostructured objects composed of organic molecules are another important field of application for electron microscopy. For instance, one-dimensional assemblies of organic molecules such as nanowires, which are perspective materials for the creation of electronic and optoelectronic nanodevices, can be easily characterized by SEM and TEM.[355,356]

Important point in the study of organic materials concerns their dielectric properties. Metal coating may cause certain changes in the observed morphology and should be avoided.[357] Therefore, low-voltage microscopy and electron deceleration mode are suggested alternatives whenever possible.

Zhao *et al.*[358] described a facile method for the preparation of single crystalline submicrotubes from 2,4,5-triphenylimidazole. Synthesized structures were characterized by a number of methods including electron microscopy and temperature-dependent $^1$H NMR. SEM study revealed the morphology of the obtained material and showed that submicrotubes had comparatively high monodispersity and uniform diameter all along their length (Fig. 49 *a*). Temperature-dependent $^1$H NMR spectroscopy indicated the downfield shift of imidazole proton signal with the decrease of temperature (Fig. 49 *b*), which proved the presence of N—H···N H—bonds in the 2,4,5-triphenylimidazole assemblies.

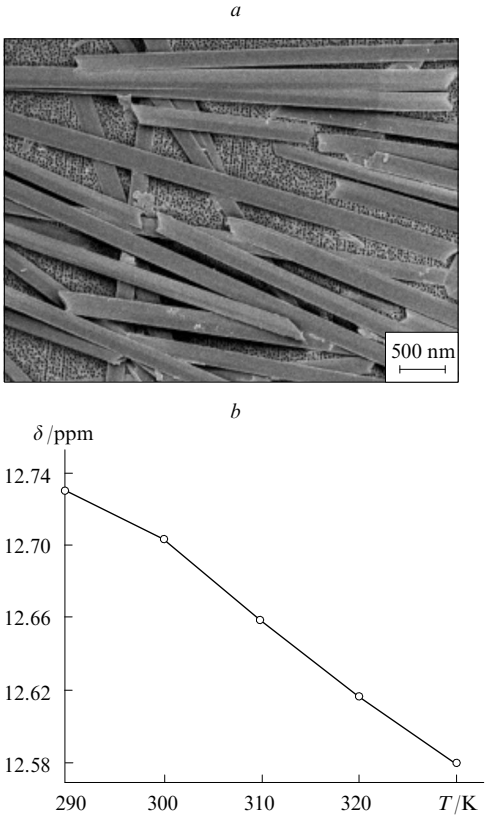



**Figure 49.** SEM image of the 2,4,5-triphenylimidazole submicrotubes (*a*) and temperature dependence of the imidazolium proton chemical shift for submicrotubes (*b*).[358]

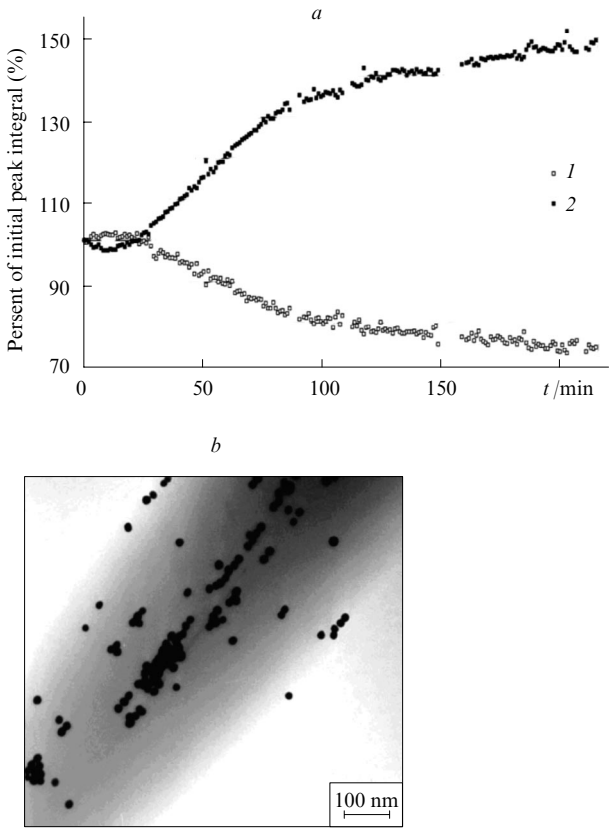



**Figure 50.** Percentage of peptide peak integrals in $^1$H NMR spectra *vs.* time during formation of nanotubes (*a*) and TEM image of the gold nanoparticles on the nanotubes (*b*).[359]
(*1*) Diphenylamine, (*2*) water.

Another interesting example of the joint structural study performed with the use of electron microscopy and NMR showed step-by-step self-assembling of peptide nanotubes to form coaxial nanocable.[359] The core of the cable was formed by the reduction of silver ions inside nanotube, and then gold shield was deposited onto the surface of nanotube modified with gold nanoparticles attached to the linker peptide. Self-assembly of the peptide was monitored by $^1$H NMR. The decrease of the integral intensity of peptide signals showed the self-assembly process in real time (Fig. 50 *a*). Transmitting electron microscopy was employed as a tool to control the metal deposition process (Fig. 50 *b*)

## VI. Conclusions and outlook

Evolution of analytical methods was a leading driving force to advance chemical science in the recent decades. However, it is important to mention the *vice versa* tendency of fascinating design of new analytical hardware challenged by requirements of novel practical applications. Very complex nature of molecular systems demanded development of target-oriented analytical approach, where important chemical tasks can be solved by a combination of analytical tools.

As illustrated in the present review, it is a proper combination of analytical tools that governs reliable structure analysis and mechanistic studies. For the organic

chemistry and related areas joining the forces of NMR spectroscopy, mass spectrometry and electron microscopy creates such a powerful complementary set of structure and reaction elucidation methods.

NMR spectroscopy and mass spectrometry (to a less extent, electron microscopy) have a diverse range of experiments, detection schemes and protocols dedicated to particular classes of compounds or reaction conditions. On the one hand, this provides great possibilities to enlarge the scope and make analysis more informative, on the other hand, many modifications and differences in the experimental set up (often missing detailed description in the articles) make it difficult to reveal and compare data obtained with different methods.

We anticipate rapid development of an improved strategy for analytical studies directed towards new practical applications. Target-oriented analysis, which has to intrinsically combine several methods, is an excellent opportunity to unify the concept of analytical measurements in modern chemical science.

## References

1. J J Thomson *The Electrician* **39** 104 (1897)
2. W Bleakney *Phys. Rev.* **34** 157 (1929)
3. W R Smythe, L H Rumbaugh, S S West *Phys. Rev.* **45** 724 (1934)
4. R D Macfarlane, D F Torgerson *Science* **191** 920 (1976)
5. F W McLafferty *Mass Spectral Correlations* (2nd Ed.) (Washington, DC: American Chemical Society, 1982)
6. *Tandem Mass Spectrometry* (Ed. F W McLafferty) (New York: Wiley, 1983)
7. R E March, R J Hughes *Quadrupole Storage Mass Spectrometry*. (New York: Wiley, 1989)
8. J B Fenn, M Mann, C K Meng, S F Wong, C M Whitehouse *Science* **246** 64 (1989)
9. M McMaster, C McMaster *GC/MS: A Practical User's Guide*. Wiley-VCH New York 1998
10. R Willoughby, E Sheehan, S Mitrovich *A Global View of LC/MS: How to Solve Your Most Challenging Analytical Problems* (2nd Ed.) (Pittsburgh, PA: Global View Publishing, 2002)
11. E de Hoffmann, V Stroobant *Mass Spectrometry: Principles and Applications* (3rd Ed.) (Chichester: Wiley, 2007)
12. J H Gross *Mass Spectrometry: A Textbook* (Berlin: Springer, 2011)
13. J L Norris, R M Caprioli *Chem. Rev.* **113** 2309 (2013)
14. *Modern Mass Spectrometry (Topics in Current Chemistry)* Vol. 225 (Ed. C A Schalley) (Berlin: Springer, 2003)
15. *Mass Spectrometry Handbook* (Ed. M S Lee) (Hoboken, NJ: Wiley, 2012)
16. V P Ananikov, L L Khemchyan, I P Beletskaya *Synlett* 2375 (2009)
17. V P Ananikov, L L Khemchyan, I P Beletskaya, Z A Starikova *Adv. Synth. Catal.* **352** 2979 (2010)
18. V P Ananikov, J V Ivanova L L Khemchyan, I P Beletskaya *Eur. J. Org. Chem.* 3830 (2012)
19. D D Laws, H-M L Bitter, A Jerschow *Angew. Chem., Int. Ed.* **41** 3096 (2002)
20. K J D MacKenzie *Solid State Ionics* **172** 383 (2004)
21. S D Courtier-Murias, H Farooq, H Masoom, A Botana, R Soong, J G Longstaffe, M J Simpson, W E Maas, M Fey, B Andrew, J Struppe, H Hutchins, S Krishnamurthy, R Kumar, M Monette, H J Stronks, A Hume, A J Simpson *J. Magn. Reson.* **217** 61 (2012)
22. *Solid-State NMR Spectroscopy: Principles and Applications* (Ed. M J Duer) (Oxford, London: Blackwell, 2002)
23. C Suarez *Chem. Educator* **3** (2) 02202-4 (1998)
24. C J Jameson *Chem. Rev.* **91** 1375 (1991)
25. R Marek, A Lycka *Curr. Org. Chem.* **6** 35 (2002)
26. M Weitman, L Lerman, S Cohen, A Nudelman, D T Major, H E Gottlieb *Tetrahedron* **66** 1465 (2010)
27. R Abraham, M Molbi *Modeling $^1$H Spectra of Organic Compounds: Theory, Applications, and NMR Prediction Software* (Oxford: Wiley, 2008)
28. T D W Claridge *High-Resolution NMR Techniques in Organic Chemistry (Tetrahedron Organic Chemistry)* Vol. 27 (2nd Ed.) (Amsterdam, Boston: Elsevier, 2009)
29. J I Goldstein, D E Newbury, D C Joy, C E Lyman, P Echlin, E Lifshin, L Sawyer, J R Michael *Scanning Electron Microscopy and X-Ray Microanalysis* (3rd Ed.) (New York: Kluwer Academic/Plenum Publishers, 2003)
30. R F Egerton *Physical Principles of Electron Microscopy: an Introduction to TEM, SEM, and AEM* (New York: Springer, 2007)
31. G Busca *Chem. Rev.* **107** 5366 (2007)
32. Val N Snytnikov, T I Mishchenko, Vl N Snytnikov, S E Malykhin, V I Avdeev, V N Parmon *Res. Chem. Intermed.* **38** 1133 (2012)
33. A Corma *Chem. Rev.* **95** 559 (1995)
34. T Durka, T Van Gerven, A Stankiewicz *Chem. Eng. Technol.* **32** 1301 (2009)
35. V S Arutyunov, R N Magomedov *Russ. Chem. Rev.* **81** 790 (2012)
36. S Yin, E R Bernstein *Int. J. Mass Spectrom.* **321** 49 (2012)
37. J Huang, M Haruta *Res. Chem. Intermed.* **38** 1 (2012)
38. A de Klerk *Green Chem.* **10** 1249 (2008)
39. M Schlangen, H Schwarz *Dalton Trans.* 10155 (2009)
40. R Kretschmer, M Schlangen, H Schwarz *Chem. – Eur. J.* **18** 40 (2012)
41. J Pola, A Ouchi *Molecules* **14** 1111 (2009)
42. A V Eremin *Prog. Energy Combust. Sci.* **38** 1 (2012)
43. T Mieno *New Diamond Front. Carbon Technol.* **16** 139 (2006)
44. J Roithová, D Schrlder *Chem. Rev.* **110** 1170 (2010)
45. L Operti R Rabezzana *Mass Spectrom. Rev.* **25** 483 (2006)
46. M K Beyer *Mass Spectrom. Rev.* **26** 517 (2007)
47. H Schwarz *Angew. Chem., Int. Ed.* **42** 4442 (2003)
48. M Speranza, F Gasparrini, B Botta, C Villani, D Subissati, C Fraschetti, A Subrizi *Chirality* **21** 69 (2009)
49. D K Bohme *Mass Spectrom. Rev.* **28** 672 (2009)
50. M N Eberlin *Int. J. Mass Spectrom.* **235** 263 (2004)
51. V P Ananikov, E G Gordeev *Chem. Sci.* **2** 2332 (2011)
52. V P Ananikov *J. Phys. Org. Chem.* **14** 109 (2001)
53. V P Ananikov *J. Phys. Org. Chem.* **16** 253 (2003)
54. H Sato *Chem. Rev.* **101** 2687 (2001)
55. P S Monks *Chem. Soc. Rev.* **34** 376 (2005)
56. I W M Smith *Annu. Rev. Astron. Astrophys.* **49** 29 (2011)
57. R Wu, T B McMahon *Mass Spectrom. Rev.* **28** 546 (2009)
58. Yu I Lyakhovetsky, E A Shilova, V V Bashilov, V I Sokolov, Yu S Nekrasov, B L Tumanskii *J. Phys. Chem. A* **113** 13700 (2009)

59. Yu I Lyakhovetsky, A P Pleshkova, E A Shilova, T V Ponomareva, R G Gasanov, B L Tumanskii, Yu A Borisov, Yu S Nekrasov *Eur. J. Mass Spectrom.* **18** 361 (2012)
60. O Martiskainen, R Gawinecki, B Ośmiałowski, K Wiinamäki, K Pihlaja *Rapid Commun. Mass Spectrom.* **23** 1075 (2009)
61. D Kim, C H Lee, J N Choi, K Y Choi, G J Zylstra, E Kim *Appl. Environ. Microbiol.* **76** 375 (2010)
62. C-Z Wang, Y Su, H-Y Wang, Y-L Guo *J. Am. Soc. Mass Spectrom.* **22** 1839 (2011)
63. M Schiorlin, E Marotta, M Dal Molin, C Paradisi *Environ. Sci. Technol.* **47** 542 (2013)
64. N Brenner, M Haapala, K Vuorensola, R Kostiainen *Anal. Chem.* **80** 8334 (2008)
65. I Dzidic, D I Carroll, R N Stillwell, E C Horning *Anal. Chem.* **48** 1763 (1976)
66. T Bristow, M Harrison, M Sims *Rapid Commun. Mass Spectrom.* **24** 1673 (2010)
67. I A Revelskii, Y S Yashin, V N Voznesenskii, V K Kurochkin, R G Kostyanovskii *Bull. Acad. Sci. USSR, Div. Chem. Sci.* **35** 1806 (1986) [*Izv. Akad. Nauk SSSR, Ser. Khim.* 1987 (1986)
68. M Haapala, L Luosujirvi, V Saarela, T Kotiaho, R A Ketola, S Franssila, R Kostiainen *Anal. Chem.* **79** 4994 (2007)
69. D Kim, P S Stevens, R A Hites *Int. J. Chem. Kinet.* **44** 821 (2012)
70. J C Harrison, J R Wells *Int. J. Chem. Kinet.* **44** 778 (2012)
71. M J Spallek, S Stockinger, R Goddard, O Trapp *Adv. Synth. Catal.* **354** 1466 (2012)
72. A Amirav, A Gordin, Y Hagooly, S Rozen, B Belgorodsky, B Seemann, H Marom, M Gozin, A B Fialkov *Tetrahedron* **68** 5793 (2012)
73. M Schenk, L Leon, K Moshammer, P Oßwald, T Zeuch, L Seidel, F Mauss, K Kohse-Höinghaus *Combust. Flame* **160** 487 (2013)
74. P Oßwald, H Güldenberg, K Kohse-Höinghaus, B Yang, T Yuan, F Qi *Combust. Flame* **158** 2 (2011)
75. A Lucassen, N Labbe, P R Westmoreland, K Kohse-Höinghaus *Combust. Flame* **158** 1647 (2011)
76. G de Petris, M Rosi, O Ursini, A Troiani *Chem. Asian J.* **8** 588 (2013)
77. H Garoiaz, M Berrabah, A Elidrissi, B Hammouti, A Ríos *Int. J. Environ. Anal. Chem.* **92** 1378 (2012)
78. F Hufsky, M Rempt, F Rasche, G Pohnert, S Böcker *Anal. Chim. Acta* **739** 67 (2012)
79. L Fiebig, H-G Schmalz, M Schäfer *Int. J. Mass Spectrom.* **308** 307 (2011)
80. A J Horan, Y Gao, W A Hall IV, M V Johnston *Anal. Chem.* **84** 9253 (2012)
81. M-Z Huang, S-C Cheng, Y-T Cho, J Shiea *Anal. Chim. Acta* **702** 1 (2011)
82. X Ma, S Zhang, X Zhang *TrAC, Trends Anal. Chem.* **35** 50 (2012)
83. M E Monge, G A Harris, P Dwivedi, F M Fernández *Chem. Rev.* **113** 2269 (2013)
84. K Tanaka, H Waki, Y Ido, S Akita, Y Yoshida, T Yoshida *Rapid Commun. Mass. Spectrom.* **2** 151 (1988)
85. *MALDI MS: a Practical Guide to Instrumentation, Methods and Applications* (Eds F Hillenkamp, J Peter-Katalinić) (Weinheim: Wiley-VCH, 2007)
86. *Surface Analysis — The Principal Techniques* (2nd Ed.) (Eds J C Vickerman, I S Gilmore) (Chichester: Wiley, 2009)
87. C N McEwen, S Trimpin *Int. J. Mass Spectrom.* **300** 167 (2011)
88. S Trimpin, B Wang, E D Inutan, J Li, C B Lietz, A Harron, V S Pagnotti, D Sardelis, C N McEwen *J. Am. Soc. Mass Spectrom.* **23** 1644 (2012)
89. A S Benk, C Roesli *Anal. Bioanal. Chem.* **404** 1039 (2012)
90. M Rainer, M N Qureshi, G K Bonn *Anal. Bioanal. Chem.* **400** 2281 (2011)
91. P A Kuzema *J. Anal. Chem.* **66** 1227 (2011)
92. O Adekunle, S Tanner, W H Binder *Beilstein J. Org. Chem.* **6** No 59 (2010)
93. W H Binder, B Pulamagatta, O Kir, S Kurzhals, H Barqawi, S Tanner *Macromolecules* **42** 9457 (2009)
94. A Matsumoto, T Kumagai, H Aota, H Kawasaki, R Arakawa *Polym. J. (Tokyo)* **41** 26 (2009)
95. R R Gowda, D Chakraborty, V Ramkumar *J. Organomet. Chem.* **696** 572 (2011)
96. R Tsunoyama, H Tsunoyama, P Pannopard, J Limtrakul, T Tsukuda *J. Phys. Chem. C* **114** 16004 (2010)
97. H Qian, Y Zhu, R Jin *ACS Nano* **3** 3795 (2009)
98. H Qian, R Jin *Chem. Commun.* **47** 11462 (2011)
99. G Li, X Li, Z Ouyang, R G Cooks *Angew. Chem., Int. Ed.* **52** 1040 (2013)
100. C J Jameson, A De Dios, A K Jameson *Chem. Phys. Lett.* **167** 575 (1990)
101. A Antušek, D Kedziera, K Jackowski, M Jaszuński, W Makulski *Chem. Phys.* **352** 320 (2008)
102. K Jackowski *J. Mol. Struct.* **786** 215 (2006)
103. A N Taha, S M Neugebauer Crawford, N S True *J. Phys. Chem. A* **102** 1425 (1998)
104. B D Ross, N S True *J. Am. Chem. Soc.* **105** 4871 (1983)
105. C Suarez, E J Nicholas, M R Bowman *J. Phys. Chem. A* **107** 3024 (2003)
106. A B Shtarov, P J Krusic, B E Smart, W R Dolbier Jr *J. Org. Chem.* **67** 3464 (2002)
107. A A Obynochny, A G Maryasov, M M Shakirov, I A Grigoriev *Chem. Phys.* **172** 295 (1993)
108. P O Moreno, N S True, C B Lemaster *J. Mol. Struct.* **243** 373 (1991)
109. P M Kating, P J Krusic, D C Roe, B E Smart *J. Am. Chem. Soc.* **118** 10000 (1996)
110. A B Shtarov, P J Krusic, B E Smart, W R Dolbier Jr *J. Am. Chem. Soc.* **123** 9956 (2001)
111. J W Nibler, P Minarik, W Fitts, R Kohnert *J. Chem. Educ.* **73** 99 (1996)
112. A A Marchione *J. Magn. Reson.* **210** 31 (2011)
113. A A Marchione, E F McCord *J. Magn. Reson.* **201** 34 (2009)
114. G E Dobereiner, R H Crabtree *Chem. Rev.* **110** 681 (2010)
115. M H Pérez-Temprano, J A Casares, P Espinet *Chem. – Eur. J.* **18** 1864 (2012)
116. K Fagnou, M Lautens *Angew. Chem., Int. Ed.* **41** 26 (2002)
117. M Moreno-Manas, R Pleixats *Acc. Chem. Res.* **36** 638 (2003)
118. M T Reetz *Angew. Chem., Int. Ed.* **47** 2556 (2008)
119. S Díez-González, N Marion, S P Nolan *Chem. Rev.* **109** 3612 (2009)
120. I P Beletskaya, V P Ananikov *Chem. Rev.* **111** 1596 (2011)
121. V P Ananikov, I P Beletskaya *Top. Organomet. Chem.* **43** 1 (2013)
122. Z Zhang, P R Schreiner *Chem. Soc. Rev.* **38** 1187 (2009)
123. S Bertelsen, K A Jørgensen *Chem. Soc. Rev.* **38** 2178 (2009)
124. A Berkessel, H Groeger *Asymmetric Organocatalysis* (Weinheim: Wiley-VCH, 2005)
125. D Enders, O Niemeier, A Henseler *Chem. Rev.* **107** 5606 (2007)
126. H Pellissier *Tetrahedron* **63** 9267 (2007)
127. D Enders, T Balensiefer *Acc. Chem. Res.* **37** 534 (2004)

128. P I Dalko, L Moisan *Angew. Chem., Int. Ed.* **43** 5138 (2004)
129. R C Wende, P R Schreiner *Green Chem.* **14** 1821 (2012)
130. F Giacalone, M Gruttadauria, P Agrigento, R Noto *Chem. Soc. Rev.* **41** 2406 (2012)
131. J Alemán, S Cabrera *Chem. Soc. Rev.* **42** 774 (2013)
132. *Asymmetric Organocatalysis (Topics in Current Chemistry)* Vol. 291 (Berlin, Heidelberg: Springer, 2009)
133. C C J Loh, D Enders *Chem. – Eur. J.* **18** 10212 (2012)
134. C Zhong, X Shi *Eur. J. Org. Chem.* 2999 (2010)
135. Z Du, Z Shao *Chem. Soc. Rev.* **42** 1337 (2013)
136. H Niedermeyer, J P Hallett, I J Villar-Garcia, P A Hunt, T Welton *Chem. Soc. Rev.* **41** 7780 (2012)
137. J P Hallett, T Welton *Chem. Rev.* **111** 3508 (2011)
138. D Betz, P Altmann, M Cokoja, W A Herrmann, F E Kühn *Coord. Chem. Rev.* **255** 1518 (2011)
139. Q Zhang, S Zhang, Y Deng *Green Chem.* **13** 2619 (2011)
140. *Ionic Liquids: Industrial Applications for Green Chemistry (ACS Sympsium Series)* Vol. 818 (Eds R D Rogers, K R Seddon) (Washington, DC: American Chemical Society, 2002)
141. *Ionic Liquids in Synthesis* (Eds P Wasserscheid, T Welton) (Wienheim: Wiley-VCH, 2003)
142. *Metal Catalysed Reactions in Ionic Liquids (Catalysis by Metal Complexes)* Vol. 29 (Eds P J Dyson, T J Geldbach) (Springer, 2005)
143. H Zhao, G A Baker *J. Chem. Technol. Biotechnol.* **88** 3 (2013)
144. J D Scholten, B C Leal, J Dupont *ACS Catal.* **2** 184 (2012)
145. M Moniruzzaman, K Nakashima, N Kamiya, M Goto *Biochem. Eng. J.* **48** 295 (2010)
146. T Welton *Chem. Rev.* **99** 2071 (1999)
147. E A Khokhlova, V V Kachala, V P Ananikov *ChemSusChem* **5** 783 (2012)
148. V P Ananikov *Chem. Rev.* **111** 418 (2011)
149. P Wasserscheid, W Keim *Angew. Chem., Int. Ed.* **39** 3772 (2000)
150. N V Plechkova, K R Seddon *Chem. Soc. Rev.* **37** 123 (2008)
151. V I Pârvulescu, C Hardacre *Chem. Rev.* **107** 2615 (2007)
152. L-A Schaper, S J Hock, W A Herrmann, F E Kühn *Angew. Chem., Int. Ed.* **52** 270 (2013)
153. S Roy, H Plenio *Adv. Synth. Catal.* **352** 1014 (2010)
154. P B Arockiam, C Fischmeister, C Bruneau, P H Dixneuf *Angew. Chem., Int. Ed.* **49** 6629 (2010)
155. *Organic Reactions in Water: Principles, Strategies and Applications* (Ed. U M Lindström) (Oxford: Blackwell, 2007)
156. *Comprehensive Organic Reactions in Aqueous Media* (Eds C-J Li, T-H Chan) (New York: Wiley, 2007)
157. A Chanda, V V Fokin *Chem. Rev.* **109** 725 (2009)
158. *Organic Synthesis in Water* (Ed. P A Grieco) (London: Blackie, 1998)
159. U M Lindstrom *Chem. Rev.* **102** 2751 (2002)
160. *Clean Solvents: Alternative Media for Chemical Reactions and Processing (ACS Symposium Series)* Vol. 819 (Eds M A Abraham, L Moens) (Washington, DC: American Chemical Society, 2002)
161. *Aqueous-Phase Organometallic Catalysis* (2nd Ed.) (Eds B Cornils, W A Herrmann) (Weinheim: Wiley-VCH, 2004)
162. N Pinault, D W Bruce *Coord. Chem. Rev.* **241** 1 (2003)
163. C I Herrertas, X Yao, Z Li, C-J Li *Chem. Rev.* **107** 2546 (2007)
164. K H Shaughnessy *Chem. Rev.* **109** 643 (2009)
165. R N Butler, A G Coyne *Chem. Rev.* **110** 6302 (2010)
166. H D Velazquez, F Verpoort *Chem. Soc. Rev.* **41** 7032 (2012)
167. C-J Li *Chem. Rev.* **105** 3095 (2005)
168. M-O Simon, C-J Li *Chem. Soc. Rev.* **41** 1415 (2012)
169. D J Cole-Hamilton *Adv. Synth. Catal.* **348** 1341 (2006)
170. X Han, M Poliakoff *Chem. Soc. Rev.* **41** 1428 (2012)
171. T Matsuda, T Harada, K Nakamura *Curr. Org. Chem.* **9** 299 (2005)
172. A Kruse, H Vogel *Chem. Eng. Technol.* **31** 23 (2008)
173. H-F Jiang, *Curr. Org. Chem.* **9** 289 (2005)
174. W Leitner *Acc. Chem. Res.* **35** 746 (2002)
175. *Chemical Synthesis Using Supercritical Fluids* (Eds P G Jessop, W Leitner) (New York: Wiley, 1999)
176. D Sanli, S E Bozbag, C Erkey *J. Mater. Sci.* **47** 2995 (2012)
177. C M Rayner *Org. Process Res. Dev.* **11** 121 (2007)
178. P G Jessop, T Ikariya, R Noyori *Chem. Rev.* **99** 475 (1999)
179. A Stobrawe, P Makarczyk, C Maillet, J-L Muller, W Leitner *Angew. Chem., Int. Ed.* **47** 6674 (2008)
180. A Baiker *Chem. Rev.* **99** 453 (1999)
181. H R Hobbs, N R Thomas *Chem. Rev.* **107** 2786 (2007)
182. S E Bozbag, D Sanli, C Erkey *J. Mater. Sci.* **47** 3469 (2012)
183. E Colacino, J Martinez, F Lamaty, L S Patrikeeva, L L Khemchyan, V P Ananikov, I P Beletskaya *Coord. Chem. Rev.* **256** 2893 (2012)
184. M A P Martins, C P Frizzo, D N Moreira, L Buriol, P Machado *Chem. Rev.* **109** 4140 (2009)
185. P Anastas, N Eghbali *Chem. Soc. Rev.* **39** 301 (2010)
186. R A Sheldon *Chem. Soc. Rev.* **41** 1437 (2012)
187. A Cappiello, G Famiglini, P Palma, F Mangani *Anal. Chem.* **74** 3547 (2002)
188. A Cappiello, G Famiglini, E Pierini, P Palma, H Trufelli *Anal. Chem.* **79** 5364 (2007)
189. A Cappiello, B Tirillini, G Famiglini, H Trufelli, V Termopoli, C Flender *Phytochem. Anal.* **23** 191 (2012)
190. O Granot, A Amirav *Int. J. Mass Spectrom.* **244** 15 (2005)
191. M Holčapek, R Jirvsko, M Ltsa *J. Chromatogr., A* **1217** 3908 (2010)
192. P Kebarle *J. Mass Spectrom.* **35** 804 (2000)
193. P Kebarle, U H Verkerk *Mass Spectrom. Rev.* **28** 898 (2009)
194. S Crotti, R Seraglia, P Traldi *Eur. J. Mass Spectrom.* **17** 85 (2011)
195. L Konermann, E Ahadi, A D Rodriguez, S Vahidi *Anal. Chem.* **85** 2 (2013)
196. J B Fenn *Angew. Chem., Int. Ed.* **42** 3871 (2003)
197. S Banerjee, S Mazumdar *Int. J. Anal. Chem.* **2012** ID 282574 (2012)
198. *Reactive Intermediates: MS Investigations in Solution* (Ed. L S Santos) (Weinheim: Wiley-VCH, 2010)
199. D Schröder *Acc. Chem. Res.* **45** 1521 (2012)
200. W Zhu, Y Yuan, P Zhou, L Zeng, H Wang, L Tang, B Guo, B Chen *Molecules* **17** 11507 (2012)
201. L S Santos *Eur. J. Org. Chem.* 235 (2008)
202. L S Santos *J. Braz. Chem. Soc.* **22** 1827 (2011)
203. P Chen *Angew. Chem., Int. Ed.* **42** 2832 (2003)
204. C A Müller, C Markert, A M Teichert, A Pfaltz *Chem. Commun.* 1607 (2009)
205. M Schäfer, M Drayß, A Springer, P Zacharias, K Meerholz *Eur. J. Org. Chem.* 5162 (2007)
206. R A J O'Hair *Chem. Commun.* 1469 (2006)
207. G Lefèvre, G Franc, A Tlili, C Adamo, M Taillefer, I Ciofini, A Jutand *Organometallics* **31** 7694 (2012)
208. P A Belyakov, V I Kadentsev, A O Chizhov, N G Kolotyrkina, A S Shashkov, V P Ananikov *Mendeleev Commun.* **20** 125 (2010)
209. D M Chisholm, J S McIndoe *Dalton Trans.* 3933 (2008)
210. J W Lee, S W Heo, S J C Lee, J Y Ko, H Kim, H I Kim *J. Am. Soc. Mass Spectrom.* **24** 21 (2013)

211. T Santa *Biomed. Chromatogr.* **25** 1 (2011)
212. K L Vikse, Z Ahmadi, C C Manning, D A Harrington, J S McIndoe *Angew. Chem., Int. Ed.* **50** 8304 (2011)
213. C Adlhart, P Chen *Helv. Chim. Acta* **83** 2192 (2000)
214. D M Chisholm, A G Oliver, J S McIndoe *Dalton Trans.* **39** 364 (2010)
215. K L Vikse, M P Woods, J S McIndoe *Organometallics* **29** 6615 (2010)
216. K L Vikse, Z Ahmadi, J Luo, N van der Wal, K Daze, N Taylor, J S McIndoe *Int. J. Mass Spectrom.* **323 – 324** 8 (2012)
217. A T Lubben, J S McIndoe, A S Weller *Organometallics* **27** 3303 (2008)
218. M A Henderson, J Luo, A Oliver, J S McIndoe *Organometallics* **30** 5471 (2011)
219. A Vasseur, D Harakat, J Muzart, J Le Bras *Adv. Synth. Catal.* **355** 59 (2013)
220. A Vasseur, D Harakat, J Muzart, J Le Bras *J. Org. Chem.* **77** 5751 (2012)
221. D Harakat, J Muzart, J Le Bras *RSC Adv.* **2** 3094 (2012)
222. C Ebner, C A Müller, C Markert, A Pfaltz *J. Am. Chem. Soc.* **133** 4710 (2011)
223. J Hyvl, D Agrawal, R Pohl, M Suri, F Glorius, D Schröder *Organometallics* **32** 807 (2013)
224. A N Comeau, J J Liu, C B Khadka, J F Corrigan, L Konermann *Anal. Chem.* **85** 1200 (2013)
225. Y-Q Hu, M-H Zeng, K Zhang, S Hu, F-F Zhou, M Kurmoo *J. Am. Chem. Soc.* **135** 7901 (2013)
226. A Eizaguirre, O Mó, M Yáñez, J Tortajada, J-Y Salpin *J. Phys. Chem. B* **117** 2088 (2013)
227. P M Mayer, C Poon *Mass Spectrom. Rev.* **28** 608 (2009)
228. R Kretschmer, M Schlangen, H Schwarz *Dalton Trans.* **42** 4153 (2013)
229. A Gholami, T D Fridgen *Dalton Trans.* **42** 3979 (2013)
230. R S Burkhalter, C L Hogue, D L Smith, S M Sonner, M J Winningham, R E Youngman *J. Organomet. Chem.* **724** 213 (2013)
231. L-G Zhuo, J-J Zhang, Z-X Yu *J. Org. Chem.* **77** 8527 (2012)
232. T Müller, A Badu-Tawiah, R G Cooks *Angew. Chem., Int. Ed.* **51** 11832 (2012)
233. T Ghislain, P Faure, R Michels *J. Am. Soc. Mass Spectrom.* **23** 530 (2012)
234. A Ahmed, C H Choi, M C Choi, S Kim *Anal. Chem.* **84** 1146 (2012)
235. P Östman, S J Marttila, T Kotiaho, S Franssila, R Kostiainen *Anal. Chem.* **76** 6659 (2004)
236. A Schmidt, M Karas, T Dülcks *J. Am. Soc. Mass Spectrom.* **14** 492 (2003)
237. A El-Faramawy, K W M Siu, B A Thomson *J. Am. Soc. Mass Spectrom.* **16** 1702 (2005)
238. N G Akhmedov, P M Gannett, B Wu, M M Cummings, B C Train *Magn. Reson. Chem.* **51** 156 (2013)
239. J B Lambert, E P Mazzola *Nuclear Magnetic Resonance Spectroscopy* (London: Pearson Education, 2004)
240. H Günther *NMR Spectroscopy* (Chichester: Wiley, 1980)
241. C M Thiele *Eur. J. Org. Chem.* 5673 (2008)
242. N Harada *Chirality* **20** 691 (2008)
243. E E Kwan, S G Huang *Eur. J. Org. Chem.* 2671 (2008)
244. T J Wenzel, C D Chisholm *Chirality* **23** 190 (2011)
245. P A Belaykov, V P Ananikov *Russ. Chem. Bull., Int. Ed.* **60** 783 (2011) [*Izv. Akad. Nauk, Ser. Khim.* 765 (2011)]
246. T Parella *NMR Guide, 4.3* (Bruker BioSpin, 2007)
247. *Avance Anniversary: 10 Years of Digital NMR. Spin Report* Vols 154/155 (Bruker BioSpin, 2004) p. 68
248. J Cavanagh, W J Fairbrother, A G Palmer III, M Rance, N J Skelton *Protein NMR Spectroscopy: Principles and Practice* (2nd Ed.) (San Diego, CA: Academic Press, CA, 2006)
249. D J Peterson, N M Loening *Magn. Reson. Chem.* **45** 937 (2007)
250. J Guo, R I Duclos Jr , V K Vemuri, A Makriyannis *Tetrahedron Lett.* **51** 3465 (2010)
251. N S Bhacca, D H Williams *Tetrahedron Lett.* **5** 3127 (1964)
252. I S Levina, E V Pokrovskaya, L E Kulikova, A V Kamernitzky, V V Kachala, A N Smirnov *Steroids* **73** 815 (2008)
253. M P Felicissimo, A A Batista, A G Ferreira, J Ellena, E E Castellano *Polyhedron* **24** 1063 (2005)
254. B Adrjan, T Szymańska-Buzar *J. Organomet. Chem.* **693** 2163 (2008)
255. A J Zozulin, H J Jakobsen, T F Moore, A R Garber, J D Odom *J. Magn. Reson.* **41** 458 (1980)
256. J Battiste, R A Newmark *Prog. Nucl. Magn. Reson. Spectrosc.* **48** 1 (2006)
257. K A M Ampt, R L E G Aspers, P Dvortsak, R M van der Werf, S S Wijmenga, M Jaeger *J. Magn. Reson.* **215** 27 (2012)
258. H Kessler, H Oschkinat, C Griesinger, W Bermel *J. Magn. Reson.* **70** 106 (1986)
259. K Stott, J Stonehouse, J Keeler, T L Hwang, A J Shaka *J. Am. Chem. Soc.* **117** 4199 (1995)
260. J Stonehouse, P Adell, J Keeler, A J Shaka *J. Am. Chem. Soc.* **116** 6037 (1994)
261. A Bax, D G Davis *J. Magn. Reson.* **65** 355 (1985)
262. I Ghiviriga *J. Org. Chem.* **77** 3978 (2012)
263. G E Martin *Annu. Rep. NMR Spectrosc.* **74** 215 (2011)
264. *Encyclopedia of Spectroscopy and Spectrometry* (2nd Ed.) (Eds J C Lindon, G E Tranter, D Koppenaal) (London: Academic Press, 2010)
265. A G Gerbst, N E Ustuzhanina, A A Grachev, E A Khatuntseva, D E Tsvetkov, A S Shashkov, A I Usov, M E Preobrazhenskaya, N A Ushakova, N E Nifantiev *J. Carbohydr. Chem.* **22** 109 (2003)
266. S Akoka, L Barantin, M Trierweiler *Anal. Chem.* **71** 2554 (1999)
267. L Frydman, A Lupulescu, T Scherf *J. Am. Chem. Soc.* **125** 9204 (2003)
268. Y Shrot, L Frydman *J. Am. Chem. Soc.* **125** 11385 (2003)
269. P Giraudeau, S Akoka *J. Magn. Reson.* **186** 352 (2007)
270. P Giraudeau, S Massou, Y Robin, E Cahoreau, J-C Portais, S Akoka *Anal. Chem.* **83** 3112 (2011)
271. M-K Lee, M Gal, L Frydman, G Varani *Proc. Natl. Acad. Sci. USA* **107** 9192 (2010)
272. Z D Pardo, G L Olsen, M E Fernández-Valle, L Frydman, R Martínez-Álvarez, A Herrera *J. Am. Chem. Soc.* **134** 2706 (2012)
273. P Giraudeau, Y Shrot, L Frydman *J. Am. Chem. Soc.* **131** 13902 (2009)
274. P Giraudeau, S Akoka *Magn. Reson. Chem.* **49** 307 (2011)
275. P Giraudeau, S Akoka *J. Magn. Reson.* **205** 171 (2010)
276. H Walderhaug, O Söderman, D Topgaard *Prog. Nucl. Magn. Reson. Spectrosc.* **56** 406 (2010)
277. W S Price *Concepts Magn. Reson.* **9** 299 (1997)
278. V P Ananikov, S S Zalesskiy, V V Kachala, I P Beletskaya *J. Organomet. Chem.* **696** 400 (2011)
279. V P Ananikov, K A Gayduk, N V Orlov, I P Beletskaya, V N Khrustalev, M Yu Antipin *Chem. – Eur. J.* **16** 2063 (2010)

280. V P Ananikov, N V Orlov, M A Kabeshov, I P Beletskaya, Z A Starikova *Organometallics* **27** 4056 (2008)
281. V P Ananikov, I P Beletskaya *Organometallics* **31** 1595 (2012)
282. J A Aguilar, S Faulkner, M Nilsson, G A Morris *Angew. Chem., Int. Ed.* **49** 3901 (2010)
283. J C Cobas, M Martín-Pastor *J. Magn. Reson.* **171** 20 (2004)
284. D H Wu, A D Chen, C S Johnson Jr *J. Magn. Reson.* **115** 260 (1995)
285. A Botana, P W A Howe, V Caër, G A Morris, M Nilsson *J. Magn. Reson.* **211** 25 (2011)
286. K Vermillion, N P J Price *J. Magn. Reson.* **198** 209 (2009)
287. J P Stamps, B Ottink, J M Visser, J P M van Duynhoven, R Hulst *J. Magn. Reson.* **151** 28 **(**2001)
288. *On-Line LC-NMR and Related Techniques* (Ed. K Albert) (Chichester, UK: Wiley, 2002)
289. M Godejohann, L-H Tseng, U Braumann, J Fuchser, M Spraul *J. Chromatogr., A* **1058** 191 (2004)
290. P A Keifer *Annu. Rep. NMR Spectrosc.* **62** 1 (2007)
291. J A Krauser, M Voehler, L-H Tseng, A B Schefer, M Godejohann, F P Guengerich *Eur. J. Biochem.* **271** 3962 (2004)
292. V A Jaravine, V Yu Orekhov *J. Am. Chem. Soc.* **128** 13421 (2006)
293. V Yu Orekhov, V A Jaravine *Prog. Nucl. Magn. Reson. Spectrosc.* **59** 271 (2011)
294. F Zhang, N Trbovic, J Wang, R Brüschweiler *J. Magn. Reson.* **174** 219 (2005)
295. T Short, L Alzapiedi, R Brüschweiler, D Snyder *J. Magn. Reson.* **209** 75 (2011)
296. K Yoshida, T Nozaki, T Hirayama, N Tanaka *J. Electron Microsc.* **56** 177 (2007)
297. S Arimoto, D Oyamatsu, T Torimoto, S Kuwabata *ChemPhysChem* **9** 763 (2008)
298. U Mansfeld, S Hoeppener, U S Schubert *Adv. Mater.* **25** 761 (2013)
299. S L James, C J Adams, C Bolm, D Braga, P Collier, T Friscic, F Grepioni, K D M Harris, G Hyett, W Jones, A Krebs, J Mack, L Maini, A G Orpen, I P Parkin, W C Shearouse, J W Steed, D C Waddell *Chem. Soc. Rev.* **41** 413 (2012)
300. R B N Baig, R S Varma *Chem. Soc. Rev.* **41** 1559 (2012)
301. A Stolle, T Szuppa, S E S Leonhardt, B Ondruschka *Chem. Soc. Rev.* **40** 2317 (2011)
302. C L Raston, J L Scott *Green Chem.* **2** 49 (2000)
303. B Rodríguez, A Bruckmann, C Bolm *Chem. – Eur. J.* **13** 4710 (2007)
304. J G Hernández, V García-López, E Juaristi *Tetrahedron* **68** 92 (2012)
305. K Tanaka, S Kishigami, F Toda *J. Org. Chem.* **56** 4333 (1991)
306. A K Bose, S Pednekar, S N Ganguly, G Chakraborty, M S Manhas *Tetrahedron Lett.* **45** 8351 (2004)
307. J Mack, M Shumba *Green Chem.* **9** 328 (2007)
308. G Kaupp, M R Naimi-Jamal, J Schmeyers *Tetrahedron* **59** 3753 (2003)
309. V P Balema, J W Wiench, M Pruski, V K Pecharsky *J. Am. Chem. Soc.* **124** 6244 (2002)
310. T L Cook, J A Walker Jr, J Mack *Green Chem.* **15** 617 (2013)
311. X Zhu, Z Li, C Jin, L Xu, Q Wu, W Su *Green Chem.* **11** 163 (2009)
312. G-W Wang, Y-W Dong, P Wu, T-T Yuan, V-B Shen *J. Org. Chem.* **73** 7088 (2008)
313. Y-W Dong, G-W Wang, L Wang *Tetrahedron* **64** 10148 (2008)
314. S Mashkouri, M R Naimi-Jamal *Molecules* **14** 474 (2009)
315. B Lee, P Kang, K H Lee, J Cho, W Nam, W K Lee, N H Hur *Tetrahedron Lett.* **54** 1384 (2013)
316. V Declerck, P Nun, J Martinez, F Lamaty *Angew. Chem., Int. Ed.* **48** 9318 (2009)
317. J G Hernández, E Juaristi *J. Org. Chem.* **75** 7107 (2010)
318. A L Garay, A Pichon, S L James *Chem. Soc. Rev.* **36** 846 (2007)
319. V A Kozlov, D V Aleksanyan, M V Korobov, N V Avramenko, R R Aysin, O A Maloshitskaya, A S Korlyukov, I L Odinets *Dalton Trans.* **40** 8768 (2011)
320. F Schneider, T Szuppa, A Stolle, B Ondruschka, H Hopf *Green Chem.* **11** 1894 (2009)
321. E Tullberg, D Peters, T Frejd *J. Organomet. Chem.* **689** 3778 (2004)
322. R Thorwirth, A Stolle, B Ondruschka *Green Chem.* **12** 985 (2010)
323. G Cravotto, D Garella, S Tagliapietra, A Stolle, S Schüßler, S E S Leonhardt, B Ondruschka *New J. Chem.* **36** 1304 (2012)
324. R Schmidt, R Thorwirth, T Szuppa, A Stolle, B Ondruschka, H Hopf *Chem. – Eur. J.* **17** 8129 (2011)
325. B Rodríguez, T Rantanen, C Bolm *Angew. Chem., Int. Ed.* **45** 6924 (2006)
326. G Guillena, M del Carmen Hita, C Najera, S F Viozquez *J. Org. Chem.* **73** 5933 (2008)
327. T Rantanen, I Schiffers, C Bolm *Org. Process Res. Dev.* **11** 592 (2007)
328. A Bruckmann, B Rodriguez, C Bolm *CrystEngComm* **11** 404 (2009)
329. M Jörres, S Mersmann, G Raabe, C Bolm *Green Chem.* **15** 612 (2013)
330. D A Fulmer, W C Shearouse, S T Medonza, J Mack *Green Chem.* **11** 1821 (2009)
331. K Biradha, R Santra *Chem. Soc. Rev.* **42** 950 (2013)
332. G K Kole, G K Tan, J J Vittal *CrystEngComm* **13** 3138 (2011)
333. L R MacGillivray, G S Papaefstathiou, T Friščić, D B Varshney, T D Hamilton, in *Templates in Chemistry I (Topics in Current Chemistry)* Vol. 248 (Eds C A Schalley, F Vögtle, K H Dötz) (Berlin, Heidelberg: Springer, 2004) p. 201
334. I G Georgiev, L R MacGillivray *Chem. Soc. Rev.* **36** 1239 (2007)
335. C Avendaño, A Briceno *CrystEngComm* **11** 408 (2009)
336. D-K Bučar, G S Papaefstathiou, T D Hamilton, Q L Chu, I G Georgiev, L R MacGillivray *Eur. J. Inorg. Chem.* 4559 (2007)
337. G K Kole, G K Tan, J J Vittal *Org. Lett.* **12** 128 (2010)
338. A M P Peedikakkal, J J Vittal *Chem. – Eur. J.* **14** 5329 (2008)
339. T Friščić, I Halasz, P J Beldon, A M Belenguer, F Adams, S A J Kimber, V Honkimäki, R E Dinnebier *Nat. Chem.* **5** 66 (2013)
340. K D M Harris *Nat. Chem.* **5** 12 (2013)
341. C G Bac, P Bernier, S Latil, V Jourdain, A Rubio, S H Jhang, S W Lee, Y W Park, M Holzinger, A Hirsch *Curr. Appl. Phys.* **1** 149 (2001)
342. T M Alam *Mater. Chem. Phys.* **85** 310 (2004)
343. E Sievänen, E Kolehmainen *Appl. Spectrosc. Rev.* **48** 50 (2013)
344. Y Zhang, D Collison, F R Livens, M Helliwell, F Heatley, A K Powell, S Wocadlo, H Eccles *Polyhedron* **21** 81 (2002)
345. S P Brown *Solid State Nucl. Magn. Reson.* **41** 1 (2012)
346. V Weis, R G Griffin *Solid State Nucl. Magn. Reson.* **29** 66 (2006)

347. A Lesage, M Lelli, D Gajan, M A Caporini, V Vitzthum, P Miéville, J Alauzun, A Roussey, C Thieuleux, A Mehdi, G Bodenhausen, C Coperet, L Emsley *J. Am. Chem. Soc.* **132** 15459 (2010)
348. V P Ananikov, N V Orlov, S S Zalesskiy, I P Beletskaya, V N Khrustalev, K Morokuma, D G Musaev *J. Am. Chem. Soc.* **134** 6637 (2012)
349. S S Zalesskiy, A E Sedykh, A S Kashin, V P Ananikov *J. Am. Chem. Soc.* **135** 3550 (2013)
350. J-D Grunwaldt, J B Wagner, R E Dunin-Borkowski *ChemCatChem* **5** 62 (2013)
351. T Takei, T Akita, I Nakamura, T Fujitani, M Okumura, K Okazaki, J Huang, T Ishida, M Haruta *Adv. Catal.* **55** 1 (2012)
352. W Zhou, I E Wachs, C J Kiely *Curr. Opin. Solid State Mater. Sci.* **16** 10 (2012)
353. J C Yang, M W Small, R V Grieshaber, R G Nuzzo *Chem. Soc. Rev.* **41** 8179 (2012)
354. J Liu *ChemCatChem* **3** 934 (2011)
355. L Zang, Y Che, J S Moore *Acc. Chem. Res.* **41** 1596 (2008)
356. Y S Zhao, H Fu, A Peng, Y Ma, D Xiao, J Yao *Adv. Mater.* **20** 2859 (2008)
357. A S Kashin, V P Ananikov *Russ. Chem. Bull. Int. Ed.* **60** 2602 (2011) [*Izv. Akad. Nauk, Ser. Khim.* 2551 (2011)]
358. Y S Zhao, W Yang, D Xiao, X Sheng, X Yang, Z Shuai, Y Luo, J Yao *Chem. Mater.* **17** 6430 (2005)
359. O Carny, D E Shalev, E Gazit *Nano Lett.* **6** 1594 (2006)